



The Use of a Multi-Degree-of-Freedom Dual Balance System to Measure Cross and Cross-Coupling Derivatives

**D.R. Haberman
Calspan Field Services, Inc.**

April 1982

Final Report for Period October 1, 1980 — November 1, 1981

Approved for public release; distribution unlimited.

**ARNOLD ENGINEERING DEVELOPMENT CENTER
ARNOLD AIR FORCE STATION, TENNESSEE
AIR FORCE SYSTEMS COMMAND
UNITED STATES AIR FORCE**

NOTICES

When U. S. Government drawings, specifications, or other data are used for any purpose other than a definitely related Government procurement operation, the Government thereby incurs no responsibility nor any obligation whatsoever, and the fact that the government may have formulated, furnished, or in any way supplied the said drawings, specifications, or other data, is not to be regarded by implication or otherwise, or in any manner licensing the holder or any other person or corporation, or conveying any rights or permission to manufacture, use, or sell any patented invention that may in any way be related thereto.

Qualified users may obtain copies of this report from the Defense Technical Information Center.

References to named commercial products in this report are not to be considered in any sense as an endorsement of the product by the United States Air Force or the Government.

This report has been reviewed by the Office of Public Affairs (PA) and is releasable to the National Technical Information Service (NTIS). At NTIS, it will be available to the general public, including foreign nations.

APPROVAL STATEMENT

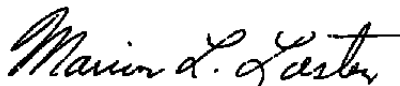
This report has been reviewed and approved.



ALVIN R. OBAL, Captain, CF
Diretorate of Technology
Deputy for Operations

Approved for publication:

FOR THE COMMANDER



MARION L. LASTER
Director of Technology
Deputy for Operations

UNCLASSIFIED

SECURITY CLASSIFICATION OF THIS PAGE (When Data Entered)

REPORT DOCUMENTATION PAGE		READ INSTRUCTIONS BEFORE COMPLETING FORM										
1. REPORT NUMBER AEDC-TR-81-34	2. GOVT ACCESSION NO.	3. RECIPIENT'S CATALOG NUMBER										
4. TITLE (and Subtitle) THE USE OF A MULTI-DEGREE-OF-FREEDOM DUAL BALANCE SYSTEM TO MEASURE CROSS AND CROSS-COUPLING DERIVATIVES		5. TYPE OF REPORT & PERIOD COVERED Final Report - Oct. 1, 1980 - Nov. 1, 1981										
		6. PERFORMING ORG. REPORT NUMBER										
7. AUTHOR(s) D. R. Haberman, Calspan Field Services, Inc.		8. CONTRACT OR GRANT NUMBER(s)										
9. PERFORMING ORGANIZATION NAME AND ADDRESS Arnold Engineering Development Center/DOT Air Force Systems Command Arnold Air Force Station, TN 37389		10. PROGRAM ELEMENT, PROJECT, TASK AREA & WORK UNIT NUMBERS Program Element 65807F										
11. CONTROLLING OFFICE NAME AND ADDRESS Arnold Engineering Development Center/DOS Air Force Systems Command Arnold Air Force Station, TN 37389		12. REPORT DATE April 1982										
		13. NUMBER OF PAGES 88										
14. MONITORING AGENCY NAME & ADDRESS (if different from Controlling Office)		15. SECURITY CLASS. (of this report) UNCLASSIFIED										
		15a. DECLASSIFICATION/DOWNGRADING SCHEDULE N/A										
16. DISTRIBUTION STATEMENT (of this Report) Approved for public release; distribution unlimited.												
17. DISTRIBUTION STATEMENT (of the abstract entered in Block 20, if different from Report)												
18. SUPPLEMENTARY NOTES Available in Defense Technical Information Center (DTIC).												
19. KEY WORDS (Continue on reverse side if necessary and identify by block number) <table border="0"> <tr> <td>balances</td> <td>deflection</td> </tr> <tr> <td>derivatives</td> <td>damping</td> </tr> <tr> <td>interferometry</td> <td>mathematical models</td> </tr> <tr> <td>degrees of freedom</td> <td>wind tunnel tests</td> </tr> <tr> <td>strain gages</td> <td>dynamics</td> </tr> </table>			balances	deflection	derivatives	damping	interferometry	mathematical models	degrees of freedom	wind tunnel tests	strain gages	dynamics
balances	deflection											
derivatives	damping											
interferometry	mathematical models											
degrees of freedom	wind tunnel tests											
strain gages	dynamics											
20. ABSTRACT (Continue on reverse side if necessary and identify by block number) <p>The equations of motion are derived for two existing dual balance systems used at the Arnold Engineering Development Center (AEDC) to obtain measurements of aerodynamic cross and cross-coupling derivatives. The complete equations of motion presented include the effects of sting motion. Each system incorporates a dynamic cross flexure balance and a five-component static balance. The primary deflection modes of the balances</p>												

UNCLASSIFIED

SECURITY CLASSIFICATION OF THIS PAGE (When Data Entered)

20. ABSTRACT (Continued)

were confirmed using a holographic interferometry measurement technique. Both laboratory and wind tunnel data are presented to illustrate dynamic effects.

UNCLASSIFIED

SECURITY CLASSIFICATION OF THIS PAGE (When Data Entered)

PREFACE

The work reported herein was performed by the Arnold Engineering Development Center (AEDC), Air Force Systems Command (AFSC), at the request of the AEDC Directorate of Technology (DOT) under Program Element 65807F. The AEDC/DOT project manager was Capt. A. R. Obal (CF). The results were obtained by Calspan Field Services, Inc./AEDC Division, operating contractor for the aerospace flight dynamics testing effort at the AEDC, AFSC, Arnold Air Force Station, Tennessee, under AEDC Project Number D215VW. The manuscript was submitted for publication on November 11, 1981.

The author acknowledges the invaluable assistance of Dr. Reinhard Menzel and Mr. Frank Hornsby, Calspan Field Services, Inc., in making the holographic interferometry measurements.

CONTENTS

	<u>Page</u>
1.0 INTRODUCTION	5
2.0 BALANCE DEFLECTION MODES AND DYNAMIC MODEL DEVELOPMENT	
2.1 Pitch/Yaw Models	7
2.2 Roll Model	9
3.0 BALANCE EQUATIONS OF MOTION	10
4.0 EQUATIONS OF MOTION WITH STING BENDING MOTION INCLUDED ...	12
5.0 DATA REDUCTION	
5.1 Pitch/Yaw Data Reduction	13
5.2 Roll Data Reduction	16
6.0 CORRECTION OF EXISTING CROSS-COUPLING ROLL DATA	17
7.0 CONCLUSIONS	19
REFERENCES	21

ILLUSTRATIONS

Figure

1. The 1,500-lb Force-Moment Balance Used for Measurement of Cross and Cross-Coupling Derivatives	23
2. The 1,500-lb Moment Balance Used for Measurement of Cross and Cross-Coupling Derivatives	24
3. Three-Degree-of-Freedom Models of the Pitch and Yaw Planes of the Force-Moment Balance	26
4. Three-Degree-of-Freedom Models of the Pitch or Yaw Plane of the Moment Balance	28
5. Two-Degree-of-Freedom Models of the Pitch and Yaw Planes of the Force-Moment Balance	29
6. Two-Degree-of-Freedom Model of the Pitch or Yaw Plane of the Moment Balance .	31
7. Yaw Plane Deflection Modes of the Force-Moment Balance	32
8. Dynamic Model in Roll	33
9. Dynamic Model of the Three-Degree-of-Freedom Force-Moment Balance System Including Two Degrees of Freedom of the Supporting Sting	34
10. Dynamic Model of the Three-Degree-of-Freedom Moment Balance System Including Two Degrees of Freedom of the Supporting Sting	36
11. Laboratory Roll Data Corrected Using the Multi-Degree-of-Freedom Approach ...	37

<u>Figure</u>	<u>Page</u>
12. Roll Data From a Current Fighter Configuration Corrected Using the Multi-Degree-of-Freedom Approach	38
13. Wind Tunnel SDM Roll Data Corrected Using the Multi-Degree-of-Freedom Approach.	39

TABLES

1. Pitch/Yaw Equations of Motion for the Force-Moment Balance	40
2. Pitch/Yaw Equations of Motion for the Moment Balance	42
3. Roll Equations of Motion	43
4. Equations of Motion for the Force-Moment Balance Including Two Degrees of Freedom of the Supporting Sting	44
5. Equations of Motion for the Moment Balance Including Two Degrees of Freedom of the Supporting Sting	46

APPENDIXES

A. BALANCE DEFLECTION MODE DETERMINATIONS	47
B. DETAILS OF BALANCE EQUATION OF MOTION DERIVATIONS	55
C. THE DETERMINATION OF CONSTANTS NEEDED FOR DATA REDUCTION	72
D. THE EFFECT OF NEGLECTING THE AERODYNAMIC DAMPING CONSTANT FROM THE DATA REDUCTION PROCEDURE	78
NOMENCLATURE	83

1.0 INTRODUCTION

During the past four to five years, two 1,500-lb balances were developed to measure aerodynamic cross and cross-coupling derivatives at the Arnold Engineering Development Center (AEDC). One of these cross-coupling (C.C.) balances was built to be mounted on the 1,500-lb forced oscillation pitch/yaw cross flexure (C.F.) balance used primarily in the Propulsion Wind Tunnel (PWT) facility. The other was developed primarily to fit the 1,200-lb pitch/yaw C.F. balance in the von Kármán Facility (VKF). The purpose of combining a C.C. balance with a C.F. balance was to enable the measurement of the forces and moments in the pitch, yaw, or roll planes that are produced by oscillating a model in a single plane with a C.F. balance. Both balance combinations have been tested in the laboratory, and, in addition, the PWT combination was used in a test in Tunnel 4T to make cross and cross-coupling measurements on the standard dynamics model (SDM) in December 1980.

Following fabrication of the balances, each was laboratory tested to determine the accuracy with which a known applied moment vector could be measured. As was expected, the use of statically obtained balance gage sensitivities to reduce dynamic data resulted in a difference between the applied laboratory moment vector and the measured moment vector. The difference in the vectors was attributable to the balance deflections, which, under dynamic loading conditions, were caused by the model and balance inertias, as well as the externally applied loads. The purpose of this report is to present the equations of motion of the subject balances which would enable a more accurate measurement of such dynamic load vectors in the future. Although other problems with making such measurements do exist, such as nonlinear load interactions between different balance gages, it is not the intent of this report to cover any subject other than the dynamic modeling of the balance motion and the development of the relevant equations of motion.

A statically obtained balance sensitivity reflects the stress imposed on a balance gage element (or beam) caused by a known statically applied load. The stress produces a strain in the beam, and a strain gage mounted on the beam converts this strain into an electrical output. Under dynamic loading conditions no distinction can be made between the strain caused by an inertia load and that caused by an external or aerodynamic load unless the system is mathematically modeled and analytically solved for the external loads. To account analytically for the inertia loads, the sting/balance/model system must be accurately modeled to include all of the degrees of freedom experienced by the system. The equations of motion for this system can then be solved for the externally applied loads. Although it is possible to write the equations to include all degrees of freedom, it is difficult to instrument a balance to measure all these quantities. Some compromises must be made to keep the

instrumentation and data reduction requirements reasonable. Therefore, only the primary degrees of freedom can be measured and accounted for in the equations of motion, and these primary degrees of freedom may vary, depending on balance type.

The equations of motion for the subject AEDC systems and the system models to which they apply are presented in this report. The methods of derivation of these equations are not new and are fairly general in applicability. However, the specific equations for a given system are unique to that system and other systems with similar primary degrees of freedom. Hanff (Ref. 1) did a similar equation development for the system at NRC in Canada, but his equations are not totally applicable to the AEDC systems because of the additional degrees of freedom added by the relatively flexible stings used at AEDC. Differences in equations of motion also arise because of the different types of balances used at AEDC. The equations of motion for the balance developed in PWT, a force-moment balance, are different from the equations of motion for the balance developed in VKF, a moment balance, because the force gage is designed for primary compliance in translation, whereas the moment gage is primarily rotational. In the application of any equation, the system model to which the equations apply must compare with the system to which the equations are to be used, or errors will result.

The roll equations are somewhat different from the pitch/yaw equations because all degrees of freedom rotate about the same axis. However, the same roll model and resulting equation apply to both of the subject systems. To illustrate the magnitude of correction resulting from the dynamic modeling of a multi-degree-of-freedom (DOF) roll balance, some cross-coupling roll data taken on an earlier test were reduced using the dynamic equation of motion in roll. These data are presented in this report, along with the same data reduced using the static roll sensitivity.

2.0 BALANCE DEFLECTION MODES AND DYNAMIC MODEL DEVELOPMENT

In principle, each cross-coupling (C.C.) balance is similar to a five-component static force balance. Each balance is designed and gaged to measure a force or a moment, i.e., a shear or bending strain, at each of two balance stations in the pitch plane and in the yaw plane. In addition, each balance has a roll element gaged to measure strain caused by roll, which brings the total loads measured to five. The roll element station is physically located between the fore and aft pitch/yaw elements on both of the subject balances. To keep the balances as rigid as possible, they lack axial force gages. The main difference from a standard static balance, however, is a result of the requirement that a cross flexure (C.F.) balance be mounted internal to the C.C. balance. To meet this requirement the C.C. balances are built in the shape of a can to fit over the C.F. balance. The force-moment and

moment balances are illustrated in Figs. 1 and 2a, respectively. The hollow center, illustrated by the cross-sectional view of each balance, is the cavity into which a C.F. balance is fit. The internal mounting of the C.F. balance within the C.C. moment balance is illustrated in the cutaway view of Fig. 2b.

In providing a measurement of the moment or force at a particular station, the balances are, in essence, providing an electrical output which is proportional to the balance deflection at that station. With the proper handling these moment and force measurements can be converted into deflections of these flexible balance stations, as will be discussed later in Sec. 3.0. The forward gaged station of the force-moment balance is designed and gaged (with strain gages) to provide an electrical output signal proportional to pitching moment and side force; i.e., it has a pitching moment element and a side force element. The pitching moment gages sense the bending strain to which they are subjected, and the side force gages sense the shear strain to which they are subjected. These two sets of gages are approximately centered about the same forward axial station of the balance, as are the two sets of gages at the aft station. Unlike the forward station, the aft gaged station is designed and gaged to provide electrical outputs proportional to yawing moment and normal force. The roll section, located between the fore and aft gaged stations, is gaged to sense shear strain produced by a rolling moment. The moment balance is different in that both the forward and aft pitch/yaw gaged stations are gaged to sense bending moment in both the pitch and yaw planes.

It is assumed that all parts of the balances are perfectly rigid except for the gaged stations. In reality each gaged station can undergo deflections other than those for which it is gaged. Although the forward station of the moment balance is gaged to sense yaw and pitch bending moment (rotational degrees of freedom), it can still undergo deflections caused by yaw and pitch shear loads (translational degrees of freedom) even though these deflections do not provide an electrical output. These extraneous degrees of freedom are limited to small deflections by making the gaged beams as short as possible, thus limiting deflection attributable to "S" bending. In like manner the forward station of the force-moment balance is given maximum compliance to side shear load and pitch bending load by designing the balance cross section to have a high second moment of area about the z axis and a relatively low second moment of area about the y axis. The aft station is similarly designed.

2.1 PITCH/YAW MODELS

If the deflections monitored by the strain gages are considered to be the primary deflection modes of the balance, then the dynamic model of the moment balance pitch and yaw planes is different from the dynamic models of the force-moment balance. The moment

balance has two rotational degrees of freedom each in the pitch and yaw planes, whereas the force-moment balance has one translational and one rotational degree of freedom in the pitch plane and the yaw plane. The roll station of each balance must also be considered to be a flexible member. It is assumed to add an additional rotational degree of freedom to each balance model. The resulting three-degree-of-freedom (3-DOF) models of the force-moment and moment balances in the pitch and yaw planes are illustrated in Figs. 3 and 4, respectively. One model applies to either the pitch or yaw plane for the moment balance, since all deflections are rotational. Two models are required for the force-moment balance, one in pitch and one in yaw. The translational degree of freedom is located at the front of the balance in the yaw plane and at the rear in the pitch plane.

Two-degree-of-freedom (2-DOF) models for the same systems are shown in Figs. 5 and 6. The 3-DOF models of the balance illustrated in Figs. 3 and 4 depict the motion of the balance more exactly than the 2-DOF models illustrated in Figs. 5 and 6, in which the roll gage elements have been omitted. The omission of the roll gage element implies that they are rigid in pitch and yaw, which is not exactly correct. However, the roll gage elements are designed to be much more rigid in pitch and yaw than the fore and aft pitch and yaw gages, and little error is introduced by their omission. In addition, the roll elements are not provided with strain gages to measure pitch or yaw deflection and their inclusion in the models and equations of motion would be of little use without a means to obtain the deflection data. Therefore, the simpler 2-DOF systems are more applicable to the balances as they now exist.

Figures 3 through 6 illustrate two types of motion that are possible in each plane: out-of-plane motion and in-plane motion. The out-of-plane motion is considered to be that motion experienced by a balance in the plane perpendicular to the oscillation plane of the C.F. balance. For example, if a balance is being oscillated in pitch, the out-of-plane motion would be the motion experienced by the balance in the yaw plane. Under ideal conditions this motion is produced by external forces only and not by the forced oscillation of the C.F. balance. In reality some inertial coupling exists between the two planes, caused by nonzero cross products of inertia causing an inertial moment as well. These cross product inertial loads represent a tare which must be subtracted from out-of-plane balance output to arrive at a measurement of the externally applied loads. Tare levels such as these are typically measured under vacuum in a laboratory where no externally applied loads, e.g., aerodynamic loads, are present.

The in-plane motion is the motion experienced by the balance in the plane of oscillation. In this plane the balance experiences the model and balance inertial loads imposed by the forced oscillation of the C.F. balances, as well as externally applied loads. These inertial

loads plus some cross product inertial loads represent a tare level on the in-plane balance output. Again, this tare level output can be obtained under vacuum conditions. When speaking in terms of aerodynamic loads, direct derivatives are sensed by the in-plane gages, and cross or cross-coupling derivatives are sensed by the out-of-plane gages.

To verify that the correct deflection modes of the force-moment balance were assumed, the balance deflections were measured under load using an holographic interferometry technique. By this technique, the deflection of the balance along its entire length was determined from a photographic record of the balance with superimposed interference fringes. Each successive fringe on the balance surface represents the deflection of the balance through one wavelength of the light used for illumination, in this case a helium-neon laser beam with a wavelength of $0.6328 \mu\text{m}$. Details of the holographic interferometry technique are presented in Appendix A. Some results of the deflection measurements are shown in Fig. 7, where the deflections of the force-moment balance in the yaw plane are graphically illustrated. The plots clearly show that the primary deflections of the balance at the flexible stations are those deflections for which it is gaged. For example, in the yaw plane the force-moment balance has a force gage at the forward flexible station and a moment gage at the aft flexible station. The deflection curve (Fig. 7) illustrates a large translational deflection at the forward station and a large rotational deflection at the aft station, as would be expected. Accompanying the large translational deflection at the forward station is a small rotational deflection. This is an example of an extraneous deflection mentioned earlier which cannot be avoided in any real physical system. The deflection curves also illustrate the deflections of the middle flexible stations, the roll gage elements, which are currently not gaged to measure these deflections. However, they are relatively small compared to the primary deflections. To measure the balance deflections (and, consequently, the model motion) more correctly, the balance would have to be gaged for all of the deflections illustrated by the deflection curve. However, as with most experimental measurements, tradeoffs between cost and ease of instrumentation must be weighed against accuracy. The dynamic data acquisition system used at AEDC does not currently have the capacity to handle the number of gages required to instrument the balances to measure the deflections in all degrees of freedom. It is unlikely that the accuracy gained would justify the additional cost.

2.2 ROLL MODEL

The rolling motion model of the balances is somewhat different from the pitch or yaw models illustrated in Figs. 3 through 6 since all degrees of freedom rotate about the same axis. For roll motion each balance is assumed to have a roll degree of freedom at each gaged station. In addition, laboratory tests of both of the counterpart C.F. balances have shown

that the C.F. balances have more flexibility in roll than the C.C. balances. Therefore, the motion of the C.F. balance in roll must be accounted for as well as the motion of the C.C. balance. The dynamic model of the system in roll is illustrated in Fig. 8. This model applies to both the force-moment and the moment balance systems.

3.0 BALANCE EQUATIONS OF MOTION

The equations of motion for the force-moment and moment balances as depicted by the models shown in Figs. 3, 4, 5, and 6 are given in Tables 1 and 2. The equation of motion in roll for the dynamic model shown in Fig. 8 is given in Table 3. The Lagrange method, as described in Ref. 2, was used for all derivations. Details of the derivations are presented in Appendix B.

Note that the balance rotational and translation deflection measurements $\bar{\Theta}_1$, $\bar{\Theta}_2$, $\bar{\Theta}_3$, \bar{Z}_1 , and \bar{Z}_3 are input into equations and not moments and forces as would be done for a static balance. This imposes the requirement that a spring constant (k) in terms of deflection/load of each gaged station must be known as well as the standard sensitivity (s) in terms of voltage/load. These two constants, used in conjunction with the voltage signal (E) from the gage, provide the proper input to the equations as follows.

$$(E)(k/s) = \Theta \text{ (or } Z) \quad (1)$$

It must also be noted that the balance gage element deflections, $\bar{\Theta}$ and \bar{Z} , are amplitudes of sinusoidal gage oscillations, since the C.C. balance is being forced to oscillate sinusoidally by the C.F. balance. A linear dependence between the balance oscillation and the forces produced from the oscillation is assumed. Therefore, the gage deflections (amplitudes) are vector quantities, i.e., they have phase, which is measured relative to the constant amplitude forcing function of the C.F. balance, as well as magnitude, and must be input as such into the equations.

The constants in the equations include some lengths and masses which are not considered for a static measurement. These masses must be calculated from the known balance dimensions and the material (usually steel) density. They represent the partial balance masses between consecutive gages (represented by springs in Figs. 3 through 6). The locations of the centers of gravity (c.g.) of these masses (ℓ_{C1} , ℓ_{C2} , and ℓ_{C3}) must also be calculated from the known balance dimensions. Although these calculations could be subject to slight error because of the neglect of the strain gage mass, connecting wire mass, and possible error in the material density assumed, a close estimate of the masses used in the equations of motion

would provide a more correct result than would complete neglect of the masses.

The equations of motion given in Tables 1, 2, and 3 also include some tare damping constants, as well as some aerodynamic damping and restoring moment constants. The tare damping constants, which are discussed in Appendix C represent the mechanical damping inherent in the gage elements themselves. The aerodynamic "constants" such as $k_{\theta_{aero}}$ and $c_{\theta_{aero}}$ represent the restoring moment (aerodynamic spring constant) and damping moment resulting from aerodynamic effects. They are the same parameters that would be obtained from a standard forced oscillation pitch, yaw, or roll test, the direct damping derivatives. If a balance could be perfectly rigid and still measure the required cross or cross-coupling moments, the inclusion of these aerodynamic terms would not be necessary. However, when a cross or cross-coupling moment is applied to a flexible balance, a motion results, and the damping and restoring moment of the air surrounding the balance (model) is a result of the balance motion and is not part of the cross or cross-coupling moment being measured. The aerodynamic restoring moment and damping moment are represented schematically by a spring and a damper attached to ground (inertial reference frame), as illustrated in Figs. 3 through 6 and Fig. 8.

The magnitude of the aerodynamic restoring moment is very small relative to other spring constants in the equations, and generally can be neglected. However, the aerodynamic damping moment can possibly be of the same magnitude or greater in magnitude than the cross or cross-coupling damping moment itself, and, if possible, it should be included in the data reduction. If it were not included in the reduction, the phase of the data signal from the balance could be misconstrued as being the phase of the cross or cross-coupling moment when, in reality, it is a phase shift caused by aerodynamic damping. In most cases if a test is being run to determine cross or cross-coupling derivatives, some knowledge of the direct damping derivatives will be available. If these direct derivatives are not known, then an analysis of the error that could result from their exclusion should be conducted before proceeding with the test. An example of the error that can result from neglecting $c_{\theta_{aero}}$ is given in Appendix D.

The roll equation of motion is somewhat simpler than the pitch or yaw equations because all of the balance masses and the model mass rotate about the same axis, the balance x axis. The system is merely a series of masses connected by a series of springs. If the moments of inertia of the intermediate balance masses are neglected, the problem reduces to a single degree-of-freedom system with a single natural frequency determined by the model mass and the total spring constant. Naturally, the total spring constant is the resultant of the series of springs represented by the three balance gages plus the C.F. balance spring. Each of these

four entities has its own spring constant in roll as well as pitch and yaw. However, only one of the gages is actually gaged to measure roll deflection, the roll gage of the C.C. balance. Through suitable substitutions, the complete equation of roll motion [Eq. (1)] given in Table 3 can be reduced to a much simpler equation [Eq. (2)] which involves the ratio of the oscillation frequency to the natural frequency of the total system in roll and the standard moment measurement from the balance.

4.0 EQUATIONS OF MOTION WITH STING BENDING MOTION INCLUDED

The equations discussed in the previous section are limited in application to cases where the balance mount is either fixed in an inertial reference frame or the balance mount is rotating about a center of rotation which is fixed in an inertial frame. In reality the sting to which the balances are mounted is not a good basis for an inertial reference frame, for the sting itself is oscillating. If it is assumed that the hub to which the sting is mounted is fairly rigid, then accounting for the sting motion between the hub and the balance will account for the total motion of the balance sections relative to an inertial frame.

As was done by Burt in Ref. 3, the sting motion was considered to be a combination of a pure rotation about the balance center of rotation (θ_s) and a pure translation of the center of rotation (z_s). Including these motions in the previous models (Figs. 3 through 6) results in the models shown in Figs. 9 and 10. The equations of motion describing these systems are given in Tables 4 and 5. These equations are similar to the previous equations of Tables 1 and 2 except they include sting translation (z_s) and rotation (θ_s) terms. The sting must be instrumented and calibrated in a manner similar to the balance gages to provide outputs proportional to the sting deflections. However, all stings that are currently used for dynamic forced oscillation testing are already instrumented and calibrated for sting deflections, so this particular requirement is not new or unusual to AEDC testing.

The equations without sting bending, Tables 1 and 2, are actually a special case of Tables 4 and 5. If the sting degrees of freedom, z_s , and θ_s , are set to zero, the equations of Tables 1 and 2 result. It must be remembered that the force or moment vector on the right-hand side of any of these equations represents the total load measured. When wind tunnel data are reduced with these equations, the total load is the aerodynamic load plus any mechanical damping or inertial tares experienced by the balance. These tares must be measured in the laboratory and subtracted from the total load to yield the aerodynamic load, as discussed in Sec. 2.1.

5.0 DATA REDUCTION

As discussed earlier in Sec. 3.0, knowing that the C.F. balance motion (θ_j) is sinusoidal and assuming a linear dependence between the balance motion and the resulting aerodynamic forces on the C.C. balance (model), the resulting balance outputs are sinusoidal, i.e., they are vector quantities with phase as well as magnitude. The time-dependent gage outputs, which reflect gage deflections, can be represented as follows:

$$\theta_j = \bar{\Theta}_j e^{i\omega t} \quad z_j = \bar{Z}_j e^{i\omega t}$$

The amplitudes of the motions ($\bar{\Theta}_j$ and \bar{Z}_j) have both phase and magnitude and can be represented as

$$\bar{\Theta}_j = \Theta_j e^{i\gamma_j} \quad \bar{Z}_j = Z_j e^{i\gamma_j}$$

These complex or vector amplitudes are the experimentally determined quantities which must be input into the equations of motion given in Tables 1 through 5. With the current AEDC data acquisition and processing technique used for acquisition of dynamic forced oscillation data, these quantities can be routinely acquired for use in the equations of motion.

5.1 PITCH/YAW DATA REDUCTION

When all of the mass constants, moment of inertia constants, length constants, spring constants, and damping constants are evaluated and input into one of the equations of motion, and after the oscillation frequency (ω) for a particular test case is measured and input, the equations reduce to the following form.

$$\begin{array}{ccccc} \sum R_j \bar{\Theta}_j & + & \sum i P_j \bar{\Theta}_j & = & \bar{M} \\ \text{(and/or } R_j \bar{Z}_j) & & \text{(and/or } i P_j \bar{Z}_j) & & \text{(or } \bar{F}) \end{array} \quad (2)$$

In this equation R_j and P_j are mass or inertia constants and \bar{M} (or \bar{F}) is the externally applied load vector measured by the balance. Combining terms and writing the equation in complex form, the above equation reduces to the following:

$$a + bi = \bar{M} \text{ (or } \bar{F}) \quad (3)$$

where

$$\bar{M} \text{ (or } \bar{F}) = M e^{i\gamma} \text{ (or } F e^{i\gamma})$$

The magnitude and phase of the measured moment or force vector is defined in the usual manner, i.e.,

$$M = \sqrt{a^2 + b^2}$$

$$\gamma = \tan^{-1} b/a$$

where a is the real and b the imaginary component of the complex number. These quantities are the magnitude and phase of the aerodynamic or other externally applied load which is applied to the particular gage in question. If the data are to be presented in an "in-phase-with-position" and an "out-of-phase-with-position" format, then these quantities are identically a and b , respectively.

In most cases the moments or forces measured at a particular gage location are not the result that is sought. Instead the balance measurements must be converted into a force and a moment about a selected reference point. For a moment balance and a force-moment balance the equations which convert the data into a force and moment about a selected reference point are as follows:

Moment Balance

$$\overline{F} = \frac{\overline{M}_1 - \overline{M}_3}{\ell} \frac{(a_1 - a_3) + i(b_1 - b_3)}{\ell} = (a + ib)_{\text{force}} \quad (4)$$

where

$$\begin{aligned} \overline{M}_1 &= \text{moment measured at forward balance station} \\ &= a_1 + i b_1 \end{aligned}$$

$$\begin{aligned} \overline{M}_3 &= \text{moment measured at rear balance station} \\ &= a_3 + i b_3 \end{aligned}$$

$$\ell = \text{absolute distance between balance gage stations}$$

and

$$\overline{F} = \text{calculated force vector.}$$

$$\overline{M}_{\text{REF}} = \overline{M}_1 + \overline{F}(x_1 - x_{\text{REF}}) = (a + ib)_{\text{MOMENT AT } x_{\text{REF}}} \quad (5)$$

where

\overline{M}_{REF} = moment referenced to reference point x_{REF}

$x_1 - x_{REF}$ = distance from the forward balance gage center to the model reference point using the sign conventions illustrated in Figs. 1 and 2.

Force-Moment Balance (Yaw Plane)

$$\begin{aligned}\overline{F}_1 &= a_1 + ib_1 & \overline{M}_3 &= a_3 + ib_3 \\ \overline{M}_{REF} &= \overline{M}_3 + \overline{F}_1(x_{\text{moment gage}} - x_{REF})\end{aligned}\quad (6)$$

where

$$\begin{aligned}\overline{F}_1 &= \text{measured force vector, } a_1 + i b_1 \\ \overline{M}_3 &= \text{measured moment vector, } a_3 + i b_3 \\ \overline{M}_{REF} &= \text{moment about reference point } x_{REF}\end{aligned}$$

and

$$x_{\text{moment gage}} - x_{REF} = \text{distance from moment gage center to reference point } x_{REF} \text{ measured positive toward the front.}$$

The pitch plane equations are similar to those presented earlier except that subscripts of the force (\overline{F}) and moment (\overline{M}) are swapped because of the position reversal of the corresponding gages in the pitch plane.

Knowledge of the magnitude and phase of both the force vector and the moment vector enables the calculation of the required derivatives. However, it must be kept in mind that the phases of the force and moment must be known relative to the total model motion, and total model motion is represented by the total rotational vector and the total translational vector, which will be called Θ_T and \bar{Z}_T for pitch plane motion. If the phase angles of the pitch plane force and moment vectors relative to Θ_T are given by γ_{TF} and γ_{TM} , then the required pitch plane damping and restoring moment derivatives are calculated as follows:

$$\begin{aligned}M_{\Theta} &= \frac{M \cos \gamma_{TM}}{\Theta_T} & M_{\dot{\Theta}} &= \frac{M \sin \gamma_{TM}}{\omega \Theta_T} \\ F_{\Theta} &= \frac{F \cos \gamma_{TF}}{\Theta_T} & F_{\dot{\Theta}} &= \frac{F \sin \gamma_{TF}}{\omega \Theta_T}\end{aligned}$$

Similar calculations are required for the yaw plane.

5.2 ROLL DATA REDUCTION

The roll data reduction equation reduces to a simple form [Eq. (2) of Table 3] which uses the standard rolling moment measurement from the balance rather than the angular deflection measurements as inputs to the equation. The equation includes several constants which must be determined experimentally, i.e., $\omega_{n_{total}}$, c_2/k_2 , and k_{total} . The remaining constant $c_{\phi_{aero}}$ is the aerodynamic roll damping constant which either must be known from the results of a previous direct derivative wind tunnel investigation, must be estimated in some manner, or must be assumed zero. The effect that $c_{\phi_{aero}}$ has on the data reduction cannot be stated in one general rule. Its relative importance depends on the phase angle of the data signal which is configuration and attitude dependent. The effect of assuming this constant to be zero is illustrated in Appendix D for a specific case.

The term k_{total} is the total spring constant of the two-balance system in roll, assuming that all of the flexible balance sections have a degree of freedom in roll, including the C.F. balance, and that these separate sections are connected in series to form a total spring constant. The roll inertia of the balance parts connecting these separate sections (springs) is ignored, and the system is assumed to exhibit one natural frequency characteristic of the total spring constant. This assumption has been shown to be accurate from spectral analysis results of both C.C. balances. Each balance exhibits one predominant natural frequency rather than one frequency for each mode of vibration. With the wind tunnel model mounted, this natural frequency is the $\omega_{n_{total}}$ mentioned earlier, and this constant may change for each model configuration for which data are taken and reduced. On the other hand the k_{total} constant will likely never change for a particular balance throughout a test program unless the balance is somehow changed. The constant c_2/k_2 is the ratio of the mechanical damping of the roll section of the balance to the spring constant of that section. The determination of this constant is discussed in Appendix C.

As with the previous pitch and yaw data, the moment signal ($k_2 \overline{\Phi_2}$) from the balance is a vector quantity and has magnitude and phase relative to the model position vector. Since the quantity in brackets [Eq. (2), Table 3] is also a vector or complex quantity, the equation takes the following form after all of the constants and the data vector are input.

$$[M'_x e^{i\gamma'}][1/\mu e^{i\Delta\gamma}] = M_x e^{i\gamma} \quad (7)$$

The equation in this form illustrates the "demagnification" and phase shifting effected by the bracketed term of Eq. (2), Table 3. The magnitude of the rolling moment signal (M'_x) is

decreased by the multiplicative constant $1/\mu$, and the phase is shifted by the phase of the bracketed vector, $\Delta\gamma$. Close examination of the bracketed term in Eq. (2), Table 3 reveals that the frequency ratio ($\omega/\omega_{n_{total}}$) is the primary influence on the multiplicative constant $1/\mu$ and that the damping constants are the primary influence on phase shift. These effects are illustrated in Appendix D.

6.0 CORRECTION OF EXISTING CROSS-COUPLING ROLL DATA

To confirm that the roll data reduction equation was indeed serving to produce a correct moment reading from the flexible C.C. balance, some previously obtained laboratory data were reduced using Eq. (2) of Table 3. The rolling moment laboratory data were induced by oscillating a dynamically unbalanced ($I_{xy} \neq 0$) calibration body in pitch. The applied rolling moment was calculated from the known I_{xy} and the oscillation frequency and amplitude. Data were taken for several values of the oscillation to total natural frequency ratio by changing the moment of inertia (I_x) of the calibration body. The rolling moment balance output was reduced in two ways: by simply applying the statically obtained roll gage sensitivity to the roll gage signal, and by using the roll equation as given in Table 3. The constant c_2/k_2 was too small to be resolved and was assumed to be zero. A plot of the results is shown in Fig. 11 where the measured to applied load ratio is plotted as the ordinate and the frequency ratio is plotted as the abscissa. The roll equation of motion of Table 3 clearly corrects the data for the majority of the dynamic effects.

To illustrate the application of the roll data reduction equation to some wind tunnel data, and to illustrate the magnitude of corrections to such data, the results from two past tests were corrected using a form of Eq. (2) of Table 3. The first source of such data was the wind tunnel tests conducted on a model of a current fighter configuration in June 1978. The uncorrected data, which were originally reduced using static calibration sensitivities, are illustrated in Ref. 4. These data were obtained with a 4,000-lb dual-balance system similar to the 1,500-lb force-moment system discussed herein. Tests of a standard dynamics model (SDM) run in December 1980 were the second source of data. These data were obtained using the 1,500-lb force-moment C.C. balance illustrated in Fig. 1.

Using the system natural frequency and the system damping factor obtained by Buchanan in Ref. 4, the roll data reduction equation was first applied to the cross-coupling roll data assuming $c_{\phi_{aero}}$ to be zero. The corrected and uncorrected data are illustrated in Fig. 12. The correction equation used was

$$\overline{M}_x = 0.868 e^{i0.033} \overline{M}_x' \quad (8)$$

The largest absolute correction was obviously made to the data of the highest magnitude. In this case the magnification effect resulting from balance dynamics was the overwhelming correction influence. On the other hand, the low magnitude data actually had a larger percentage correction in many cases attributable to the gage mechanical damping phase shift effects. In one case where $C_{\ell_q} + C_{\ell_\alpha}$ was near zero, the correction even caused a sign reversal from the original data. However, these magnitudes are too low to be of practical interest to a user of the data.

Since the direct roll damping data were also available from this test program, the same data were reduced, including the effects of the aerodynamic damping ($c_{\phi_{aero}}$) on the data. The correction equation including the effects of $c_{\phi_{aero}}$ is

$$\overline{M}_x = 0.869 e^{i0.053} \overline{M}_x' \quad (9)$$

These data have not been plotted since the added aerodynamic damping effect produced no noticeable change in the corrected data.

The effects of the correction of the SDM data are illustrated in Fig. 13. Because of the low moment of inertia (I_x) of the SDM model, the ratio of the oscillation to total natural frequency was relatively low and, consequently, the correction was fairly small. The equation used to correct these data was

$$\overline{M}_x = 0.971 e^{i0.001} \overline{M}_x' \quad (10)$$

This correction equation includes the effect of aerodynamic damping, which was known from direct derivative tests of the same model.

The correction equations for the fighter data and the SDM data indicate minimum corrections of 13 and 3 percent, respectively. In these cases no extremely large corrections occurred because the phase angle of the balance signal was not near a multiple of 90 deg. Had this occurred in conjunction with the phase correction required for the fighter data, large corrections in the data could have occurred. In fact, this did occur on several of the data points, but the magnitude of the coefficients in these cases was small enough to render the moments themselves, let alone the correction, unimportant. Since the phase of the cross or cross-coupling rolling moment is configuration and attitude sensitive, it is almost impossible to predict from one model to another whether the corrections will be significant.

7.0 CONCLUSIONS

The equations of motion for the two C.C. balances used at AEDC have been derived and presented for use in future cross and cross-coupling data reduction procedures. These equations enable statically obtained balance gage sensitivities to be used in the reduction of dynamic loads. Although all balance motions must be measured and accounted for in order to define an external load exactly, only the primary motions have been included in these derivations. These include the motions for which the balances are gaged, the lateral rotation of the balance roll gage element, and two degrees of freedom of sting motion. The primary deflections of the balance, i.e., the motions for which the balance is gaged, have been measured under load, and have been shown to be the most significant deflections of the balance. On the other hand, the lateral rotational motion of the roll gage, which was also included in the equations of motion, proved to be insignificant.

Selected cross-coupling roll data previously obtained in the laboratory, as well as some selected wind tunnel roll data, were corrected using the dynamic equations. The effects of corrections afforded by the dynamic equation, the effects of ignoring aerodynamic damping in the measurement of cross and cross-coupling derivatives, and the results of the balance deflection measurements are summarized in the following concluding remarks:

1. The primary deflections undergone by the two subject balances are indeed the deflections for which the balances are gaged.
 - a. The lateral rotational deflections of the roll gage elements are small if at all measurable and can be excluded from the equations of motion.
 - b. The rotational (bending) deflection of a gage element primarily designed for translational (shear) deflection is measureable. The definition of the externally applied dynamic loads would be more exact by including measurements of these deflections, although the effect on accuracy would be small.
2. The use of the dynamic equations of motion in correcting cross-coupling roll data has shown varied effects on dynamic moment calculation.
 - a. The roll equation, for which the correction magnitude varies inversely with the natural frequency of the dual-balance system in roll ($\omega_{n_{total}}$), corrected the laboratory roll data to within two percent of the applied cross-coupling load.

- b. Application of the dynamic roll equation to data from a modern fighter aircraft resulted in significant correction (13 percent) to the higher magnitude data.
 - c. Application of the dynamic roll equation to data from the Standard Dynamics Model taken with the subject force-moment balance system resulted in relatively small corrections (<3 percent).
 - d. It is unlikely that a general rule regarding the significance of the correction to dynamic data from varied models will be established, since the magnitude of the correction depends on the phase of the cross-coupling moment signal, which is configuration and attitude dependent.
3. Neglecting aerodynamic damping in the calculation of cross or cross-coupling moments could result in significant percentage errors in the damping moment when measured phase angles are near 0 or 180 deg.

The details of the work which led to these conclusions are presented in Appendixes A through D. The balance deflection mode determinations and the equation of motion derivations which result from mathematically modeling the confirmed deflection modes are presented in Appendixes A and B, respectively. Methods for determining the equation constants are discussed in Appendix C, and the possible effects of neglecting the aerodynamic damping constants when they are not available are discussed in Appendix D.

In the process of providing a systematic development of the equations of motion, several forms of the equations have been presented in Tables 1 through 5. The equations which provide the most accurate reduction of the aerodynamic moments, and which require only those measurements for which the subject AEDC balances are currently instrumented, are the roll equation of Table 3 and the pitch/yaw equations including sting motion of Tables 4 and 5. Inclusion of additional degrees of freedom in the equations of motion is ineffectual unless the measurement of additional balance or support deflections is made possible through additional balance instrumentation.

REFERENCES

1. Hanff, E.S. and Kapoor, K.B. "Measurement of Dynamic Direct and Cross-Coupling Derivatives Due to Oscillatory Roll." *1979 Record*, International Congress on Instrumentation in Aerospace Simulation Facilities, 186, September 1979.
2. Greenwood, Donald T. *Principles of Dynamics*. Prentice-Hall, Inc., Englewood Cliffs, New Jersey, 1965 (First Edition).
3. Burt, Glen E. and Uselton, James C. "Effect of Sting Oscillations on the Measurement of Dynamic Stability Derivatives." *AIAA Journal of Aircraft*, Vol. 13, No. 3, March 1976, pp. 210-216.
4. Buchanan, T. D., Coulter, S. M., and Marquart, E. J. "Evaluation and Wind Tunnel Tests of the 4,000-lb (Normal-Force) Pitch/Yaw and Roll-Damping Stability Balance Systems for Measuring Direct, Cross and Cross-Coupling Derivatives." AEDC-TR-80-12, (AD-A205122), September 1981.

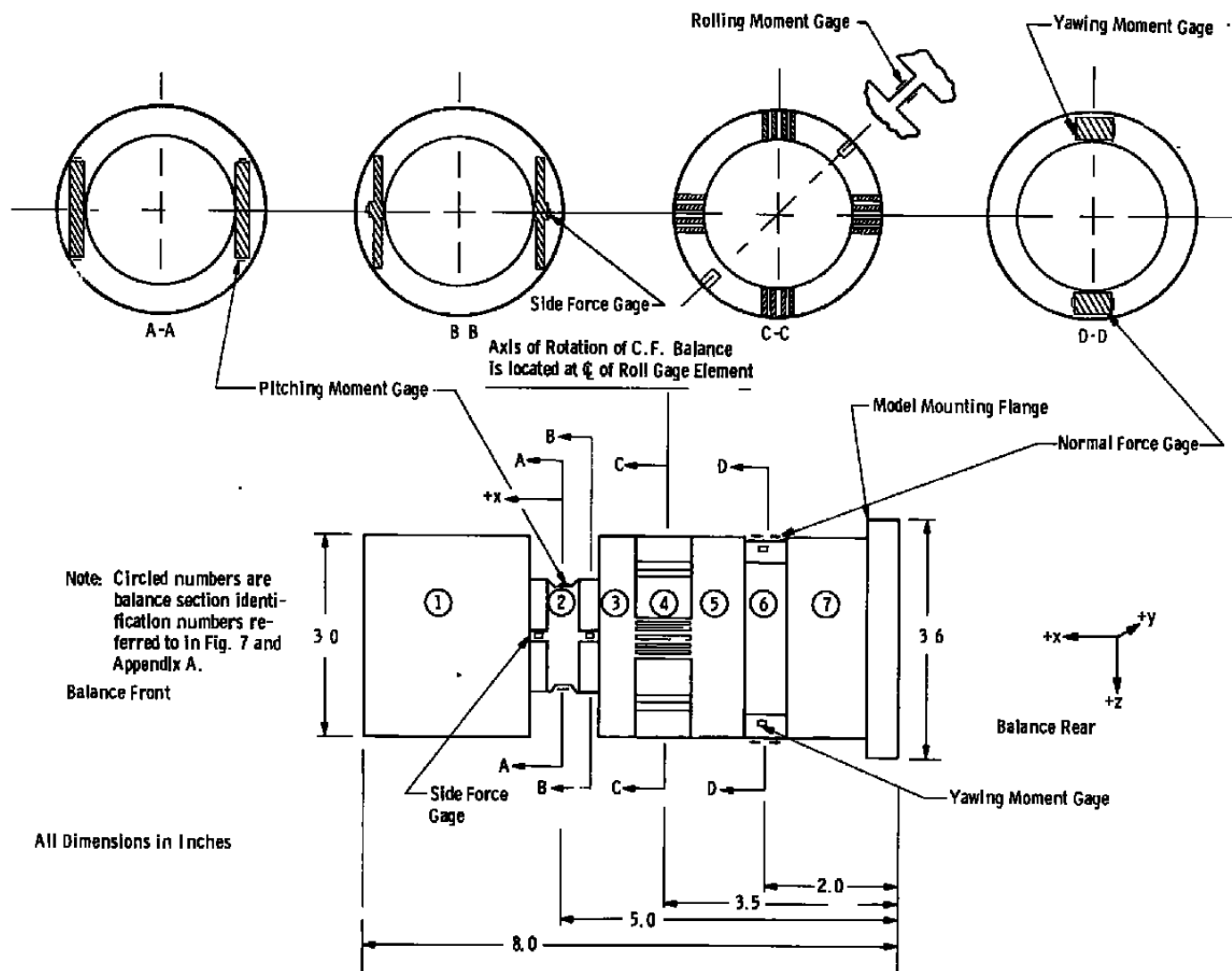
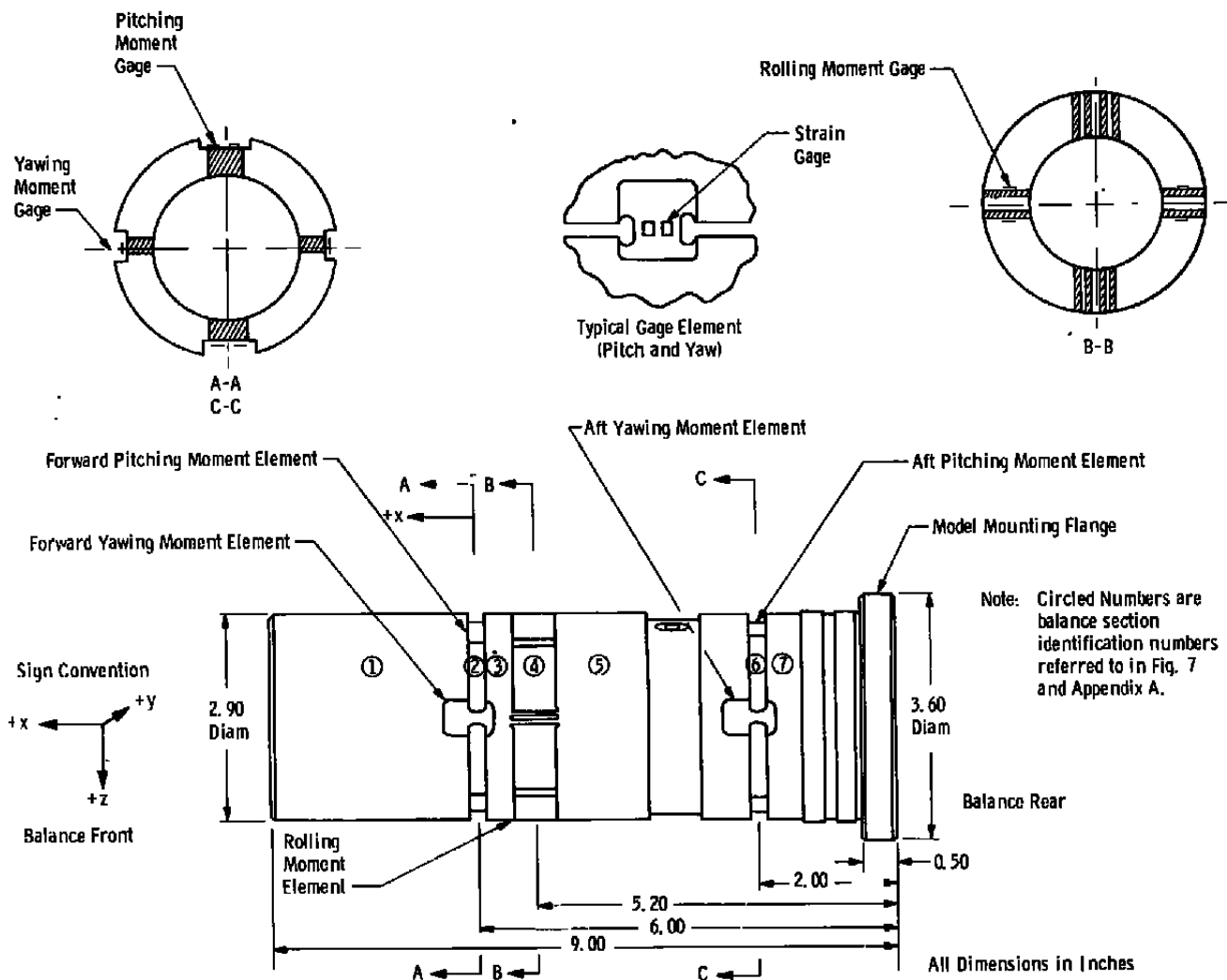


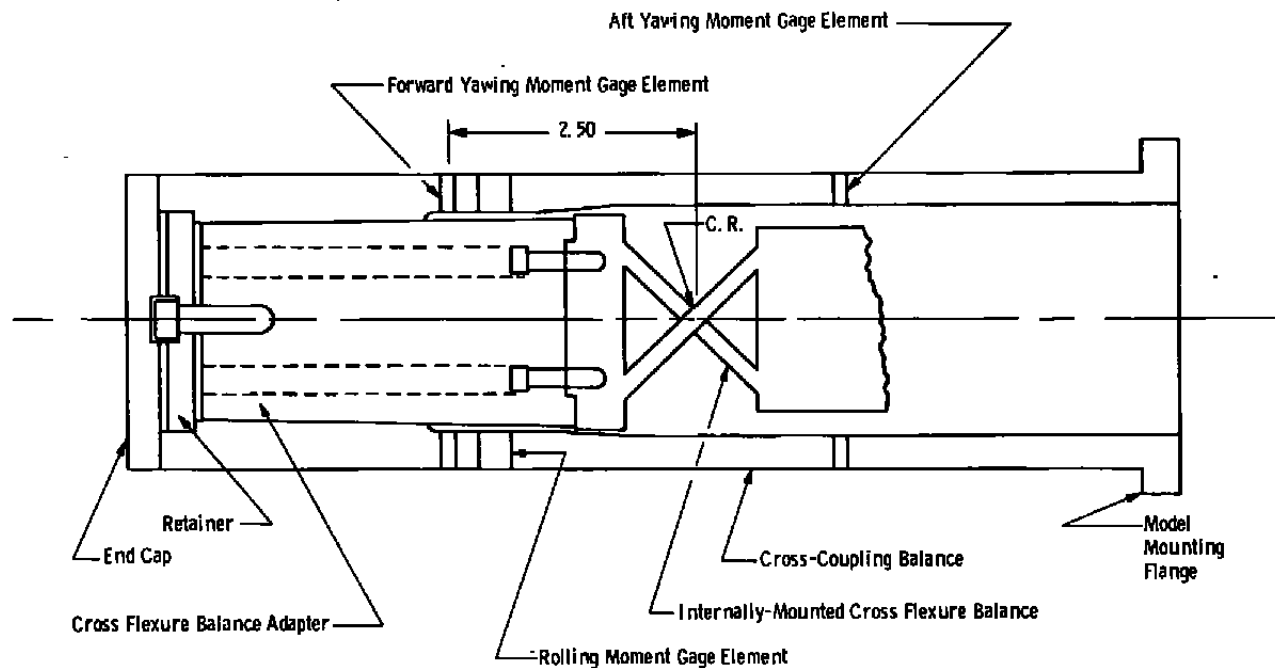
Figure 1. The 1,500-lb force-moment balance used for measurement of cross and cross-coupling derivatives.



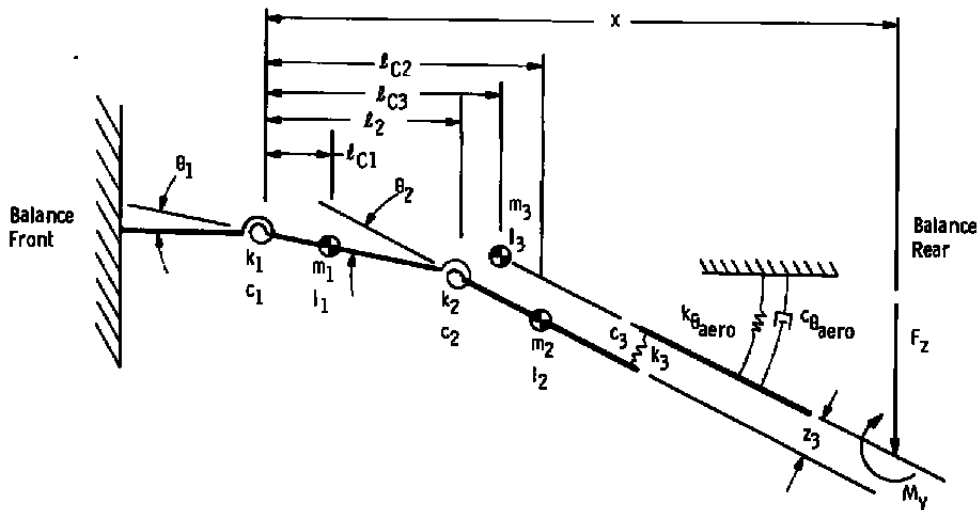
a. Cross-coupling moment balance details

Figure 2. The 1,500-lb moment balance used for measurement of cross and cross-coupling derivatives.

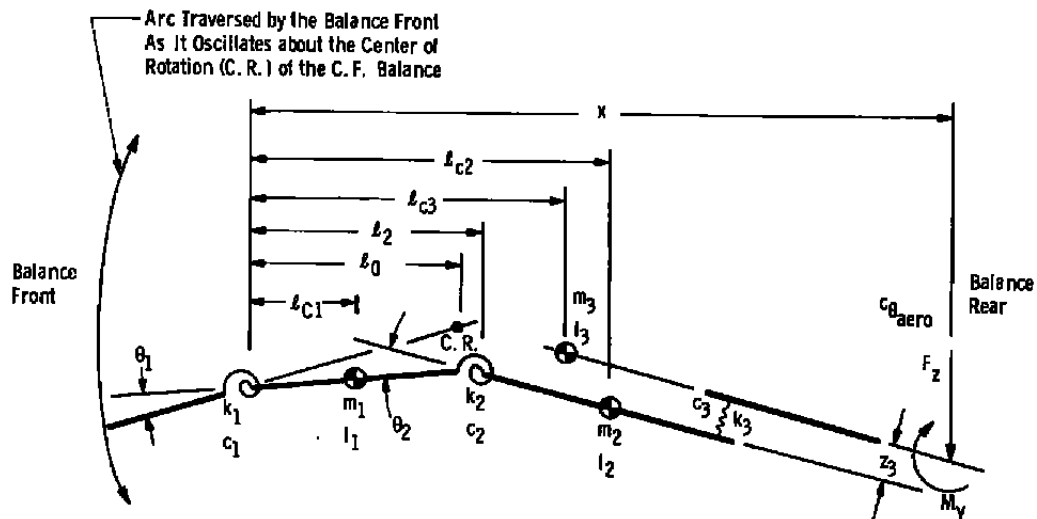
Note: Balances as shown are in the proper mounting orientation for oscillation of a wind tunnel model in yaw. For pitch oscillation the cross flexure balance must be rotated 90 deg relative to the cross-coupling balance. The force-moment balance system permits similar mounting orientations between the cross flexure and the cross-coupling balances.



b. Cutaway view of cross flexure balance mounted internal to the cross-coupling moment balance.
Figure 2. Concluded.



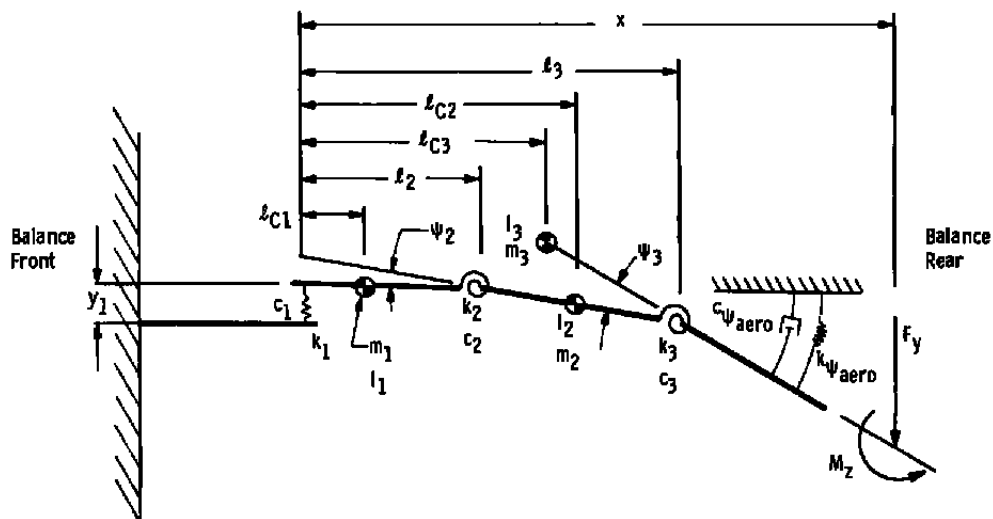
Out-of-plane motion (Balance motion in the pitch plane resulting from the forced oscillation of the balance in the yaw plane with the C. F. balance)



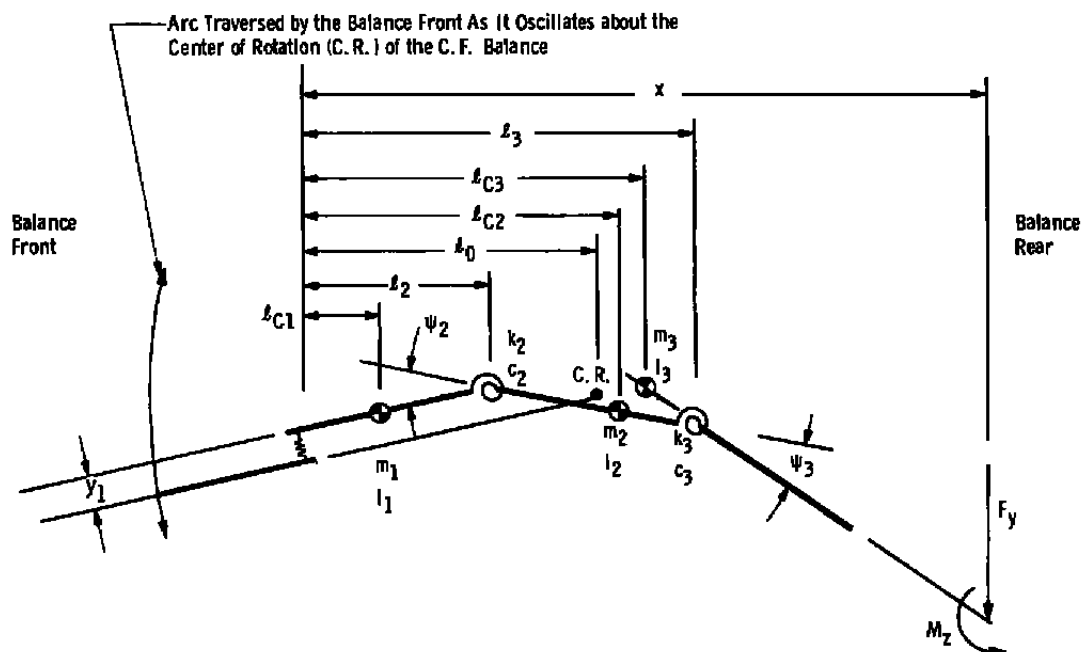
In-Plane Motion (Balance motion in the pitch plane resulting from the forced oscillation of the balance in the pitch plane with the C. F. balance)

a. Pitch plane models (side view of balance)

Figure 3. Three-degree-of-freedom models of the pitch and yaw planes of the force-moment balance.



Out-of-Plane Motion (Balance motion in the yaw plane resulting from the forced oscillation of the balance in the pitch plane with the C. F. balance)

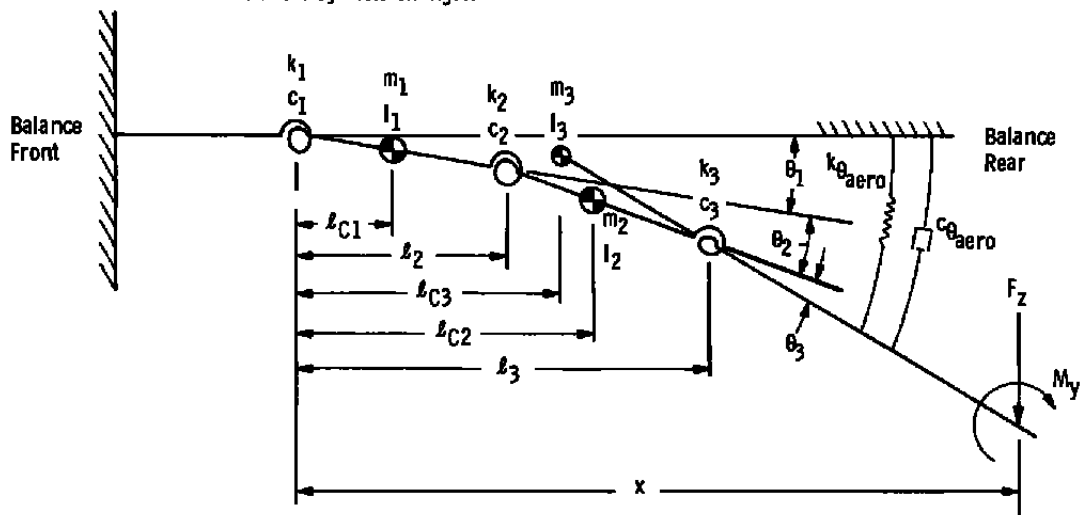


In-Plane Motion (Balance motion in the yaw plane resulting from the forced oscillation of the balance in the yaw plane with the C. F. balance)

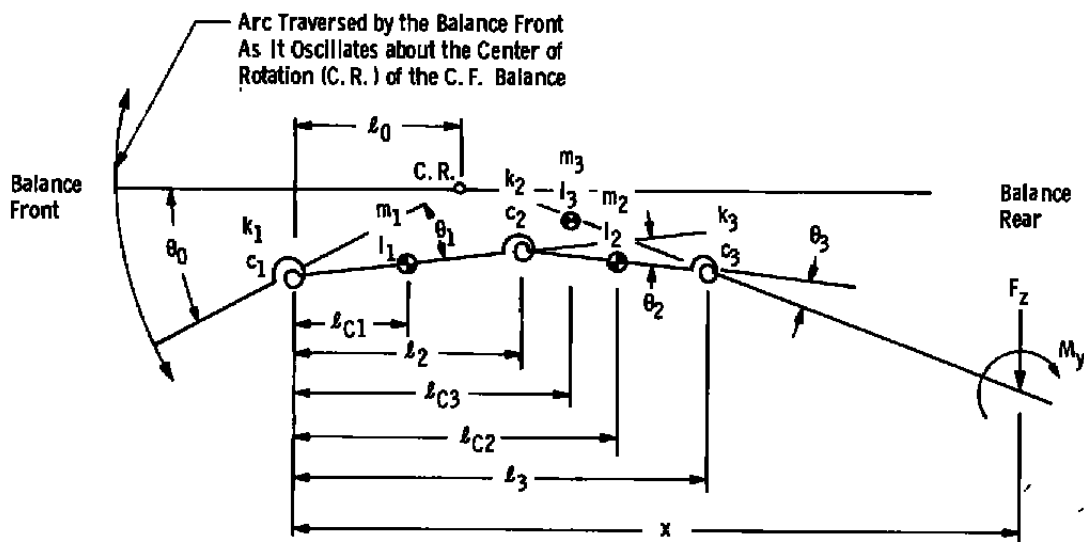
b. Yaw plane models (elevation view of balance)

Figure 3. Concluded.

Note: Models are illustrated with pitch plane nomenclature. Models also apply to the yaw plane with the deflection and load symbols changed.

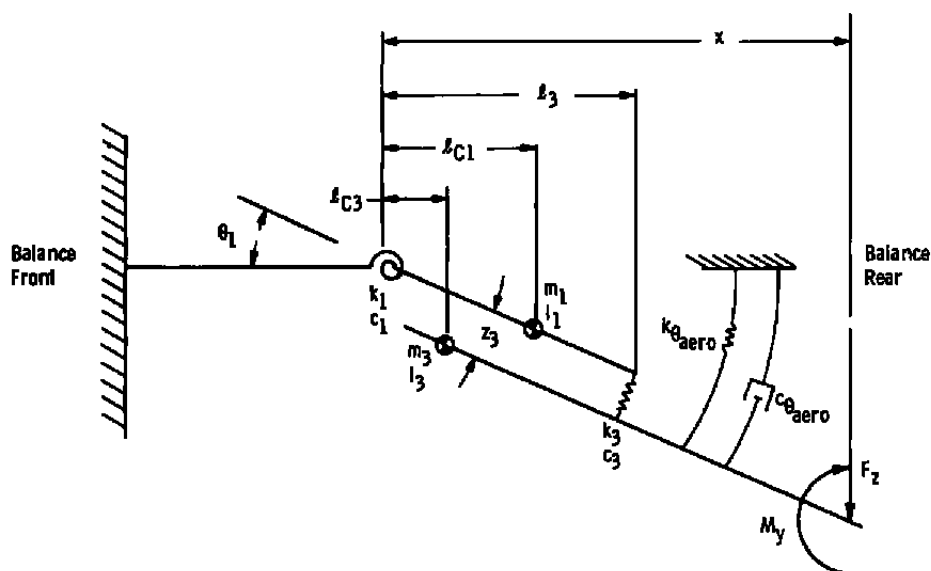


- a. Out-of-plane motion (balance motion in the pitch (or yaw) plane resulting from the forced oscillation of the balance in the yaw (or pitch) plane with the C.F. balance)

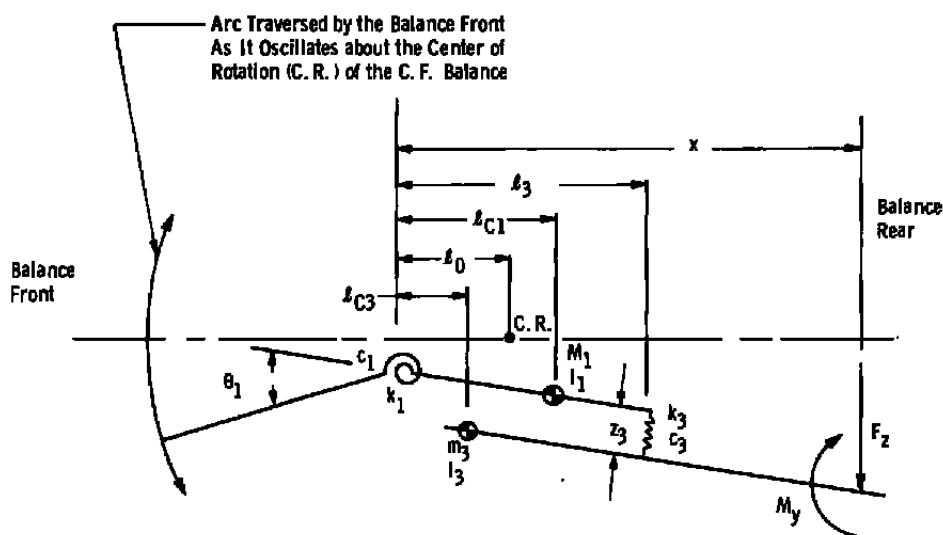


- b. In-plane motion (balance motion in the pitch (or yaw) plane resulting from the forced oscillation of the balance in the pitch (or yaw) plane with the C.F. balance)

Figure 4. Three-degree-of-freedom models of the pitch or yaw plane of the moment balance.



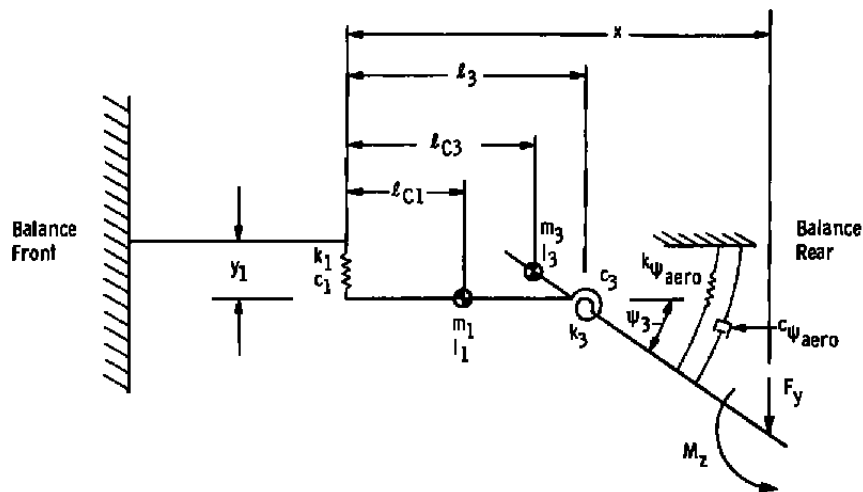
Out-of-Plane Motion (Balance motion in the pitch plane resulting from the forced oscillation of the balance in the yaw plane with the C. F. balance)



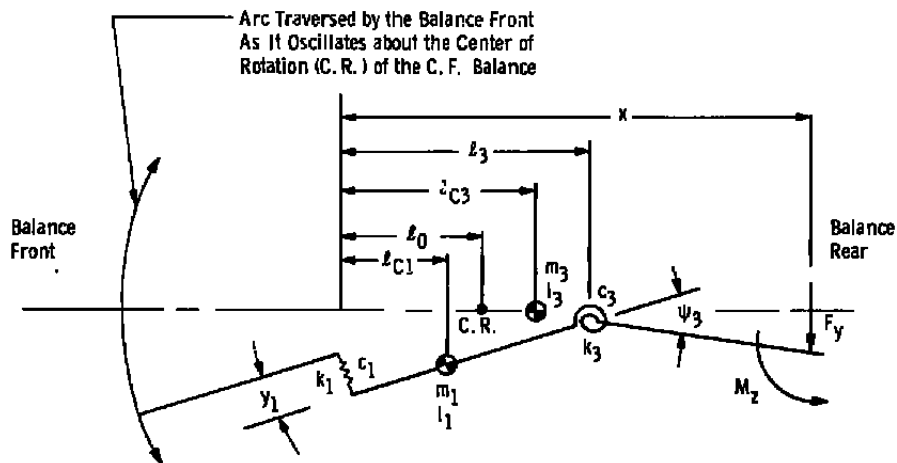
In-Plane Motion (Balance motion in the pitch plane resulting from the forced oscillation of the balance in the yaw plane with the C. E. balance)

a. Pitch plane (side view of balance)

Figure 5. Two-degree-of-freedom models of the pitch and yaw planes of the force-moment balance.



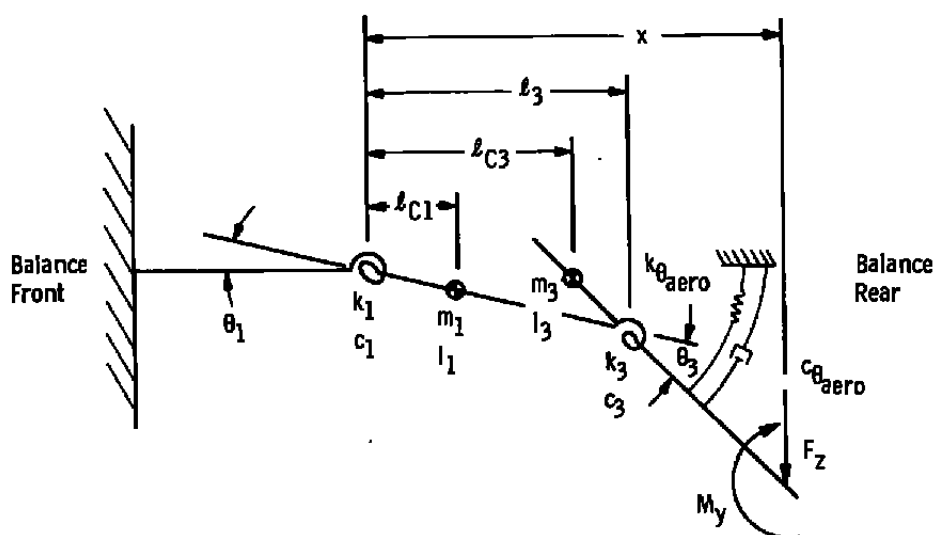
Out-of-Plane Motion (Balance motion in the yaw plane resulting from the forced oscillation of the balance in the pitch plane with the C. F. balance)



In-Plane Motion (Balance motion in the yaw plane resulting from the forced oscillation of the balance in the yaw plane with the C. F. balance)

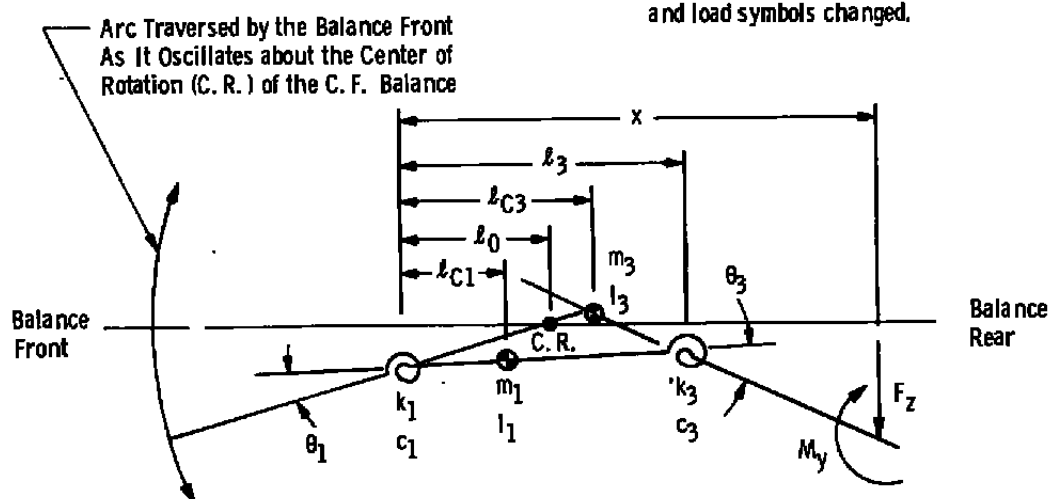
b. Yaw plane models (elevation view of balance)

Figure 5. Concluded.

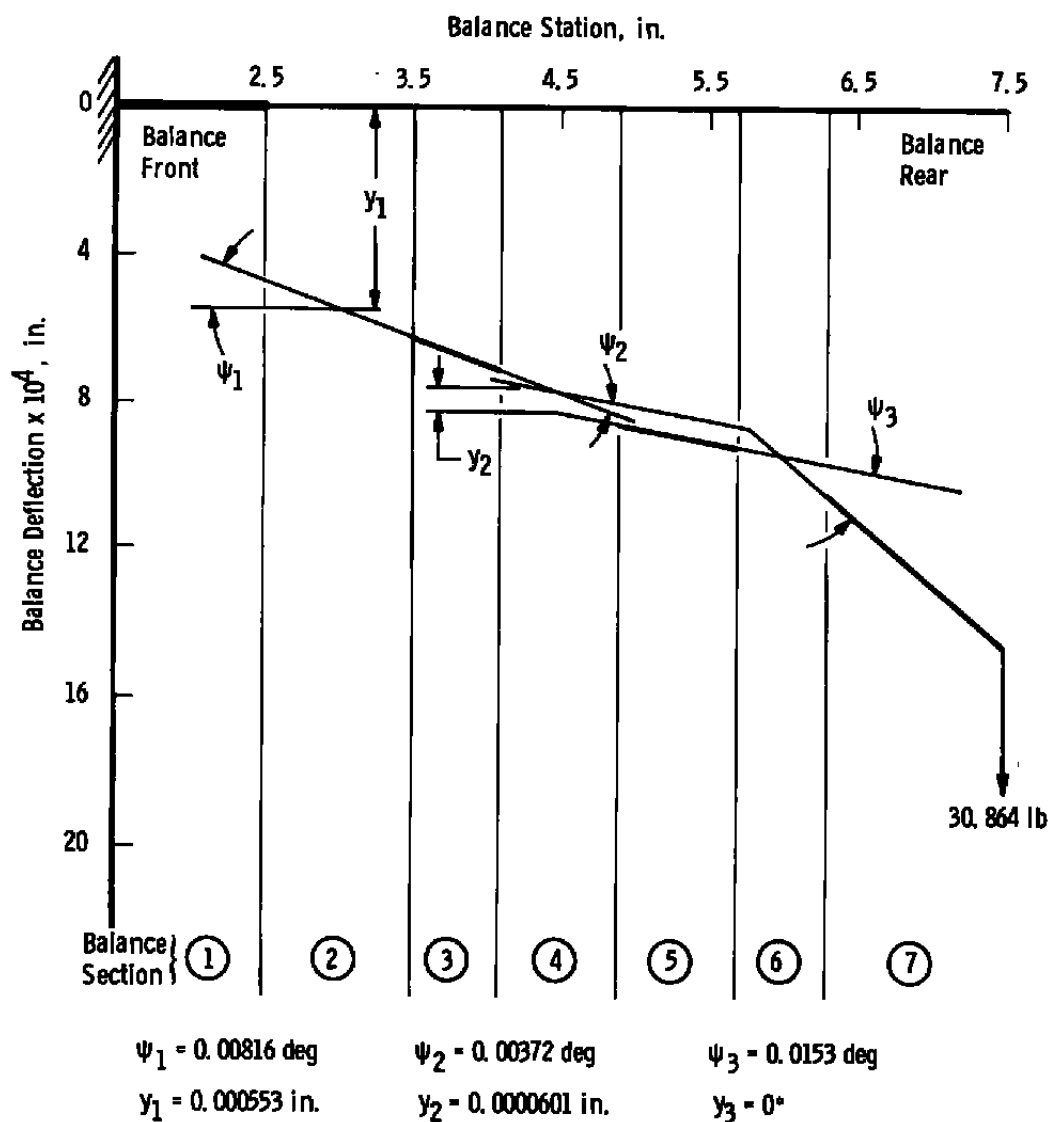


- a. Out-of-plane motion (balance motion in the pitch (or yaw) plane resulting from forced oscillation of the balance in the yaw (or pitch) plane with the C.F. balance)

Note: Models are illustrated with pitch plane nomenclature. Models also apply to the yaw plane with the deflection and load symbols changed.



- b. In-plane motion (balance motion in the pitch (or yaw) plane resulting from the forced oscillation of the balance in the pitch (or yaw) plane with the C.F. balance)
- Figure 6. Two-degree-of-freedom model of the pitch or yaw plane of the moment balance.



* y_3 was assumed to be zero since this measurement was not possible with the measurement technique used.

Balance Section	Load Measured
2	Side Force
4	Rolling Moment
6	Yawing Moment

Note: Balance Sections 1, 3, 5, and 7 are assumed to be rigid.

Figure 7. Yaw plane deflection modes of the force-moment balance.

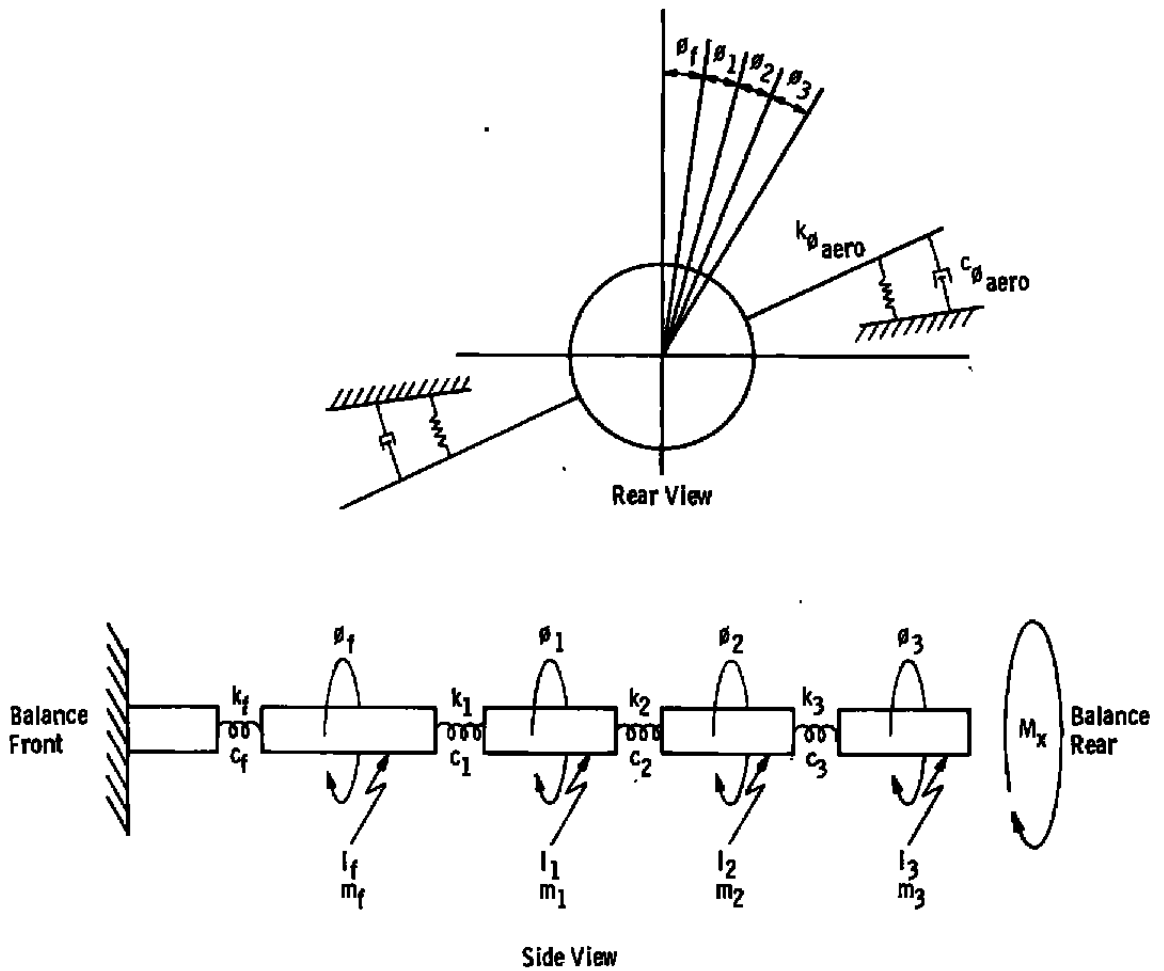
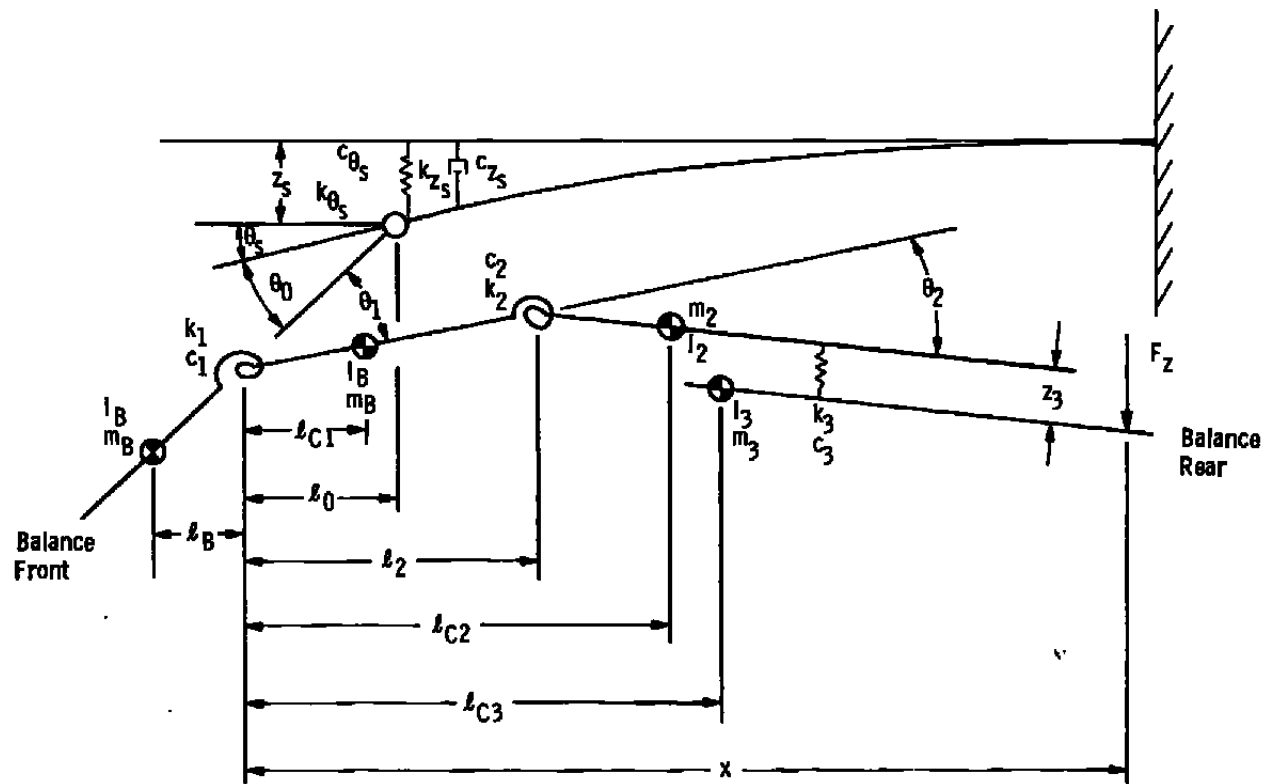


Figure 8. Dynamic model in roll.

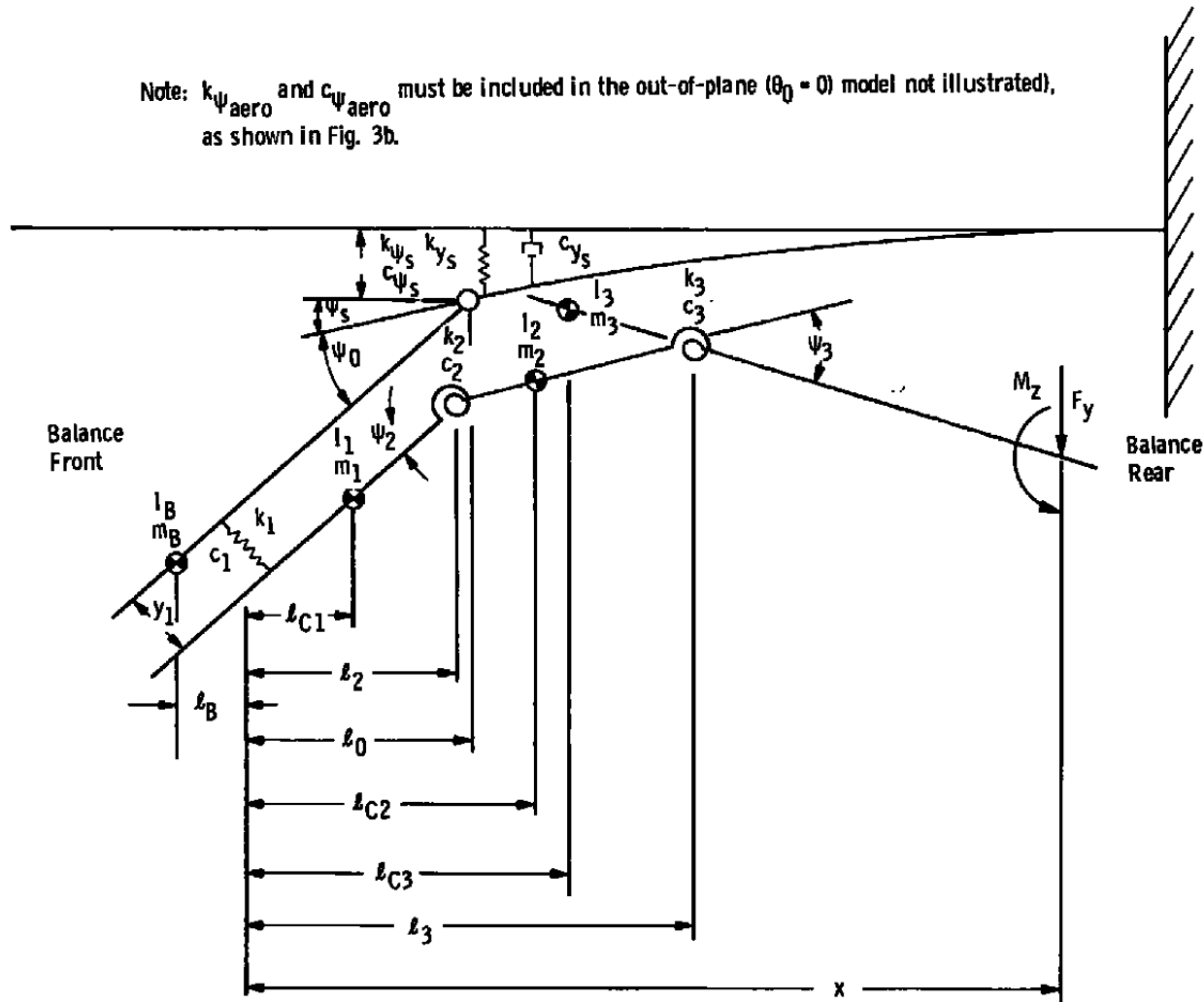


Note: $k_{0\text{aero}}$ and $c_{0\text{aero}}$ must be included in the out-of-plane ($\theta_0 = 0$) model (not illustrated), as shown in Fig. 3a.

a. Pitch plane model of in-plane motion (side view of balance and sting)

Figure 9. Dynamic model of the three-degree-of-freedom force-moment balance system including two degrees of freedom of the supporting sting.

35



AEDC-TR-81-34

- Note: (1) Model is illustrated with pitch plane nomenclature.
 Model also applies to the yaw plane with the deflection and load symbols changed.
- (2) $k_{\theta_{aero}}$ and $c_{\theta_{aero}}$ must be included in the out-of-plane ($\theta_0 = 0$) model (not illustrated), as shown in Fig. 4a.

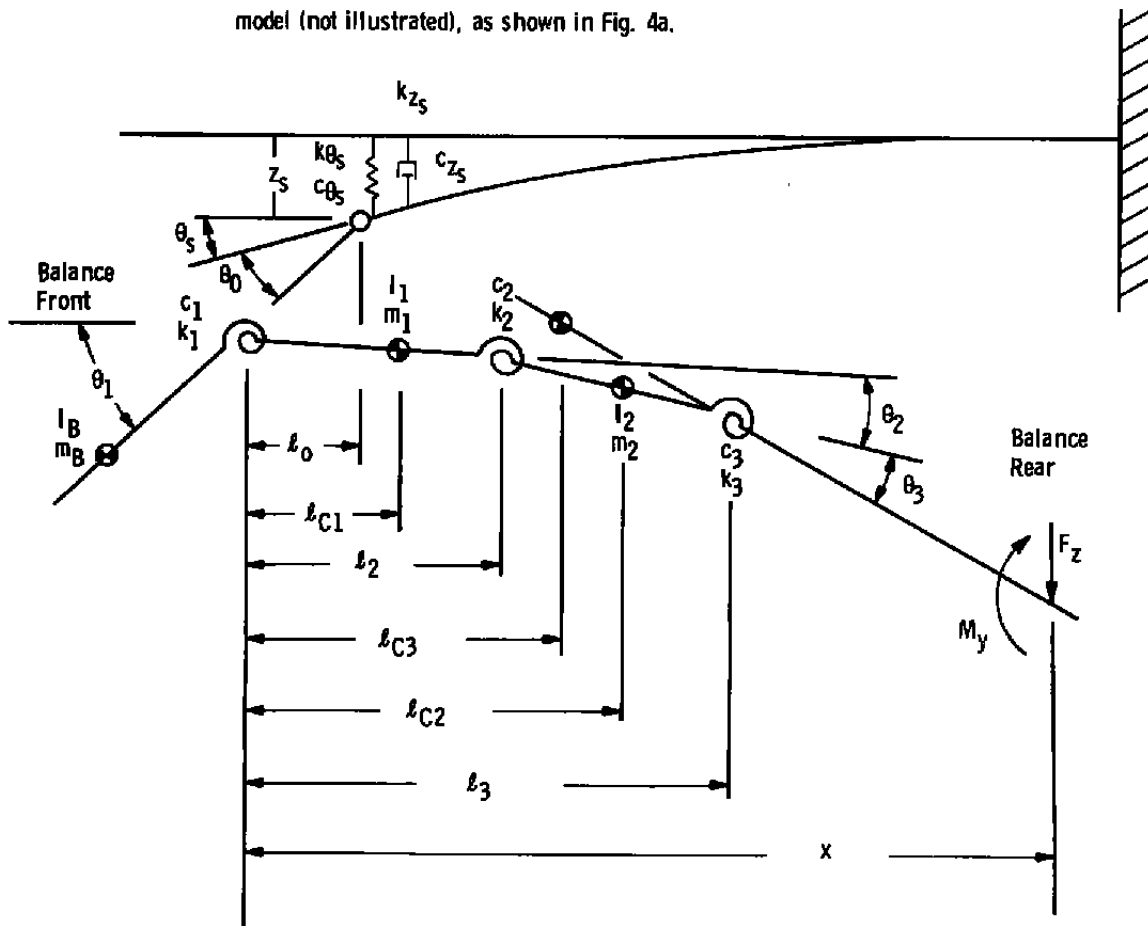


Figure 10. Dynamic model of the three-degree-of-freedom moment balance system including two degrees of freedom of the supporting sting.

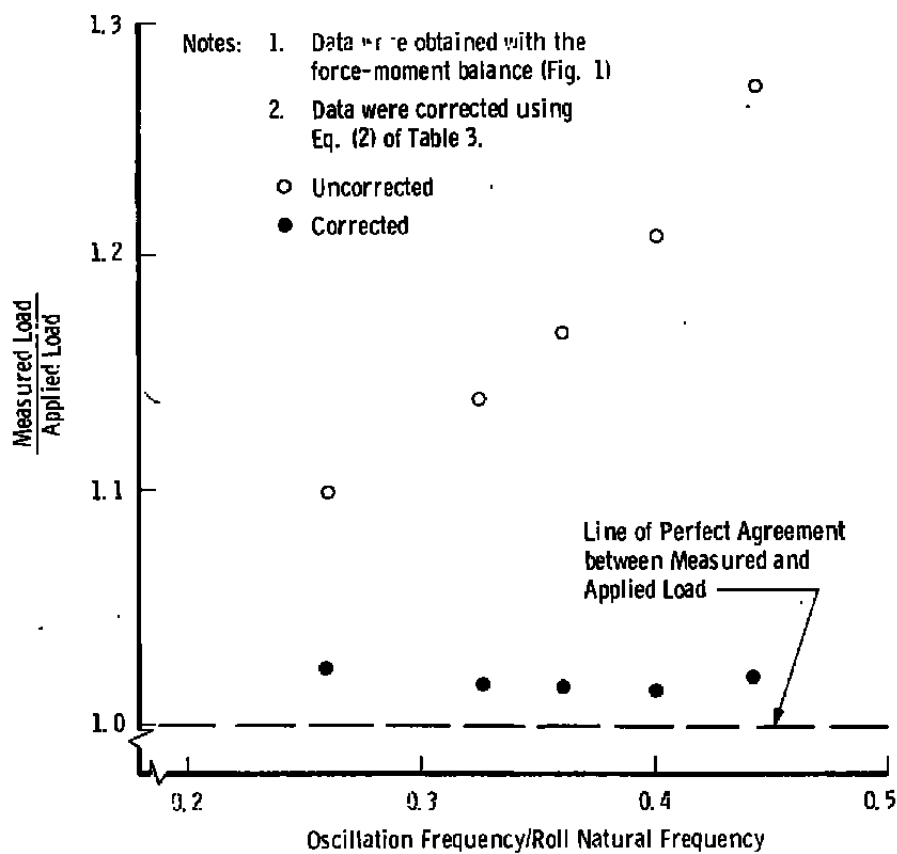


Figure 11. Laboratory roll data corrected using the multi-degree-of-freedom approach.

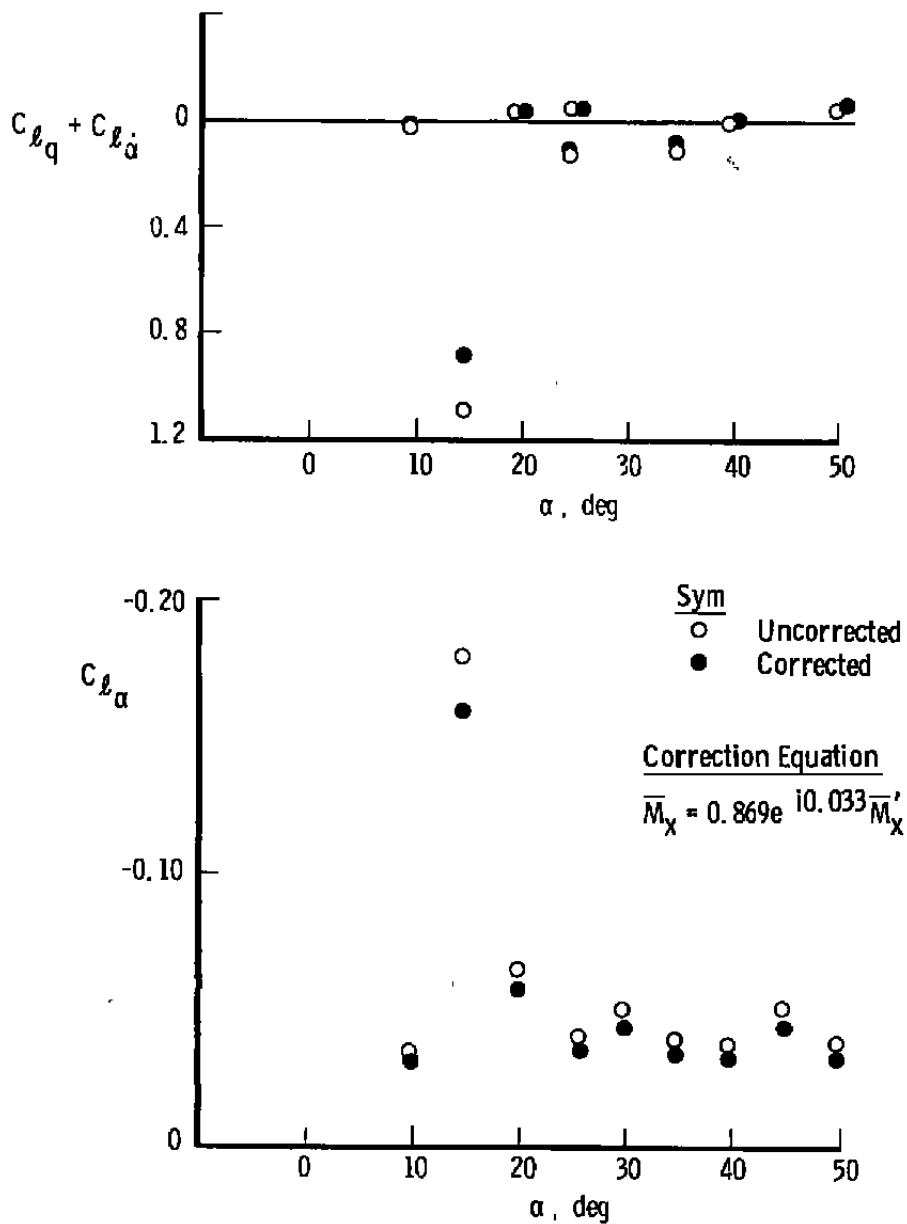


Figure 12. Roll data from a current fighter configuration corrected using the multi-degree-of-freedom approach.

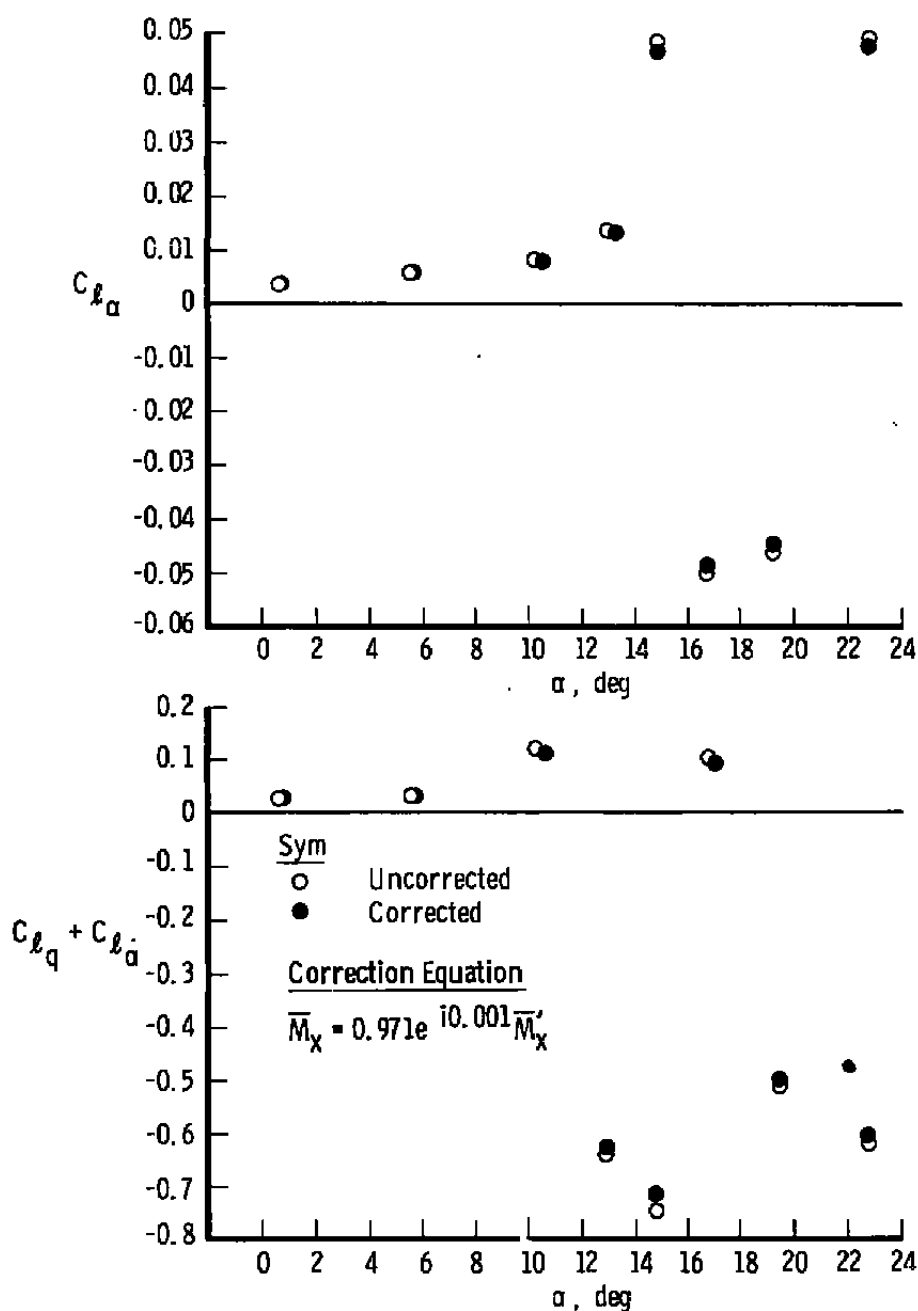


Figure 13. Wind tunnel SDM roll data corrected using the multi-degree-of-freedom approach.

Table 1. Pitch/Yaw Equations of Motion for the Force-Moment Balance
a. Pitch Plane

Out-Of-Plane 2-DOF Motion (Assumes Roll Section Rigid in Pitch and Yaw)

$$\begin{aligned}
 & -\omega^2 \bar{\Theta}_1 [I_1 + I_3 + m_1 \ell_{C1}^2 + m_3 \ell_{C3}^2] + \omega^2 \bar{Z}_3 [m_3 \ell_{C3}] + k_1 \bar{\Theta}_1 + k_{\theta_{aero}} (\bar{\Theta}_1) + c_1 \omega i \bar{\Theta}_1 \\
 & + c_{\theta_{aero}} \omega i \bar{\Theta}_1 = \bar{M}_1 \\
 & \omega^2 \bar{\Theta}_1 [m_3 \ell_{C3}] - \omega^2 \bar{Z}_3 [m_3] + k_3 \bar{Z}_3 + c_3 \omega i \bar{Z}_3 = \bar{F}_Z
 \end{aligned}$$

Out-Of-Plane 3-DOF Motion (Assumes Roll Section Compliant in Pitch and Yaw)

$$\begin{aligned}
 & -\omega^2 \bar{\Theta}_1 [I_1 + I_2 + I_3 + m_1 \ell_{C1}^2 + m_2 \ell_{C2}^2 + m_3 \ell_{C3}^2] - \omega^2 \bar{\Theta}_2 [I_2 + I_3 + m_2 \ell_{C2} (\ell_{C2} - \ell_2) \\
 & + m_3 \ell_{C3} (\ell_{C3} - \ell_2)] + \omega^2 \bar{Z}_3 [m_3 \ell_{C3}] + k_1 \bar{\Theta}_1 + k_{\theta_{aero}} (\bar{\Theta}_1 + \bar{\Theta}_2) + c_1 i \omega \bar{\Theta}_1 + c_{\theta_{aero}} i \omega \\
 & (\bar{\Theta}_1 + \bar{\Theta}_2) = \bar{M}_1 \\
 & \omega^2 \bar{\Theta}_1 [m_3 \ell_{C3}] + \omega^2 \bar{\Theta}_2 [m_3 (\ell_{C3} - \ell_2)] - \omega^2 \bar{Z}_3 [m_3] + k_3 \bar{Z}_3 + c_3 \omega i \bar{Z}_3 = \bar{F}_Z
 \end{aligned}$$

In-Plane 2-DOF Motion (Assumes Roll Section Rigid in Pitch and Yaw)

$$\begin{aligned}
 & -\omega^2 \bar{\Theta}_1 [I_1 + I_3 + m_1 \ell_{C1}^2 + m_3 \ell_{C3}^2] + \omega^2 \bar{Z}_3 [m_3 \ell_{C3}] + k_1 \bar{\Theta}_1 + c_1 \omega i \bar{\Theta}_1 - \omega^2 \bar{\Theta}_0 \\
 & [I_1 + I_3 + m_1 \ell_{C1} (\ell_{C1} - \ell_0) + m_3 \ell_{C3} (\ell_{C3} - \ell_0)] = \bar{M}_1 \\
 & \omega^2 \bar{\Theta}_1 [m_3 \ell_{C3}] - \omega^2 \bar{Z}_3 [m_3] + k_3 \bar{Z}_3 + c_3 \omega i \bar{Z}_3 - \omega^2 \bar{\Theta}_0 [m_3 (\ell_0 - \ell_{C3})] = \bar{F}_Z
 \end{aligned}$$

In-Plane 3-DOF Motion (Assumes Roll Section Compliant in Pitch and Yaw)

$$\begin{aligned}
 & -\omega^2 \bar{\Theta}_1 [I_1 + I_2 + I_3 + m_1 \ell_{C1}^2 + m_2 \ell_{C2}^2 + m_3 \ell_{C3}^2] - \omega^2 \bar{\Theta}_2 [I_2 + I_3 + m_2 \ell_{C2} (\ell_{C2} - \ell_2) + m_3 \ell_{C3} \\
 & (\ell_{C3} - \ell_2)] + \omega^2 \bar{Z}_3 [m_3 \ell_{C3}] - \omega^2 \bar{\Theta}_0 [I_1 + I_2 + I_3 + m_1 \ell_{C1} (\ell_{C1} - \ell_0) + m_2 \ell_{C2} (\ell_{C2} - \ell_0) \\
 & + m_3 \ell_{C3} (\ell_{C3} - \ell_0)] + k_1 \bar{\Theta}_1 + c_1 \omega i \bar{\Theta}_1 = \bar{M}_1 \\
 & \omega^2 \bar{\Theta}_1 [m_3 \ell_{C3}] + \omega^2 \bar{\Theta}_2 [m_3 (\ell_{C3} - \ell_2)] - \omega^2 \bar{Z}_3 [m_3] - \omega^2 \bar{\Theta}_0 [m_3 (\ell_0 - \ell_{C3})] + k_3 \bar{Z}_3 + c_3 \omega i \bar{Z}_3 = \bar{F}_Z
 \end{aligned}$$

Table 1. Concluded
b. Yaw Plane

Out-Of-Plane 2-DOF Motion (Assumes Roll Section Rigid in Pitch and Yaw)

$$\begin{aligned}
 & -\omega^2 \bar{Y}_1 [m_1 + m_3] + \omega^2 \bar{\Psi}_3 [m_3 (\ell_{C3} - \ell_3)] + k_1 \bar{Y}_1 + c_1 \omega i \bar{Y}_1 = \bar{F}_Y \\
 & -\omega^2 \bar{Y}_1 [(-m_3)(\ell_{C3} - \ell_3)] - \omega^2 \bar{\Psi}_3 [I_3 + (m_3)(\ell_{C3} - \ell_3)^2] + k_3 \bar{\Psi}_3 + c_3 \omega i \bar{\Psi}_3 + k_{\psi_{aero}} \bar{\Psi}_3 \\
 & + c_{\psi_{aero}} \omega i \bar{\Psi}_3 = \bar{M}_3
 \end{aligned}$$

Out-Of-Plane 3-DOF Motion (Assumes Roll Section Compliant in Pitch and Yaw)

$$\begin{aligned}
 & -\omega^2 \bar{Y}_1 [m_1 + m_2 + m_3] + \omega^2 \bar{\Psi}_2 [m_2 (\ell_{C2} - \ell_2) + m_3 (\ell_{C3} - \ell_2)] + \omega^2 \bar{\Psi}_3 \\
 & [m_3 (\ell_{C3} - \ell_3)] + k_1 \bar{Y}_1 + c_1 \omega i \bar{Y}_1 = \bar{F}_Y \\
 & -\omega^2 \bar{Y}_1 [(-m_3)(\ell_{C3} - \ell_3)] - \omega^2 \bar{\Psi}_2 [I_3 + (m_3)(\ell_{C3} - \ell_2)(\ell_{C3} - \ell_3)] - \omega^2 \bar{\Psi}_3 [I_3 + (m_3) \\
 & (\ell_{C3} - \ell_3)^2] + k_3 \bar{\Psi}_3 + c_3 \omega i \bar{\Psi}_3 + k_{\psi_{aero}} [\bar{\Psi}_2 + \bar{\Psi}_3] + c_{\psi_{aero}} \omega i [\bar{\Psi}_2 + \bar{\Psi}_3] = \bar{M}_3
 \end{aligned}$$

In-Plane 2-DOF Motion (Assumes Roll Section Rigid in Pitch and Yaw)

$$\begin{aligned}
 & -\omega^2 \bar{Y}_1 [m_1 + m_3] + \omega^2 \bar{\Psi}_3 [m_3 (\ell_{C3} - \ell_3)] - \omega^2 \bar{\Psi}_0 [m_1 \ell_0 + m_3 (\ell_0 - \ell_{C3})] + k_1 \bar{Y}_1 \\
 & + c_1 \omega i \bar{Y}_1 = \bar{F}_Y \\
 & -\omega^2 \bar{Y}_1 [(-m_3)(\ell_{C3} - \ell_3)] - \omega^2 \bar{\Psi}_3 [I_3 + (m_3)(\ell_{C3} - \ell_3)^2] - \omega^2 \bar{\Psi}_0 [I_3 - (m_3)(\ell_0 - \ell_{C3}) \\
 & (\ell_{C3} - \ell_3)] + k_3 \bar{\Psi}_3 + c_3 \omega i \bar{\Psi}_3 = \bar{M}_3
 \end{aligned}$$

In-Plane 3-DOF Motion (Assumes Roll Section Compliant in Pitch and Yaw)

$$\begin{aligned}
 & -\omega^2 \bar{Y}_1 [m_1 + m_2 + m_3] + \omega^2 \bar{\Psi}_2 [m_2 (\ell_{C2} - \ell_2) + m_3 (\ell_{C3} - \ell_2)] + \omega^2 \bar{\Psi}_3 [(\ell_{C3} - \ell_3)(m_3)] \\
 & -\omega^2 \bar{\Psi}_0 [m_1 \ell_0 + m_2 (\ell_0 - \ell_{C3}) + m_3 (\ell_0 - \ell_{C3})] + k_1 \bar{Y}_1 - c_1 \omega i \bar{Y}_1 = \bar{F}_Y \\
 & -\omega^2 \bar{Y}_1 [(-m_3)(\ell_{C3} - \ell_3)] - \omega^2 \bar{\Psi}_2 [I_3 + (m_3)(\ell_{C3} - \ell_2)(\ell_{C3} - \ell_3)] - \omega^2 \bar{\Psi}_3 [I_3 + (m_3)(\ell_{C3} - \ell_3)^2] \\
 & -\omega^2 \bar{\Psi}_0 [I_3 - (m_3)(\ell_0 - \ell_{C3})(\ell_{C3} - \ell_3)] + k_3 \bar{\Psi}_3 + c_3 \omega i \bar{\Psi}_3 = \bar{M}_3
 \end{aligned}$$

Table 2. Pitch-Yaw Equations of Motion for the Moment Balance**Out-Of-Plane Motion (2-DOF-Assumes Rigid Roll Section)**

$$\begin{aligned}
& -\omega^2 \bar{\Theta}_1 [I_1 + m_1 \ell_{C1}^2 + I_3 + m_3 \ell_{C3}^2] - \omega^2 \bar{\Theta}_3 [I_3 + m_3 \ell_{C3} (\ell_{C3} - \ell_3)] + k_1 \bar{\Theta}_1 + i\omega c_1 \bar{\Theta}_1 \\
& + k_{\theta_{aero}} [\bar{\Theta}_1 + \bar{\Theta}_3] + i\omega c_{\theta_{aero}} [\bar{\Theta}_1 + \bar{\Theta}_3] = \bar{M}_1 \\
& - \omega^2 \bar{\Theta}_1 [I_3 + m_3 \ell_{C3} (\ell_{C3} - \ell_3)] - \omega^2 \bar{\Theta}_3 [I_3 + m_3 (\ell_{C3} - \ell_3)^2] + k_3 \bar{\Theta}_3 + i\omega c_3 \bar{\Theta}_3 \\
& + k_{\theta_{aero}} [\bar{\Theta}_1 + \bar{\Theta}_3] + i\omega c_{\theta_{aero}} [\bar{\Theta}_1 + \bar{\Theta}_3] = \bar{M}_3
\end{aligned}$$

Out-Of-Plane Motion (3-DOF-Assumes Complaint Roll Section)

$$\begin{aligned}
& -\omega^2 \bar{\Theta}_1 [I_1 + I_2 + I_3 + m_1 \ell_{C1}^2 + m_2 \ell_{C2}^2 + m_3 \ell_{C3}^2] - \omega^2 \bar{\Theta}_2 \\
& [I_2 + I_3 + m_2 \ell_{C2} (\ell_{C2} - \ell_2) + m_3 \ell_{C3} (\ell_{C3} - \ell_2)] - \omega^2 \bar{\Theta}_3 [I_3 + m_3 \ell_{C3} (\ell_{C3} - \ell_3)] \\
& + k_1 \bar{\Theta}_1 + i\omega c_1 \bar{\Theta}_1 + k_{\theta_{aero}} [\bar{\Theta}_1 + \bar{\Theta}_2 + \bar{\Theta}_3] + i\omega c_{\theta_{aero}} [\bar{\Theta}_1 + \bar{\Theta}_2 + \bar{\Theta}_3] = \bar{M}_1 \\
& - \omega^2 \bar{\Theta}_1 [I_3 + m_3 \ell_{C3} (\ell_{C3} - \ell_3)] - \omega^2 \bar{\Theta}_2 [I_3 + m_3 (\ell_{C3} - \ell_3) (\ell_{C3} - \ell_2)] \\
& - \omega^2 \bar{\Theta}_3 [I_3 + m_3 (\ell_{C3} - \ell_3)^2] + k_3 \bar{\Theta}_3 + i\omega c_3 \bar{\Theta}_3 + k_{\theta_{aero}} [\bar{\Theta}_1 + \bar{\Theta}_2 + \bar{\Theta}_3] \\
& + i\omega c_{\theta_{aero}} [\bar{\Theta}_1 + \bar{\Theta}_2 + \bar{\Theta}_3] = \bar{M}_3
\end{aligned}$$

In-Plane Motion (2-DOF-Assumes Rigid Roll Section)

$$\begin{aligned}
& -\omega^2 \bar{\Theta}_1 [I_1 + m_1 \ell_{C1}^2 + I_3 + m_3 \ell_{C3}^2] - \omega^2 \bar{\Theta}_3 [I_3 + m_3 \ell_{C3} (\ell_{C3} - \ell_3)] + k_1 \bar{\Theta}_1 + i\omega c_1 \bar{\Theta}_1 \\
& - \omega^2 \bar{\Theta}_0 [I_1 + I_3 + m_1 \ell_{C1} (\ell_{C1} - \ell_0) + m_3 \ell_{C3} (\ell_{C3} - \ell_0)] = \bar{M}_1 \\
& - \omega^2 \bar{\Theta}_1 [I_3 + m_3 \ell_{C3} (\ell_{C3} - \ell_3)] - \omega^2 \bar{\Theta}_3 [I_3 + m_3 (\ell_{C3} - \ell_3)^2] + k_3 \bar{\Theta}_3 + i\omega c_3 \bar{\Theta}_3 - \omega^2 \bar{\Theta}_0 \\
& [I_3 + m_3 (\ell_{C3} - \ell_3) (\ell_{C3} - \ell_0)] = \bar{M}_3
\end{aligned}$$

In-Plane Motion (3-DOF-Assumes Compliant Roll Section)

$$\begin{aligned}
& -\omega^2 \bar{\Theta}_1 [I_1 + I_2 + I_3 + m_1 \ell_{C1}^2 + m_2 \ell_{C2}^2 + m_3 \ell_{C3}^2] - \omega^2 \bar{\Theta}_2 [I_2 + I_3 + m_2 \ell_{C2} (\ell_{C2} - \ell_2) \\
& + m_3 \ell_{C3} (\ell_{C3} - \ell_2)] - \omega^2 \bar{\Theta}_3 [I_3 + m_3 \ell_{C3} (\ell_{C3} - \ell_3)] + k_1 \bar{\Theta}_1 + i\omega c_1 \bar{\Theta}_1 - \omega^2 \bar{\Theta}_0 \\
& [I_1 + I_2 + I_3 + m_1 \ell_{C1} (\ell_{C1} - \ell_0) + m_2 \ell_{C2} (\ell_{C2} - \ell_0) + m_3 \ell_{C3} (\ell_{C3} - \ell_0)] = \bar{M}_1 \\
& - \omega^2 \bar{\Theta}_1 [I_3 + m_3 \ell_{C3} (\ell_{C3} - \ell_3)] - \omega^2 \bar{\Theta}_2 [I_3 + m_3 (\ell_{C3} - \ell_3) (\ell_{C3} - \ell_2)] - \omega^2 \bar{\Theta}_3 [I_3 \\
& + m_3 (\ell_{C3} - \ell_3)^2] + k_3 \bar{\Theta}_3 + i\omega c_3 \bar{\Theta}_3 - \omega^2 \bar{\Theta}_0 [I_3 + m_3 (\ell_{C3} - \ell_3) (\ell_{C3} - \ell_0)] = \bar{M}_3
\end{aligned}$$

Table 3. Roll Equations of Motion

$$- \omega^2 I_3 (\bar{\Phi}_1 + \bar{\Phi}_2 + \bar{\Phi}_3 + \bar{\Phi}_f) + k_2 \bar{\Phi}_2 + i\omega c_2 \bar{\Phi}_2 + i\omega c_{\phi_{aero}} (\bar{\Phi}_1 + \bar{\Phi}_2 + \bar{\Phi}_3 + \bar{\Phi}_f) = \bar{M}_X \quad (1)$$

$$\left\{ \left[1 - \left(\frac{\omega}{\omega_{n_{total}}} \right)^2 \right] + i\omega \left[\frac{c_2}{k_2} + \frac{c_{\phi_{aero}}}{k_{total}} \right] \right\} \bar{M}'_X = \bar{M}_X \quad (2)$$

$k_2 \bar{\Phi}_2$ = Standard moment measurement obtained from the balance roll gage using a static gage sensitivity

$\omega_{n_{total}}$ = Natural frequency of the total model/balance system in roll

c_2 = Mechanical damping of roll gage
 k_2 = Spring constant of roll gage
 }
 See Appendix C for these constant determination details

$c_{\phi_{aero}}$ = Aerodynamic damping in roll

k_{total} = Spring gage constant of total two-balance system in roll

Table 4. Equations of Motion for the Force-Moment Balance Including Two Degrees of the Supporting Sting
a. Pitch Plane

$$\begin{aligned}
 & -\omega^2(A_2\bar{\Theta}_1 + B_2\bar{\Theta}_2 + C_2\bar{Z}_3 + D_2\bar{\Theta}_s + E_2\bar{Z}_s + F_2\bar{\Theta}_0) + k_3\bar{Z}_3 + c_3\omega i\bar{Z}_3 = \bar{F}_Z \\
 & -\omega^2(A_1\bar{\Theta}_1 + B_1\bar{\Theta}_2 + C_1\bar{Z}_3 + D_1\bar{\Theta}_s + E_1\bar{Z}_s + F_1\bar{\Theta}_0) + k_1\bar{\Theta}_1 + k_{\theta_{aero}} \\
 & (\bar{\Theta}_0 + \bar{\Theta}_s + \bar{\Theta}_1 + \bar{\Theta}_2) + c_1\omega i\bar{\Theta}_1 + c_{\theta_{aero}}\omega i(\bar{\Theta}_0 + \bar{\Theta}_s + \bar{\Theta}_1 + \bar{\Theta}_2) = \bar{M}_1
 \end{aligned}$$

Constant Definitions

3-Degree-Of-Freedom Balance (Fig. 3a)

$$\begin{aligned}
 A_1 &= I_1 + I_2 + I_3 + m_1\ell_{C1}^2 + m_2\ell_{C2}^2 + m_3\ell_{C3}^2 \\
 B_1 &= I_2 + I_3 + m_2\ell_{C2}(\ell_{C2} - \ell_2) + m_3\ell_{C3}(\ell_{C3} - \ell_2) \\
 C_1 &= -m_3\ell_{C3} \\
 F_1 = D_1 &= I_1 + I_2 + I_3 + m_1\ell_{C1}(\ell_{C1} - \ell_0) + m_2\ell_{C2}(\ell_{C2} - \ell_0) + m_3\ell_{C3}(\ell_{C3} - \ell_0) \\
 E_1 &= -m_1\ell_{C1} - m_2\ell_{C2} - m_3\ell_{C3} \\
 A_2 &= -m_3\ell_{C3} \\
 B_2 &= -m_3(\ell_{C3} - \ell_2)
 \end{aligned}$$

2-Degree-Of-Freedom Balance (Fig. 5a)

$$\begin{aligned}
 A_1 &= I_1 + I_3 + m_1\ell_{C1}^2 + m_3\ell_{C3}^2 \\
 B_1 &= 0 \\
 C_1 &= -m_3\ell_{C3} \\
 F_1 = D_1 &= I_1 + I_3 + m_1\ell_{C1}(\ell_{C1} - \ell_0) + m_3\ell_{C3}(\ell_{C3} - \ell_0) \\
 E_1 &= -m_1\ell_{C1} - m_3\ell_{C3} \\
 A_2 &= -m_3\ell_{C3} \\
 B_2 &= 0
 \end{aligned}$$

Notes: (1) For out-of-plane motion $\bar{\Theta}_0 = 0$

(2) For in-plane motion $k_{\theta_{aero}}$ and $c_{\theta_{aero}}$ terms should be omitted since they are the measured loads, i.e., the direct derivatives.

Table 4. Concluded
b. Yaw Plane

$$\begin{aligned}
 & -\omega^2(A_1\bar{Y}_1 + B_1\bar{\Psi}_2 + C_1\bar{\Psi}_3 + D_1\bar{\Psi}_s + E_1\bar{\Psi}_s + F_1\bar{\Psi}_0) + k_1\bar{Y}_1 + c_1i\omega\bar{Y}_1 = \bar{F}_Y \\
 & -\omega^2(A_2\bar{Y}_1 + B_2\bar{\Psi}_2 + C_2\bar{\Psi}_3 + D_2\bar{\Psi}_s + E_2\bar{Y}_s + F_2\bar{\Psi}_0) + k_3\bar{\Psi}_3 + c_3i\omega\bar{\Psi}_3 \\
 & + k_{\psi_{aero}}(\bar{\Psi}_3 + \bar{\Psi}_2 + \bar{\Psi}_0 + \bar{\Psi}_s) + c_{\psi_{aero}}i\omega(\bar{\Psi}_3 + \bar{\Psi}_2 + \bar{\Psi}_0 + \bar{\Psi}_s) = \bar{M}_3
 \end{aligned}$$

Constant Definitions

3-Degree-Of-Freedom Balance (Fig. 3b)

$$\begin{aligned}
 E_1 &= A_1 = m_1 + m_2 + m_3 \\
 B_1 &= -m_2(\ell_{C2} - \ell_2) - m_3(\ell_{C3} - \ell_2) \\
 C_1 &= -m_3(\ell_{C3} - \ell_3) \\
 F_1 &= D_1 = m_1\ell_0 + m_2(\ell_0 - \ell_{C2}) + m_3(\ell_0 - \ell_{C3}) \\
 E_2 &= A_2 = (-m_3)(\ell_{C3} - \ell_3) \\
 B_2 &= I_3 + (m_3)(\ell_{C3} - \ell_2)(\ell_{C3} - \ell_3) \\
 C_2 &= I_3 + (m_3)(\ell_{C3} - \ell_3)^2 \\
 F_2 &= D_2 = I_3 - (m_3)(\ell_{C3} - \ell_3)(\ell_0 - \ell_{C3})
 \end{aligned}$$

2-Degree-Of-Freedom Balance (Fig. 5b)

$$\begin{aligned}
 E_1 &= A_1 = m_1 + m_3 \\
 B_1 &= 0 \\
 C_1 &= -m_3(\ell_{C3} - \ell_3) \\
 F_1 &= D_1 = m_1\ell_0 + m_3(\ell_0 - \ell_{C3}) \\
 E_2 &= A_2 = -m_3(\ell_{C3} - \ell_3) \\
 B_2 &= 0 \\
 C_2 &= I_3 + (m_3)(\ell_{C3} - \ell_3)^2 \\
 F_2 &= D_2 = I_3 - (m_3)(\ell_{C3} - \ell_3)(\ell_0 - \ell_{C3})
 \end{aligned}$$

Notes: (1) For out-of-plane motion $\bar{\Theta}_0 = 0$

(2) For in-plane motion $k_{\psi_{aero}}$ and $c_{\psi_{aero}}$ terms should be omitted since they are the measured loads, i.e., the direct derivatives.

Table 5. Equations of Motion for the Moment Balance Including Two Degrees of Freedom of the Supporting Sting

$$-\omega^2(A_1\bar{\Theta}_1 + B_1\bar{\Theta}_2 + C_1\bar{\Theta}_3 + D_1\bar{\Theta}_s + E_1\bar{Z}_s + F_1\bar{\Theta}_0) + k_1\bar{\Theta}_1 + k_{\theta_{aero}}(\bar{\Theta}_3 + \bar{\Theta}_2 + \bar{\Theta}_1 + \bar{\Theta}_s + \bar{\Theta}_0) + c_1\omega i\bar{\Theta}_1 + c_{\theta_{aero}}\omega i(\bar{\Theta}_3 + \bar{\Theta}_2 + \bar{\Theta}_1 + \bar{\Theta}_s + \bar{\Theta}_0) = \bar{M}_1$$

$$-\omega^2(A_2\bar{\Theta}_1 + B_2\bar{\Theta}_2 + C_2\bar{\Theta}_3 + D_2\bar{\Theta}_s + E_2\bar{Z}_s + F_2\bar{\Theta}_0) + k_3\bar{\Theta}_3 + k_{\theta_{aero}}(\bar{\Theta}_3 + \bar{\Theta}_2 + \bar{\Theta}_1 + \bar{\Theta}_s + \bar{\Theta}_0) + c_2\omega i\bar{\Theta}_2 + c_{\theta_{aero}}\omega i(\bar{\Theta}_3 + \bar{\Theta}_2 + \bar{\Theta}_1 + \bar{\Theta}_s + \bar{\Theta}_0) = \bar{M}_3$$

Constant Definitions

3-Degree-Of-Freedom Balance (Fig. 4)

$$A_1 = I_1 + I_2 + I_3 + m_1\ell_{C1}^2 + m_2\ell_{C2}^2 + m_3\ell_{C3}^2$$

$$B_1 = I_2 + I_3 + m_2\ell_{C2}(\ell_{C2} - \ell_2) + m_3\ell_{C3}(\ell_{C3} - \ell_2)$$

$$A_2 = C_1 = I_3 + m_3\ell_{C3}(\ell_{C3} - \ell_3)$$

$$D_1 = F_1 = I_1 + I_2 + I_3 + m_1\ell_{C1}(\ell_{C1} - \ell_0) + m_2\ell_{C2}(\ell_{C2} - \ell_0) + m_3\ell_{C3}(\ell_{C3} - \ell_0)$$

$$E_1 = -\ell_{C1}m_1 - \ell_{C2}m_2 - \ell_{C3}m_3$$

$$B_2 = I_3 + m_3(\ell_{C3} - \ell_2)(\ell_{C3} - \ell_3)$$

$$C_2 = I_3 + m_3(\ell_{C3} - \ell_3)^2$$

$$D_2 = F_2 = I_3 + m_3(\ell_{C3} - \ell_0)(\ell_{C3} - \ell_3)$$

$$E_2 = -m_3(\ell_{C3} - \ell_3)$$

2-Degree-Of-Freedom Balance (Fig. 6)

$$A_1 = I_1 + I_3 + m_1\ell_{C1}^2 + m_3\ell_{C3}^2$$

$$B_1 = 0$$

$$A_2 = C_1 = I_3 + m_3\ell_{C3}(\ell_{C3} - \ell_3)$$

$$D_1 = F_1 = I_1 + I_3 + m_1\ell_{C1}(\ell_{C1} - \ell_0) + m_3\ell_{C3}(\ell_{C3} - \ell_0)$$

$$E_1 = -\ell_{C1}m_1 - \ell_{C3}m_3$$

$$B_2 = 0$$

$$C_2 = I_3 + m_3(\ell_{C3} - \ell_3)^2$$

$$D_2 = F_2 = I_3 + m_3(\ell_{C3} - \ell_0)(\ell_{C3} - \ell_3)$$

$$E_2 = -m_3(\ell_{C3} - \ell_3)$$

Notes: (1) For out-of-plane motion $\Theta_0 = 0$.

(2) For in-plane motion $k_{\theta_{aero}}$ and $c_{\theta_{aero}}$ terms should be omitted since they are the measured loads, i.e., the direct derivatives.

APPENDIX A

BALANCE DEFLECTION MODE DETERMINATIONS

To interpret data obtained from a dynamic balance system correctly, an accurate model of the system must be assumed from which the equations of motion are derived. Naturally, the most accurate model would include both a translational and a rotational degree of freedom at each flexible balance station and in each plane, i.e., six degrees of freedom must be assumed and measured at each flexible station. However, the physical size of strain gages relative to the space available for gage placement on a small balance renders this approach all but impossible. Even if the instrumentation were possible, the additional accuracy gained from measuring all of these deflections would not be cost efficient. The most practical approach is to determine the primary deflection modes of a balance at each flexible station, instrument the balance to measure these deflections and corresponding loads, and write the system equations in terms of these primary deflections only.

If a balance is designed to measure a moment at a particular station, its primary compliance is in rotation at that station since the gage must sense strain attributable to bending to provide an electrical output proportional to moment. It is kept as rigid as possible in all other degrees of freedom to limit the extraneous motions which are not measured. In a similar manner, if a balance is designed to measure a force at a particular station, its primary compliance is translational at that station. To confirm these primary modes of deflection of the force-moment C.C. balance, holographic interferometry was used to provide a graphic illustration of the balance deflections under load over the entire length of the balance. The technique involves the superpositioning of a deflected balance image onto the holographically reconstructed image of an undeflected balance. To the extent that the wavefront propagation directions of the two images have changed, interference fringes form that are observed superimposed on the image of the balance. The wavefronts will interfere destructively at points where the distance of deflection is an odd multiple of half the light wavelength, and constructively where the distance is an even multiple of half the wavelength. Each successive fringe represents the deflection of an additional wavelength. A raw data record of such measurements takes the form of a photograph as illustrated in Fig. A-1, where the force-moment balance is illustrated under a nominal 30-lb load (directed into the page) along with the optical fringes.

To obtain the deflection data the balance was rigidly mounted horizontally on an optical isolation table by the end which is normally attached to the sting. A load was applied to the free end of the balance horizontal to the table and in a direction normal to the balance axis, as illustrated in Fig. A-2. The balance was viewed and data images recorded from the side of the balance opposite to that of the load application, i.e., the free end of the balance

deflected away from the imaging plane. The balance was illuminated with a He-Ne laser providing a coherent light source with a wavelength of $0.6328\ \mu\text{m}$. A diagram of the optical set-up is shown in Fig. A-2.

The deflection curves illustrated by the balance while under a nominal 30-lb load are illustrated in Fig. A-3. The deflection curve of the yaw plane shown in Fig. A-3a was obtained from the raw data photograph shown in Fig. A-1. The difference between the deflection mode of the forward station (force gage) and the aft station should be noted. The yaw plane of the forward station is gaged for force measurement and is, therefore, designed for primary compliance in translation, whereas the aft station is gaged for moment measurement and undergoes a primarily rotational deflection. The deflection curve (Fig. A-3a) shows this station indeed to be undergoing a translational deflection much larger than the translational deflections of the other stations.

Besides providing a verification of the primary deflection modes of the balance, the balance deflection measurements used in conjunction with the known loads applied to each of the balance's flexible stations provided data for obtaining spring constants of each. From the series of three different loads hung in each balance plane, both the translational and the rotational spring constants of each of the three flexible stations of the force-moment balance were calculated. The resulting constants are tabulated in Table A-1. The translational spring constants of the aft yaw station and the forward pitch station were impossible to calculate because of the discontinuity in the model surface at these points, as illustrated for the aft yaw station in Fig. A-1. However, knowledge of these constants is only academic since these are not the primary degrees of freedom of their respective stations.

The measurements discussed above and the resulting constants tabulated in Table A-1 were obtained during a feasibility study of this proposed calibration technique. The data obtained do not reflect the kind of precision required from a pretest calibration to be used for actual wind tunnel data reduction. The study did lead to some conclusions regarding some possible improvements that could be made to enable a more accurate calibration. The conclusions are listed below along with some discussion:

1. A calibration body should be used which allows the application of a broad range of applied moments about each gage while keeping the shear force constant, or vice versa.

2. Rather than displaying the fringes on the balance itself to get angular deflections, long fringe imaging planes should be attached to the balance sections on either side of the element to be calibrated. This would enable a higher fringe count over a known distance, reducing the uncertainty in the angle of rotation. This would necessitate the calibration of one element at a time.
3. For calibration of the force (translational) gages or springs, the beam which is undergoing "S" bending and on which the fringes must be displayed and counted should be viewed and illuminated perpendicular to the center of the beam such that shadows do not hamper the accurate fringe count on the beam.
4. A large number of points should be taken on each spring, enabling a better definition of the uncertainty of the resulting spring constant.
5. Each spring should be calibrated in both directions of load application.
6. The use of a dual beam interferometry technique should be attempted to obtain a more accurate measurement of the translation across a force gage. This technique would use a laser beam reflected from each side of the translational gage using two retroreflectors secured to the balance surface. If the distance between the parallel beams, the angular deflection from a previous angular calibration, and the phase shift between the two light beams are known, the translational deflection could be determined.

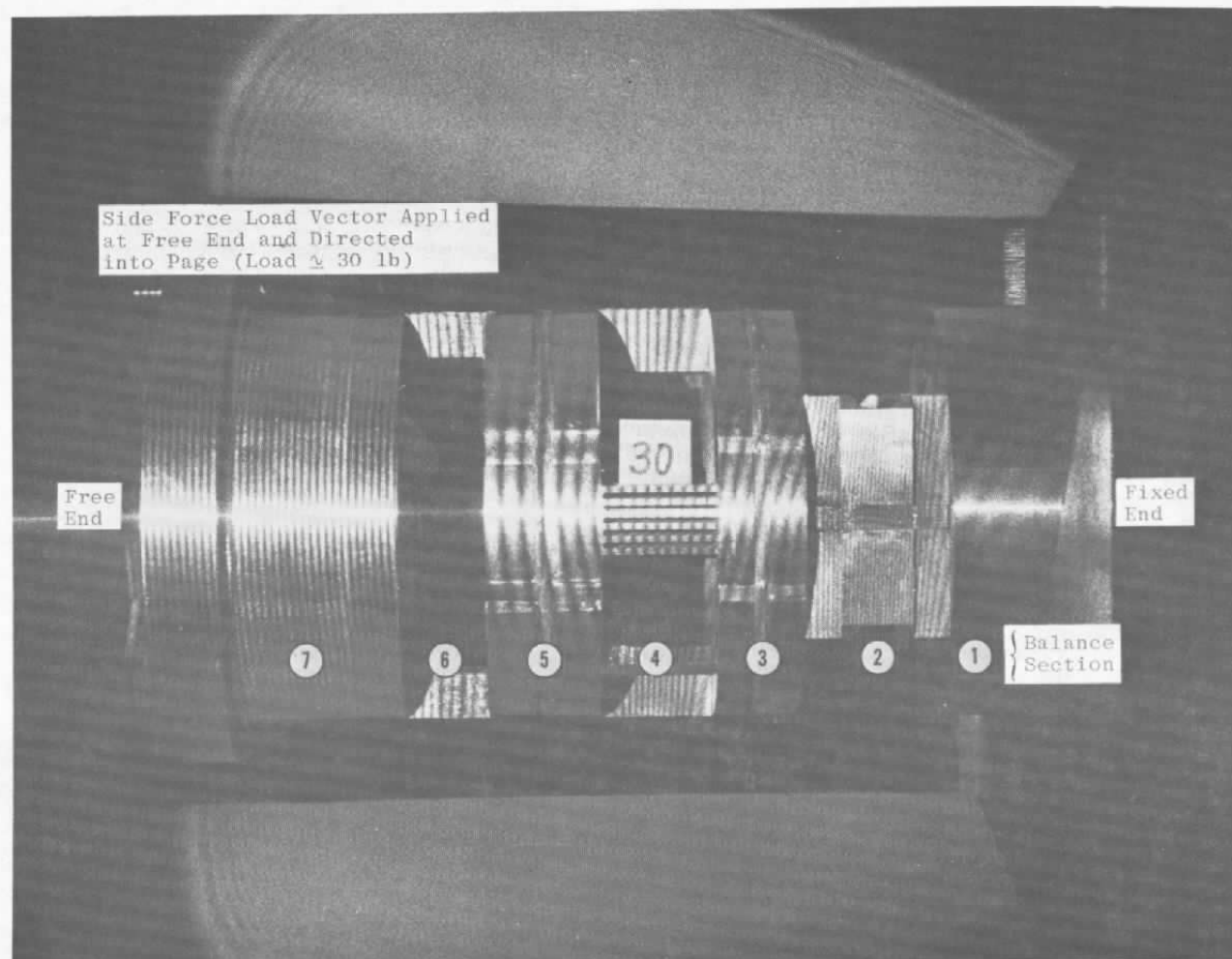


Figure A-1. Photographic record of the yaw plane deflection of the force-moment balance.

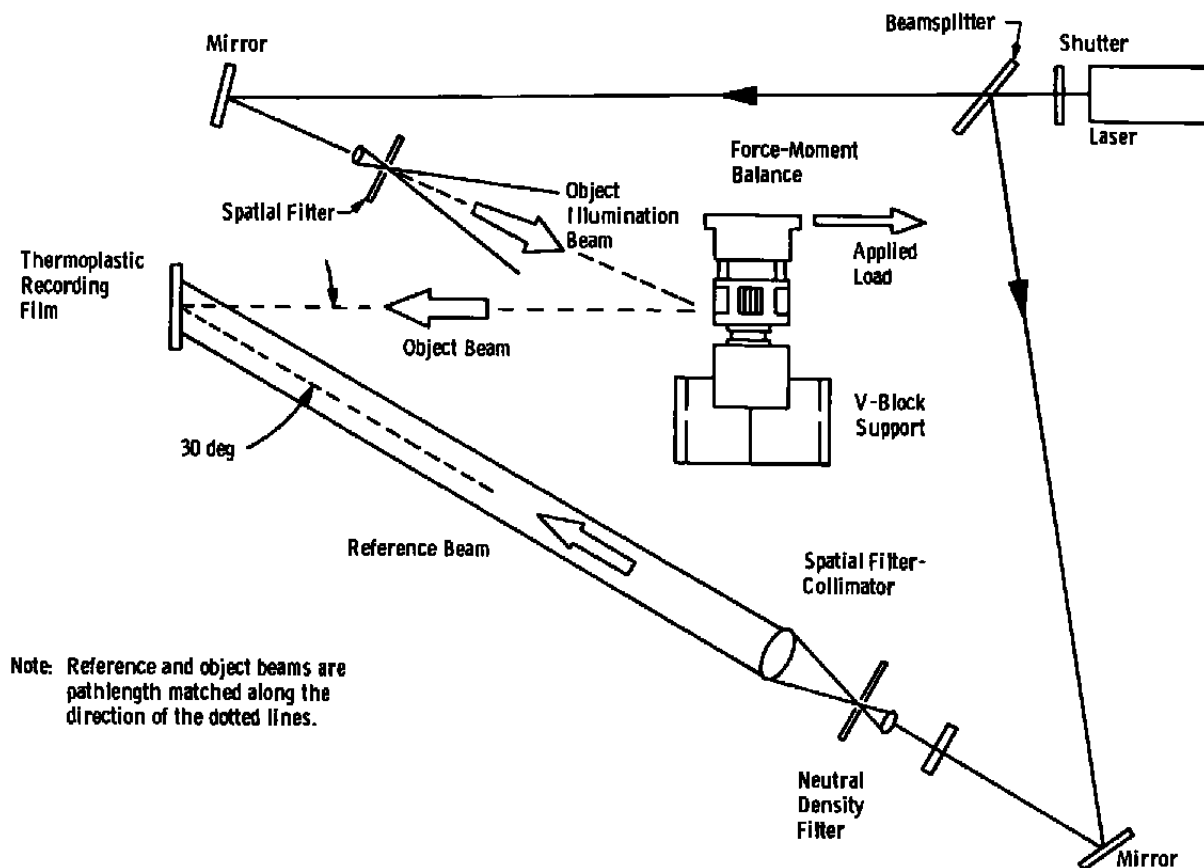
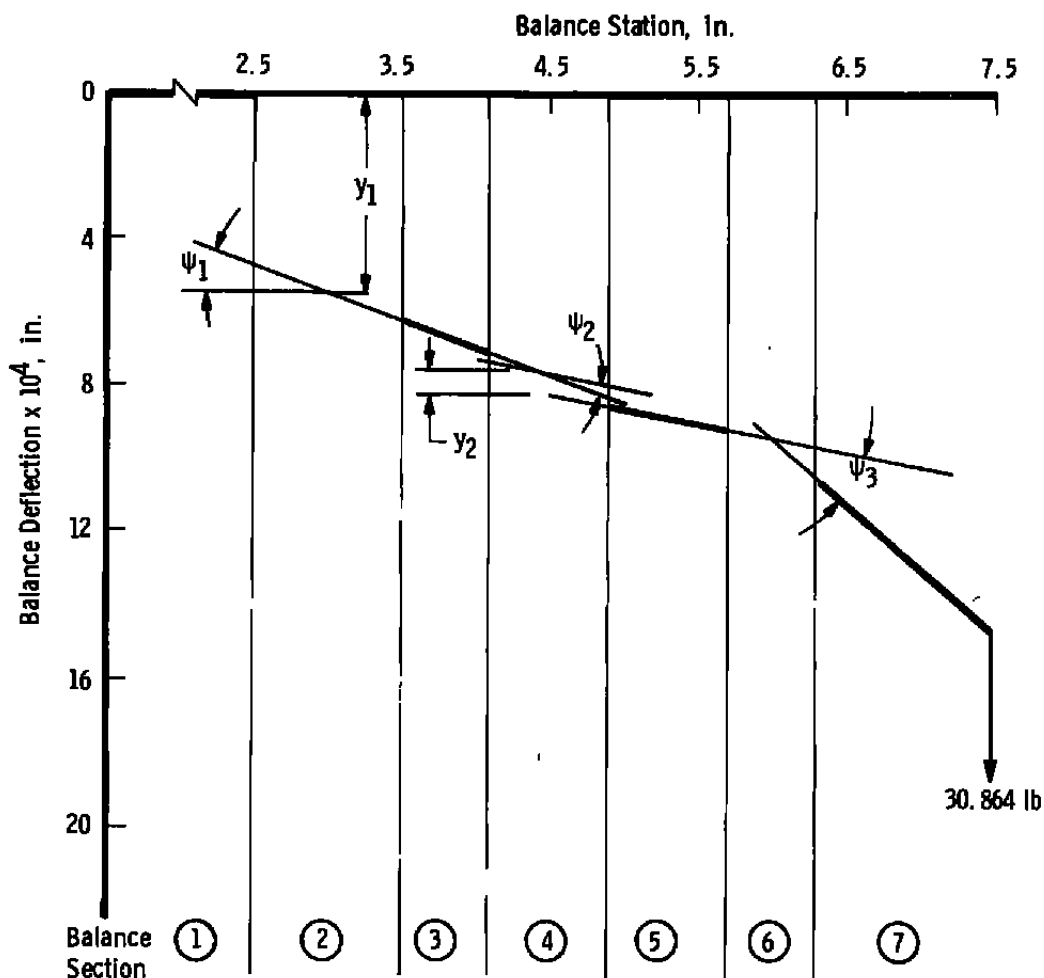


Figure A-2. Optical arrangement for holographic interferometry measurements.



$$\psi_1 = 0.00816 \text{ deg} \quad \psi_2 = -0.00372 \text{ deg} \quad \psi_3 = 0.0153 \text{ deg}$$

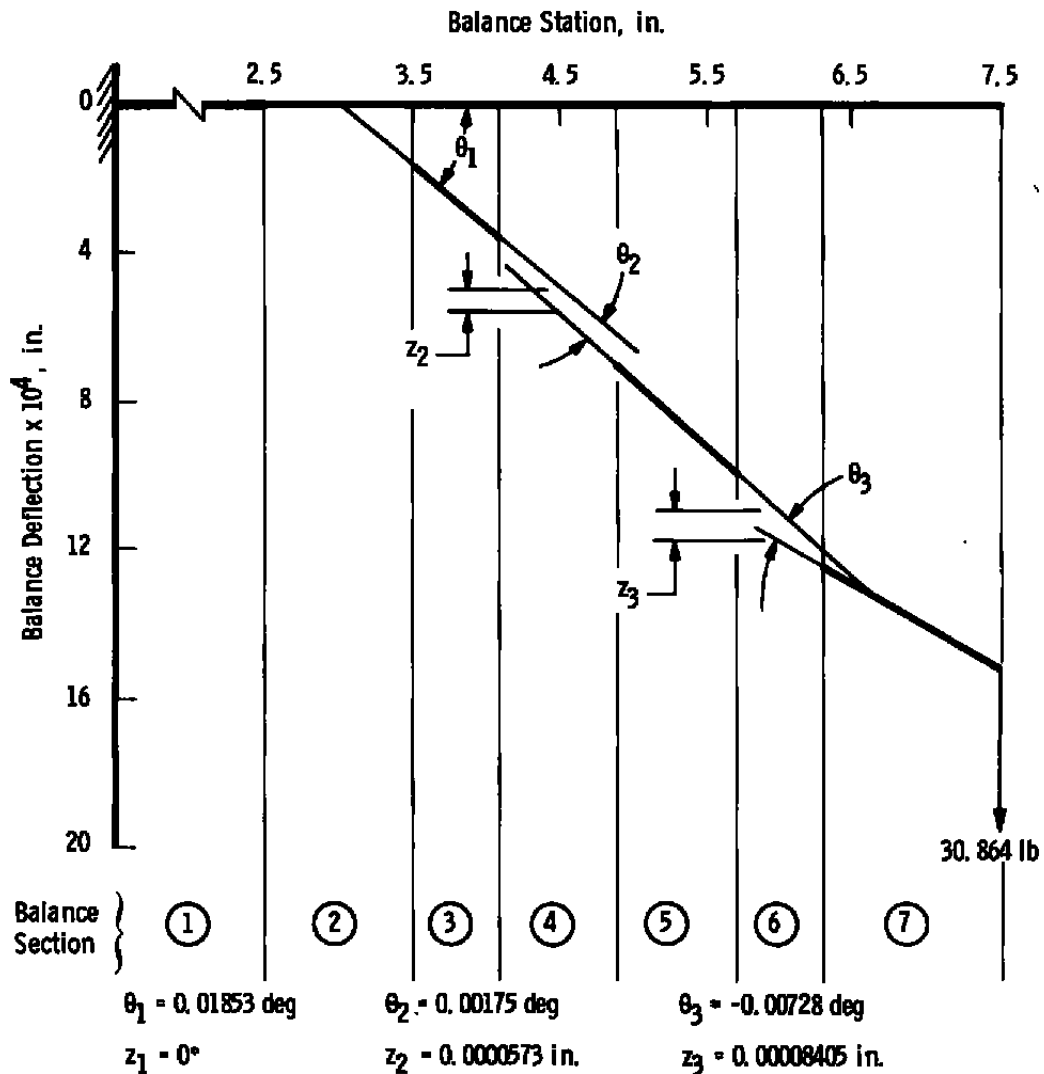
$$y_1 = 0.000553 \text{ in.} \quad y_2 = 0.0000601 \text{ in.} \quad y_3 = 0^*$$

* y_3 was assumed to be zero since this measurement was not possible with the measurement technique used.

Balance Section	Load Measured
2	Side Force
4	Rolling Moment
6	Yawing Moment

a. Yaw plane deflections

Figure A-3. Deflections of the force-moment balance.



* z_1 was assumed to be zero since this measurement was not possible with the technique used.

Balance Section	Load Measured
2	Pitching Moment
4	Rolling Moment
6	Normal Force

b. Pitch plane deflections
Figure A-3. Concluded.

Table A-1. Force-Moment Balance Spring Constants Determined From Interferometer Measurements

	Pitch Translation (lb/in.)	Pitch Rotation (in.-lb/deg)	Yaw Translation (lb/in.)	Yaw Rotation (in.-lb/deg)
Aft Gage Station (Balance Section Six)	425,000* ($\pm 14\%$)	Note 2	Note 3	2,910* ($\pm 7\%$)
Roll Gage Station (Balance Section Four)	711,000 ($\pm 32\%$)	49,400 ($\pm 6\%$)	556,000 ($\pm 11\%$)	Note 2
Forward Gage Station (Balance Section Two)	Note 3	7,110* ($\pm 6\%$)	59,300* ($\pm 8\%$)	17,300 ($\pm 6\%$)

- NOTES: (1) The spring constants quoted represent the average of three measurements. The uncertainty band centered about this average which would include all three values is indicated below each average spring constant.
- (2) These spring constants were negative. Because of the unlikely event that a negative deflection could result from a positive load, these spring constants were considered to be in error. It is likely that this error resulted from the inability to measure this deflection accurately because of the short balance surface available for viewing fringes.
- (3) The interferometry method used did not provide a means for measurement of this deflection.
- (4) The spring constants for the degrees of freedom for which the balance is gaged are denoted with an asterisk (*).

APPENDIX B

DETAILS OF BALANCE EQUATION OF MOTION DERIVATIONS

The details of the derivations of the equations of motion for each of the two AEDC dual-balance, cross-coupling systems are given on the following pages. The equations were formulated with the Lagrange approach. The moment balance system required only one derivation for both the pitch and yaw plane since all gages on this balance are moment gages and the side and pitch planes can be modeled identically. On the other hand the force-moment balance required a different model for each of the two planes of motion since one force and one moment gage are used in each plane, and the force gage is forward in the yaw plane and aft in the pitch plane. This different relative orientation of the force and moment gages in the two planes results in a different model and a somewhat different derivation for each plane.

The three pitch and yaw derivations presented represent the most complex cases that would be experienced by the balances, i.e., the balance roll section is modeled as an additional rotational degree of freedom, the sting motion attributable to bending is included, and the primary forcing motion of the C.F. balance is included to simulate in-plane motion. The simpler cases which may be of interest, such as the case of two degree-of-freedom, out-of-plane motion without sting motion, can be obtained from these derivations by setting the variables and related constants equal to zero which do not apply to the simpler system. For example, if a system is to be considered which has a completely rigid roll section, then the θ_2 variable can be set equal to zero. The two sets of mass and moment of inertia constants included between gaged stations 1 and 3 must also be combined into one mass and one moment of inertia. Although it would be possible to present a derivation for any type of simpler system which could be made from the more complex system, an identical result could be much more easily obtained by simply cancelling terms in the equations of the more complex system.

The equations of motion were derived from Lagrange's equations, as illustrated below.

$$\frac{d}{dt} \left(\frac{\partial L}{\partial \dot{q}_j} \right) - \frac{\partial L}{\partial q_j} + \frac{\partial D}{\partial \dot{q}_j} = Q_j \quad (B-1)$$

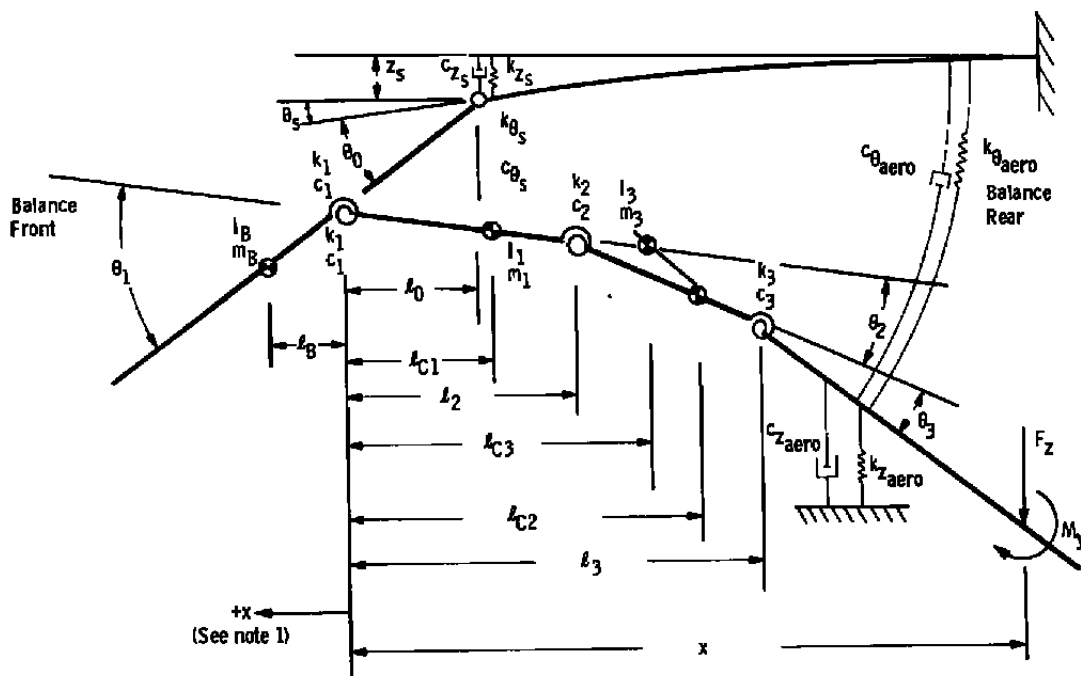
Lagrange's formulation requires the definition of the dissipation function D , the generalized forces Q_{ij} , and the Lagrangian L , which is a function of kinetic energy (T) and potential energy (V).

Four separate derivations are presented in the pages that follow. Since each derivation was formulated with a specific model in mind, each one is begun with a diagram of the dynamic model to which it applies. Following a sketch of the dynamic model, each

derivation includes the following steps: (1) definition of the center of gravity translations and translational velocities from which kinetic energy is calculated, (2) definition of the potential and kinetic energies, (3) definition of the dissipation function from the velocities and damping constants, and (4) definition of the generalized forces which apply to the various generalized coordinates. Following these definitions, the quantities are differentiated and substituted into the general formula for Lagrange's equations given earlier to yield the equations of motion.

The derivation of the roll equation of motion applies to either balance since they are modeled identically. The roll derivation was somewhat simpler since the masses between the springs were neglected. This was thought to be a good assumption since the spectral analyses of the roll gage signals from both balances exhibited a single predominant frequency, indicating a relative absence of multiple modes. The final roll equation has been written in a form involving the rolling moment gage reading (in moment units rather than displacement units) and the natural frequency of the total dual-balance/sting system.

Derivation 1. The Moment Balance Equation Derivation



- Notes: (1) The constants $l_B, l_0, l_{C1}, l_{C2}, l_{C3}, l_2$, and l_3 are measured positive (+) forward from the forward gage center.
- (2) F_z and M_y are the aerodynamic force and moment applied at some location (x) on the model surface.
- (3) For in-plane motion the terms involving the aerodynamic damping spring constants should be omitted from the above illustration and from the derivation since they are the loads (F_z and M_y) being measured.
- (4) For out-of-plane motion $\theta_0 = 0$.

C.G. Translations

$$z_{C1} = z_s + \ell_0(\theta_0 + \theta_s) - \ell_{C1}(\theta_1 + \theta_0 + \theta_s)$$

$$z_{C2} = z_s + \ell_0(\theta_0 + \theta_s) - \ell_2(\theta_1 + \theta_0 + \theta_s) - (\ell_{C2} - \ell_2)(\theta_1 + \theta_0 + \theta_s + \theta_2)$$

$$z_{C3} = z_s + \ell_0(\theta_0 + \theta_s) - \ell_2(\theta_1 + \theta_0 + \theta_s) - (\ell_3 - \ell_2)(\theta_1 + \theta_0 + \theta_s + \theta_2) \\ - (\ell_{C3} - \ell_3)(\theta_1 + \theta_0 + \theta_s + \theta_2 + \theta_3)$$

$$z_B = z_s - (\ell_B - \ell_0)(\theta_0 + \theta_s)$$

C.G. Translational Velocities:

$$\dot{z}_B = \dot{z}_s - (\ell_B - \ell_0)(\dot{\theta}_0 + \dot{\theta}_s)$$

$$\dot{z}_{C1} = \dot{z}_s + \ell_0(\dot{\theta}_0 + \dot{\theta}_s) - \ell_{C1}(\dot{\theta}_1 + \dot{\theta}_0 + \dot{\theta}_s)$$

$$\dot{z}_{C2} = \dot{z}_s + \ell_0(\dot{\theta}_0 + \dot{\theta}_s) - \ell_2(\dot{\theta}_1 + \dot{\theta}_0 + \dot{\theta}_s) - (\ell_{C2} - \ell_2)(\dot{\theta}_1 + \dot{\theta}_0 + \dot{\theta}_s + \dot{\theta}_2)$$

$$\dot{z}_{C3} = \dot{z}_s + \ell_0(\dot{\theta}_0 + \dot{\theta}_s) - \ell_2(\dot{\theta}_1 + \dot{\theta}_0 + \dot{\theta}_s) - (\ell_3 - \ell_2)(\dot{\theta}_1 + \dot{\theta}_0 + \dot{\theta}_s + \dot{\theta}_2) \\ - (\ell_{C3} - \ell_3)(\dot{\theta}_1 + \dot{\theta}_0 + \dot{\theta}_s + \dot{\theta}_2 + \dot{\theta}_3)$$

Kinetic Energy:

$$T = \frac{1}{2}m_s\dot{z}_s^2 + \frac{1}{2}I_s\dot{\theta}_s^2 + \frac{1}{2}I_B(\dot{\theta}_0 + \dot{\theta}_s)^2 + \frac{1}{2}I_1(\dot{\theta}_1 + \dot{\theta}_0 + \dot{\theta}_s)^2 \\ + \frac{1}{2}I_2(\dot{\theta}_1 + \dot{\theta}_0 + \dot{\theta}_s + \dot{\theta}_2)^2 + \frac{1}{2}I_3(\dot{\theta}_1 + \dot{\theta}_0 + \dot{\theta}_s + \dot{\theta}_2 + \dot{\theta}_3)^2 \\ + \frac{1}{2}m_B[\dot{z} + \ell_B(\dot{\theta}_0 + \dot{\theta}_s)]^2 + \frac{1}{2}m_1[\dot{z}_s + \ell_0(\dot{\theta}_0 + \dot{\theta}_s) \\ - \ell_{C1}(\dot{\theta}_1 + \dot{\theta}_0 + \dot{\theta}_s)]^2 + \frac{1}{2}m_2[\dot{z}_s + \ell_0(\dot{\theta}_0 + \dot{\theta}_s) - \ell_2(\dot{\theta}_1 + \dot{\theta}_0 + \dot{\theta}_s) \\ - (\ell_{C2} - \ell_2)(\dot{\theta}_1 + \dot{\theta}_0 + \dot{\theta}_s + \dot{\theta}_2)]^2 + \frac{1}{2}m_3[\dot{z}_s + \ell_0(\dot{\theta}_0 + \dot{\theta}_s) \\ - \ell_2(\dot{\theta}_1 + \dot{\theta}_0 + \dot{\theta}_s) - (\ell_3 - \ell_2)(\dot{\theta}_1 + \dot{\theta}_0 + \dot{\theta}_s + \dot{\theta}_2) \\ - (\ell_{C3} - \ell_3)(\dot{\theta}_1 + \dot{\theta}_0 + \dot{\theta}_s + \dot{\theta}_2 + \dot{\theta}_3)]^2$$

Potential Energy:

$$\begin{aligned}
V = & \frac{1}{2}k_z z_s^2 + \frac{1}{2}k_{\theta_s} \theta_s^2 + \frac{1}{2}k_1 \theta_1^2 + \frac{1}{2}k_2 \theta_2^2 + \frac{1}{2}k_3 \theta_3^2 \\
& + \frac{1}{2}k_{\theta_{aero}} (\theta_3 + \theta_2 + \theta_1 + \theta_0 + \theta_s)^2 + \frac{1}{2}k_{z_{aero}} \\
& [z_s + \ell_0(\theta_0 + \theta_s) - \ell_2(\theta_1 + \theta_0 + \theta_s) - (\ell_3 - \ell_2) \\
& (\theta_1 + \theta_0 + \theta_s + \theta_2) - (\ell_{C2} - \ell_3)(\theta_1 + \theta_0 + \theta_s + \theta_2 + \theta_3)]^2
\end{aligned}$$

Dissipation Function:

$$\begin{aligned}
D = & \frac{1}{2}c_z \dot{z}_s^2 + \frac{1}{2}c_{\theta_s} \dot{\theta}_s^2 + \frac{1}{2}c_1 \dot{\theta}_1^2 + \frac{1}{2}c_2 \dot{\theta}_2^2 + \frac{1}{2}c_3 \dot{\theta}_3^2 + \frac{1}{2}c_{\theta_{aero}} (\dot{\theta}_3 + \dot{\theta}_2 + \dot{\theta}_1 \\
& + \dot{\theta}_0 + \dot{\theta}_s)^2 + \frac{1}{2}c_{z_{aero}} [\dot{z}_s + \ell_0(\dot{\theta}_0 + \dot{\theta}_s) - \ell_2(\dot{\theta}_1 + \dot{\theta}_0 + \dot{\theta}_s) - (\ell_3 - \ell_2) \\
& (\dot{\theta}_1 + \dot{\theta}_0 + \dot{\theta}_s + \dot{\theta}_2)]
\end{aligned}$$

Generalized Forces ($Q_i = \mathcal{F}_j \frac{\partial x_j}{\partial q_i}$):

$$\mathcal{F}_1 = F_z \quad x_1 = z = f(\theta_1, \theta_2, \theta_3, z_s, \theta_0, \theta_s)$$

$$\begin{aligned}
z = & z_s + \ell_0(\theta_0 + \theta_s) - \ell_2(\theta_1 + \theta_0 + \theta_s) - (\ell_3 - \ell_2)(\theta_1 + \theta_0 + \theta_s \\
& + \theta_2) - (x - \ell_3)(\theta_1 + \theta_0 + \theta_s + \theta_2 + \theta_3)
\end{aligned}$$

$$\mathcal{F}_3 = M_y \quad x_2 = \theta$$

$$\theta = \theta_0 + \theta_s + \theta_1 + \theta_2 + \theta_3$$

$$Q_1 = F_z \left(\frac{\partial z}{\partial \theta_1} \right) + M_y \left(\frac{\partial \theta}{\partial \theta_1} \right) = F_z(-x) + M_y(1)$$

$\therefore Q_1 =$ the moment causing the deflection $\theta_1 \equiv M_1$

$$Q_3 = F_z \left(\frac{\partial z}{\partial \theta_2} \right) + M_y \left(\frac{\partial \theta}{\partial \theta_2} \right) = -F(x - \ell_2) + M_y$$

$\therefore Q_2 =$ the moment causing the deflection $\theta_2 \equiv M_3$

Lagrange's equation for θ_1 , the forward moment gage deflection:

$$\frac{d}{dt} \left(\frac{\partial L}{\partial \dot{\theta}_1} \right) - \frac{\partial L}{\partial \theta_1} + \frac{\partial D}{\partial \dot{\theta}_1} = M_1$$

$$\begin{aligned}
& I_1(\ddot{\theta}_1 + \ddot{\theta}_0 + \ddot{\theta}_s) + I_2(\ddot{\theta}_1 + \ddot{\theta}_0 + \ddot{\theta}_s + \ddot{\theta}_2) + I_3(\ddot{\theta}_1 + \ddot{\theta}_0 + \ddot{\theta}_s + \ddot{\theta}_2 + \ddot{\theta}_3) \\
& + m_1[\ddot{z}_s + \ell_0(\ddot{\theta}_0 + \ddot{\theta}_s) - \ell_{C1}(\ddot{\theta}_1 + \ddot{\theta}_0 + \ddot{\theta}_s)][-\ell_{C1}] \\
& + m_2[\ddot{z}_s + \ell_0(\ddot{\theta}_0 + \ddot{\theta}_s) - \ell_2(\ddot{\theta}_1 + \ddot{\theta}_0 + \ddot{\theta}_s) - (\ell_{C2} - \ell_2) \\
& (\ddot{\theta}_1 + \ddot{\theta}_0 + \ddot{\theta}_s + \ddot{\theta}_2)][-\ell_{C2}] + m_3[\ddot{z}_s + \ell_0(\ddot{\theta}_0 + \ddot{\theta}_s) \\
& - \ell_2(\ddot{\theta}_1 + \ddot{\theta}_0 + \ddot{\theta}_s) - (\ell_3 - \ell_2)(\ddot{\theta}_1 + \ddot{\theta}_0 + \ddot{\theta}_s + \ddot{\theta}_2) - (\ell_{C3} - \ell_3) \\
& (\ddot{\theta}_1 + \ddot{\theta}_0 + \ddot{\theta}_s + \ddot{\theta}_2 + \ddot{\theta}_3)][-\ell_{C3}] + k_1\theta_1 + k_{\theta_{aero}}(\theta_3 + \theta_2 \\
& + \theta_1 + \theta_0 + \theta_s) + c_1\dot{\theta}_1 + c_{\theta_{aero}}(\dot{\theta}_3 + \dot{\theta}_2 + \dot{\theta}_1 + \dot{\theta}_0 + \dot{\theta}_s) = M_1
\end{aligned}$$

Note: $k_{z_{aero}}$ and $c_{z_{aero}}$ have been assumed to be negligible in arriving at the above equation.

$$\begin{aligned}
& [I_1 + I_2 + I_3 + m_1\ell_{C1}^2 + m_2\ell_{C2}^2 + m_3\ell_{C3}^2]\ddot{\theta}_1 + [I_2 + I_3 + m_2\ell_{C2}(\ell_{C2} - \ell_2) \\
& + m_3\ell_{C3}(\ell_{C3} - \ell_2)]\ddot{\theta}_2 + [I_3 + m_3\ell_{C3}(\ell_{C3} - \ell_3)]\ddot{\theta}_3 + [-\ell_{C1}m_1 - \ell_{C2}m_2 \\
& - \ell_{C3}m_3]\ddot{z}_s + [I_1 + I_2 + I_3 + m_1\ell_{C1}(\ell_{C1} - \ell_0) + m_2\ell_{C2}(\ell_{C2} - \ell_0) + m_3\ell_{C3} \\
& (\ell_{C3} - \ell_0)]\ddot{\theta}_s + [I_1 + I_2 + I_3 + m_1\ell_{C1}(\ell_{C1} - \ell_0) + m_2\ell_{C2}(\ell_{C2} - \ell_0) \\
& + m_3\ell_{C3}(\ell_{C3} - \ell_0)]\ddot{\theta}_0 + k_1\theta_1 + k_{\theta_{aero}}(\theta_3 + \theta_2 + \theta_1 + \theta_0 + \theta_s) \\
& + c_1\dot{\theta}_1 + c_{\theta_{aero}}(\dot{\theta}_3 + \dot{\theta}_2 + \dot{\theta}_1 + \dot{\theta}_0 + \dot{\theta}_s) = M_1
\end{aligned}$$

Assume that the balance and sting deflections are sinusoidal, e.g.,

$$\theta_j = \bar{\Theta}_j e^{i\omega t} \text{ and } z_s = \bar{Z}_s e^{i\omega t}.$$

$$\begin{aligned}
& A_1(-\omega^2 \bar{\Theta}_1) + B_1(-\omega^2 \bar{\Theta}_2) + C_1(-\omega^2 \bar{\Theta}_3) + D_1(-\omega^2 \bar{\Theta}_s) + E_1(-\omega^2 \bar{Z}_s) \\
& + F_1(-\omega^2 \bar{\Theta}_0) + k_1 \bar{\Theta}_1 + k_{\theta_{aero}}(\bar{\Theta}_3 + \bar{\Theta}_2 + \bar{\Theta}_1 + \bar{\Theta}_0 + \bar{\Theta}_s) + c_1 i \omega \bar{\Theta}_1 \\
& + c_{\theta_{aero}}(\bar{\Theta}_3 + \bar{\Theta}_2 + \bar{\Theta}_1 + \bar{\Theta}_0 + \bar{\Theta}_s) = \bar{M}_1
\end{aligned}$$

The constants A_1 through F_1 are defined in the preceding equation and are tabulated in Table 5.

Lagrange's Equation for Θ_3 , the aft moment gage deflection:

$$\frac{d}{dt} \left(\frac{\partial L}{\partial \dot{\theta}_3} \right) - \frac{\partial L}{\partial \theta_3} + \frac{\partial D}{\partial \dot{\theta}_3} = M_3$$

$$\begin{aligned}
& I_3(\ddot{\theta}_3 + \ddot{\theta}_2 + \ddot{\theta}_1 + \ddot{\theta}_0 + \ddot{\theta}_s) + m_3[\ddot{z}_s + \ell_0)\ddot{\theta}_0 + \ddot{\theta}_s) - \ell_2(\ddot{\theta}_1 + \ddot{\theta}_0 + \ddot{\theta}_s) \\
& (\ell_3 - \ell_2)(\ddot{\theta}_2 + \ddot{\theta}_1 + \ddot{\theta}_0 + \ddot{\theta}_s) - (\ell_{C3} - \ell_3)(\ddot{\theta}_3 + \ddot{\theta}_2 + \ddot{\theta}_1 + \ddot{\theta}_0 + \ddot{\theta}_s)] \\
& [- (\ell_{C3} - \ell_3)] + k_3\theta_3 - k_{\theta_{aero}}(\theta_3 + \theta_2 + \theta_1 + \theta_0 + \theta_s) + c_3\dot{\theta}_3 \\
& + c_{\theta_{aero}}(\dot{\theta}_3 + \dot{\theta}_2 + \dot{\theta}_1 + \dot{\theta}_0 + \dot{\theta}_s) = M_3
\end{aligned}$$

Note: $k_{z_{aero}}$ and $c_{z_{aero}}$ have been assumed to be negligible in arriving at the above equation.

$$\begin{aligned}
& [I_3 + m_3\ell_{C3}(\ell_{C3} - \ell_3)]\ddot{\theta}_1 + [I_3 + m_3(\ell_{C3} - \ell_2)(\ell_{C3} - \ell_3)]\ddot{\theta}_2 + [I_3 + m_3(\ell_{C3} - \ell_3)^2]\ddot{\theta}_3 \\
& + [- m_3(\ell_{C3} - \ell_3)]\ddot{z}_s + [I_3 + m_3(\ell_{C3} - \ell_0)(\ell_{C3} - \ell_3)]\ddot{\theta}_0 + [I_3 + m_3(\ell_{C3} - \ell_0) \\
& (\ell_{C3} - \ell_3)]\ddot{\theta}_s + k_3\theta_3 + k_{\theta_{aero}}(\theta_3 + \theta_2 + \theta_1 + \theta_0 + \theta_s) + c_3\dot{\theta}_3 + c_{\theta_{aero}}(\dot{\theta}_3 + \dot{\theta}_2 \\
& + \dot{\theta}_1 + \dot{\theta}_0 + \dot{\theta}_s) = M_3
\end{aligned}$$

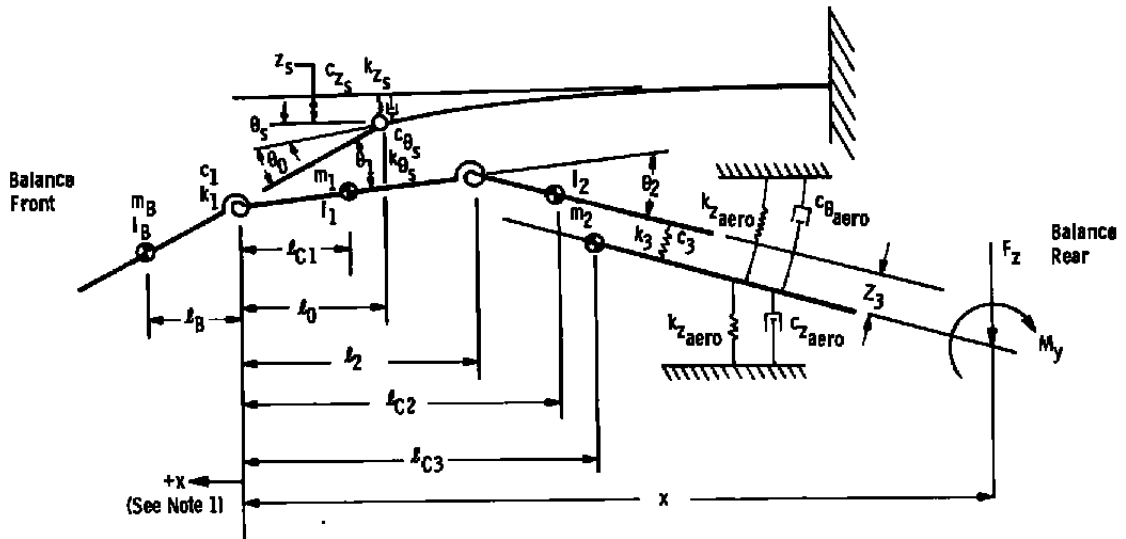
Assume that the balance and sting deflections are sinusoidal, e.g.,

$$\theta_j = \bar{\Theta}_j e^{i\omega t} \text{ and } z_s = \bar{Z}_s e^{i\omega t}$$

$$\begin{aligned}
& A_2(-\omega^2 \bar{\Theta}_1) + B_2(-\omega^2 \bar{\Theta}_2) + C_2(-\omega^2 \bar{\Theta}_3) + D_2(-\omega^2 \bar{\Theta}_s) - E_2(-\omega^2 \bar{Z}_s) \\
& + F_2(-\omega^2 \bar{\Theta}_0) + k_3 \bar{\Theta}_3 + k_{\theta_{aero}}(\bar{\Theta}_3 + \bar{\Theta}_2 + \bar{\Theta}_1 + \bar{\Theta}_0 + \bar{\Theta}_s) + c_3 i \omega \bar{\Theta}_3 \\
& + c_{\theta_{aero}} i \omega (\bar{\Theta}_3 + \bar{\Theta}_2 + \bar{\Theta}_1 + \bar{\Theta}_0 + \bar{\Theta}_s) = \bar{M}_3
\end{aligned}$$

The constants A_2 through F_2 are defined in the preceding equation and are tabulated in Table 5.

Derivation 2. The Force-Moment Balance Pitch Plane Equation Derivation



- Notes: (1) The constants l_B , l_0 , l_{C1} , l_{C2} , l_{C3} , and l_2 are measured positive (+) forward from the forward gage center.
- (2) F_z and M_y are the aerodynamic force and moment applied at some location (x) on the model surface.
- (3) For in-plane motion the terms involving the aerodynamic damping and spring constants should be omitted from the above illustration and from the derivation since they are the loads (F_z and M_y) being measured.
- (4) For out-of-plane motion $\theta_0 = 0$.

C.G. Translations:

$$z_B = z_s - (l_B - l_0)(\theta_0 + \theta_s)$$

$$z_{C1} = z_s + l_0(\theta_0 + \theta_s) - l_{C1}(\theta_0 + \theta_s + \theta_1)$$

$$z_{C2} = z_s + l_0(\theta_0 + \theta_s) - l_2(\theta_0 + \theta_s + \theta_1) - (l_{C2} - l_2)(\theta_2 + \theta_1 + \theta_0 + \theta_s)$$

$$z_{C3} = z_s + l_0(\theta_0 + \theta_s) - l_2(\theta_0 + \theta_1 + \theta_s) - (l_{C3} - l_2)(\theta_2 + \theta_1 + \theta_0 + \theta_s) + z_3$$

C.G. Translational Velocities:

$$\dot{z}_B = \dot{z}_s - (\ell_B - \ell_0)(\dot{\theta}_0 + \dot{\theta}_s)$$

$$\dot{z}_{C1} = \dot{z}_s + \ell_0(\dot{\theta}_0 + \dot{\theta}_s) - \ell_{C1}(\dot{\theta}_0 + \dot{\theta}_s + \dot{\theta}_1)$$

$$\dot{z}_{C2} = \dot{z}_s + \ell_0(\dot{\theta}_0 + \dot{\theta}_s) - \ell_2(\dot{\theta}_0 + \dot{\theta}_s + \dot{\theta}_1) - (\ell_{C2} - \ell_2)(\dot{\theta}_2 + \dot{\theta}_1 + \dot{\theta}_0 + \dot{\theta}_s)$$

$$\dot{z}_{C3} = \dot{z}_s + \ell_0(\dot{\theta}_0 + \dot{\theta}_s) - \ell_2(\dot{\theta}_0 + \dot{\theta}_1 + \dot{\theta}_s) - (\ell_{C3} - \ell_2)(\dot{\theta}_2 + \dot{\theta}_1 + \dot{\theta}_0 + \dot{\theta}_s) + \dot{z}_3$$

Kinetic Energy:

$$\begin{aligned} T = & \frac{1}{2}m_s\dot{z}_s^2 + \frac{1}{2}I_s\dot{\theta}_s^2 + \frac{1}{2}m_B[\dot{z}_s - (\ell_B - \ell_0)(\dot{\theta}_0 + \dot{\theta}_s)]^2 + \frac{1}{2}I_B(\dot{\theta}_0 + \dot{\theta}_s)^2 \\ & + \frac{1}{2}m_1[\dot{z}_s + \ell_0(\dot{\theta}_0 + \dot{\theta}_s) - \ell_{C1}(\dot{\theta}_0 + \dot{\theta}_s + \dot{\theta}_1)]^2 + \frac{1}{2}I_1(\dot{\theta}_0 + \dot{\theta}_s + \dot{\theta}_1)^2 \\ & + \frac{1}{2}m_2[\dot{z}_s + \ell_0(\dot{\theta}_0 + \dot{\theta}_s) - \ell_2(\dot{\theta}_0 + \dot{\theta}_s + \dot{\theta}_1) - (\ell_{C2} - \ell_2) \\ & (\dot{\theta}_0 + \dot{\theta}_s + \dot{\theta}_1 + \dot{\theta}_2)]^2 + \frac{1}{2}I_2[\dot{\theta}_0 + \dot{\theta}_s + \dot{\theta}_1 + \dot{\theta}_2]^2 + \frac{1}{2}m_3[\dot{z}_s + \ell_0 \\ & (\dot{\theta}_0 + \dot{\theta}_s) - \ell_2(\dot{\theta}_0 + \dot{\theta}_s + \dot{\theta}_1) - (\ell_{C3} - \ell_2)(\dot{\theta}_0 + \dot{\theta}_s + \dot{\theta}_1 + \dot{\theta}_2) \\ & + \dot{z}_3]^2 + \frac{1}{2}I_3(\dot{\theta}_0 + \dot{\theta}_s + \dot{\theta}_1 + \dot{\theta}_2)^2 \end{aligned}$$

Potential Energy:

$$\begin{aligned} V = & \frac{1}{2}k_{z_s}z_s^2 + \frac{1}{2}k_{\theta_s}\theta_s^2 + \frac{1}{2}k_1\theta_1^2 + \frac{1}{2}k_2\theta_2^2 + \frac{1}{2}k_3z_3^2 + \frac{1}{2}k_{z_{aero}} \\ & z_{C3}^2 + \frac{1}{2}k_{\theta_{aero}}(\theta_2 + \theta_1 + \theta_0 + \theta_s)^2 \end{aligned}$$

Dissipation Function:

$$\begin{aligned} D = & \frac{1}{2}c_{z_s}\dot{z}_s^2 + \frac{1}{2}c_{\theta_s}\dot{\theta}_s^2 + \frac{1}{2}c_1\dot{\theta}_1^2 + \frac{1}{2}c_2\dot{\theta}_2^2 + \frac{1}{2}c_3\dot{z}_3^2 + \frac{1}{2}c_{z_{aero}}\dot{z}_{C3}^2 \\ & + \frac{1}{2}c_{\theta_{aero}}(\dot{\theta}_2 + \dot{\theta}_1 + \dot{\theta}_0 + \dot{\theta}_s)^2 \end{aligned}$$

$$\text{Generalized Forces } (Q_i = \mathcal{F}_j \frac{\partial x_j}{\partial q_i}):$$

$$\mathcal{F}_1 = F_Z \quad x_1 = z = f(\theta_1, \theta_2, z_3, z_s, \theta_0, \theta_s)$$

$$\begin{aligned} z = & z_s + \ell_0(\theta_0 + \theta_s) - \ell_2(\theta_0 + \theta_1 + \theta_s) - (x - \ell_2) \\ & (\theta_2 + \theta_1 + \theta_0 + \theta_s) + z_3 \end{aligned}$$

$$\begin{aligned} \mathcal{F}_2 &= M_y & x_2 &= \theta \\ & & \theta &= \theta_2 + \theta_1 + \theta_0 + \theta_s \end{aligned}$$

$$q_1 = \theta_1$$

$$Q_1 = F_z \left(\frac{\partial z}{\partial \theta_1} \right) + M_y \left(\frac{\partial \theta}{\partial \theta_1} \right) = F_z(-x) + M_y'(1)$$

$$Q_1 = M_1 \equiv \text{the moment causing the deflection } \theta_1$$

$$q_3 = z_3$$

$$Q_3 = F_z \left(\frac{\partial z}{\partial z_3} \right) + M_y \left(\frac{\partial \theta}{\partial z_3} \right) = F_z(1) + M_y(0) = F_z$$

$$Q_3 = F_z \equiv \text{the force causing the deflection } z_3$$

Lagrange's Equation for θ_1 , the aft moment gage deflection:

$$\frac{d}{dt} \left(\frac{\partial L}{\partial \dot{\theta}_1} \right) - \frac{\partial L}{\partial \theta_1} + \frac{\partial D}{\partial \dot{\theta}_1} = M_1$$

$$\begin{aligned} & m_1[\ddot{z}_s + \ell_0(\ddot{\theta}_0 + \ddot{\theta}_s) - \ell_{C1}(\ddot{\theta}_0 + \ddot{\theta}_s + \ddot{\theta}_1)][-\ell_{C1}] + I_1[\ddot{\theta}_1 + \ddot{\theta}_0 + \ddot{\theta}_s] \\ & + m_2[\ddot{z}_s + \ell_0(\ddot{\theta}_0 + \ddot{\theta}_s) - \ell_2(\ddot{\theta}_1 + \ddot{\theta}_0 + \ddot{\theta}_s) - (\ell_{C2} - \ell_2)(\ddot{\theta}_2 + \ddot{\theta}_1 \\ & + \ddot{\theta}_0 + \ddot{\theta}_s)][-\ell_{C2}] + I_2[\ddot{\theta}_2 + \ddot{\theta}_1 + \ddot{\theta}_0 + \ddot{\theta}_s] + m_3[\ddot{z}_s + \ell_0(\ddot{\theta}_0 + \ddot{\theta}_s) \\ & - \ell_2(\ddot{\theta}_1 + \ddot{\theta}_0 + \ddot{\theta}_s) - (\ell_{C3} - \ell_2)(\ddot{\theta}_2 + \ddot{\theta}_1 + \ddot{\theta}_0 + \ddot{\theta}_s) + \ddot{z}_3][-\ell_{C3}] \\ & + I_3[\ddot{\theta}_2 + \ddot{\theta}_1 + \ddot{\theta}_0 + \ddot{\theta}_s] + k_1\theta_1 + k_{\theta_{aero}}(\theta_2 + \theta_1 + \theta_0 + \theta_s) + c_1\dot{\theta}_1 \\ & + c_{\theta_{aero}}(\dot{\theta}_2 + \dot{\theta}_1 + \dot{\theta}_0 + \dot{\theta}_s) = M_1 \end{aligned}$$

Note: $k_{\theta_{aero}}$ and $c_{\theta_{aero}}$ have been assumed to be negligible in arriving at the above equation.

$$\begin{aligned} & [m_1\ell_{C1}^2 + I_1 + m_2\ell_{C2}^2 + I_2 + m_3\ell_{C3}^2 + I_3]\ddot{\theta}_1 + [m_2\ell_{C2}(\ell_{C2} - \ell_2) + I_2 \\ & + m_3\ell_{C3}(\ell_{C3} - \ell_2) + I_3]\ddot{\theta}_2 + [-m_3\ell_{C3}]\ddot{z}_3 + [m_1\ell_{C1}(\ell_{C1} - \ell_0) + I_1 + m_2\ell_{C2} \\ & (\ell_{C2} - \ell_0) + I_2 + m_3\ell_{C3}(\ell_{C3} - \ell_0) + I_3]\ddot{\theta}_0 + [m_1\ell_{C1}(\ell_{C1} - \ell_0) + I_1 + m_2\ell_{C2} \\ & (\ell_{C2} - \ell_0) + I_2 + m_3\ell_{C3}(\ell_{C3} - \ell_0) + I_3]\ddot{\theta}_s + [-m_1\ell_{C1} - m_2\ell_{C2} - m_3\ell_{C3}]\ddot{z}_s \\ & + k_1\theta_1 + k_{\theta_{aero}}(\theta_2 + \theta_1 + \theta_0 + \theta_s) + c_1\dot{\theta}_1 + c_{\theta_{aero}}(\dot{\theta}_2 + \dot{\theta}_1 + \dot{\theta}_0 + \dot{\theta}_s) = M_1 \end{aligned}$$

Assume that the balance and sting deflections are sinusoidal, e.g.,

$$\theta_j = \bar{\Theta}_j e^{i\omega t} \text{ and } z_j = \bar{Z}_j e^{i\omega t}$$

$$\begin{aligned} & A_1(-\omega^2 \bar{\Theta}_1) + B_1(-\omega^2 \bar{\Theta}_2) + C_1(-\omega^2 \bar{Z}_3) + D_1(-\omega^2 \bar{\Theta}_s) + E_1(-\omega^2 \bar{Z}_s) \\ & + F_1(-\omega^2 \bar{\Theta}_0) + k_1 \bar{\Theta}_1 + k_{\theta_{aero}}(\bar{\Theta}_2 + \bar{\Theta}_1 + \bar{\Theta}_0 + \bar{\Theta}_s) + c_1 \omega i \bar{\Theta}_1 \\ & + c_{\theta_{aero}} \omega i (\bar{\Theta}_2 + \bar{\Theta}_1 + \bar{\Theta}_0 + \bar{\Theta}_s) = \bar{M}_1 \end{aligned}$$

The constants A_1 through F_1 are defined in the preceding equation and are tabulated in Table 4.

Lagrange's Equation for z_3 , the aft moment gage deflection:

$$\frac{d}{dt} \left(\frac{\partial L}{\partial \dot{z}_3} \right) - \frac{\partial L}{\partial z_3} + \frac{\partial D}{\partial \dot{z}_3} = F_z$$

$$\begin{aligned} & m_3[\ddot{z}_s + \ell_0(\ddot{\theta}_0 + \ddot{\theta}_s) - \ell_2(\ddot{\theta}_1 + \ddot{\theta}_0 + \ddot{\theta}_s) - (\ell_{C3} - \ell_2)(\ddot{\theta}_2 + \ddot{\theta}_1 + \ddot{\theta}_0 + \ddot{\theta}_s) \\ & + \ddot{z}_3] + k_3 z_3 + k_{zaero} z_{C3} + c_3 \dot{z}_3 + c_{zaero} \dot{z}_{C3} = F_z \\ & [-m_3 \ell_{C3}] \ddot{\theta}_1 + [-m_3(\ell_{C3} - \ell_2)] \ddot{\theta}_2 + [m_3(\ell_0 - \ell_{C3})] \ddot{\theta}_0 + [m_3(\ell_0 - \ell_{C3})] \ddot{\theta}_s \\ & + [m_3] \ddot{z}_s + [m_3] \ddot{z}_3 + k_3 z_3 + c_3 \dot{z}_3 = F_z \end{aligned}$$

Note: k_{zaero} and c_{zaero} have been assumed to be negligible in arriving at the above equation.

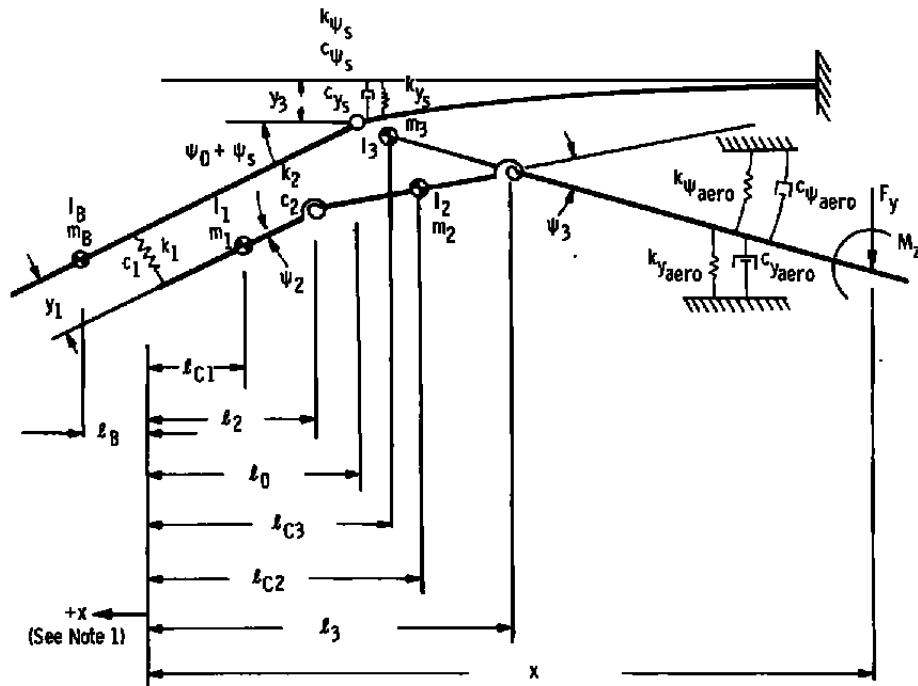
Assume that the balance and sting deflections are sinusoidal, e.g.,

$$\theta_j = \bar{\Theta}_j e^{i\omega t} \text{ and } z_j = \bar{Z}_j e^{i\omega t}$$

$$\begin{aligned} & A_2(-\omega^2 \bar{\Theta}_1) + B_2(-\omega^2 \bar{\Theta}_2) + C_2(-\omega^2 \bar{Z}_3) + D_2(-\omega^2 \bar{\Theta}_s) + E_2(-\omega^2 \bar{Z}_s) \\ & + F_2(-\omega^2 \bar{\Theta}_0) + k \bar{Z}_3 + c_3 \omega i \bar{Z}_3 = \bar{F}_z \end{aligned}$$

The constants A_2 through F_2 are defined in the preceding equation and are tabulated in Table 4.

Derivation 3. The Force-Moment Balance Yaw Plane Equation Derivation



- Notes: (1) The constants l_B , l_0 , l_{C1} , l_{C2} , l_{C3} , l_2 , and l_3 are measured positive (+) forward from the forward gage center.
 (2) F_y and M_z are the aerodynamic force and moment applied at some location (x) on the model surface.
 (3) For in-plane motion the terms involving the aerodynamic damping and spring constants should be omitted from the above illustration and from the derivation since they are the loads (F_y and M_z) being measured.
 (4) For out-of-plane motion $\theta_0 = 0$.

C.G. Translations:

$$y_B = y_s - (l_B - l_0)(\psi_0 + \psi_s)$$

$$y_{C1} = y_s + l_0(\psi_0 + \psi_s) + y_1$$

$$y_{C2} = y_s + l_0(\psi_0 + \psi_s) + y_1 - l_2(\psi_0 + \psi_s) - (l_{C2} - l_2)(\psi_2 + \psi_0 + \psi_s)$$

$$y_{C3} = y_s + (l_0 - l_2)(\psi_0 + \psi_s) + y_1 - (l_3 - l_2)(\psi_2 + \psi_0 + \psi_s) - (l_{C3} - l_3)(\psi_3 + \psi_2 + \psi_0 + \psi_s)$$

C.G. Translational Velocities:

$$\dot{y}_B = \dot{y}_s - (\ell_B - \ell_0)(\dot{\psi}_0 + \dot{\psi}_s)$$

$$\dot{y}_{C1} = \dot{y}_s + \ell_0(\dot{\psi}_0 + \dot{\psi}_s) + \dot{y}_1$$

$$\dot{y}_{C2} = \dot{y}_s + (\ell_0 - \ell_2)(\dot{\psi}_0 + \dot{\psi}_s) + \dot{y}_1 - (\ell_{C2} - \ell_2)(\dot{\psi}_2 + \dot{\psi}_0 + \dot{\psi}_s)$$

$$\begin{aligned} \dot{y}_{C3} = & \dot{y}_s + (\ell_0 - \ell_2)(\dot{\psi}_0 + \dot{\psi}_s) + \dot{y}_1 - (\ell_3 - \ell_2)(\dot{\psi}_2 + \dot{\psi}_0 + \dot{\psi}_s) \\ & - (\ell_{C3} - \ell_3)(\dot{\psi}_3 + \dot{\psi}_2 + \dot{\psi}_0 + \dot{\psi}_s) \end{aligned}$$

Kinetic Energy:

$$\begin{aligned} T = & \frac{1}{2}m_s\dot{y}_s^2 + \frac{1}{2}I_s\dot{\psi}_s^2 + \frac{1}{2}m_B[\dot{y}_s - (\ell_B - \ell_0)(\dot{\psi}_0 + \dot{\psi}_s)]^2 + \frac{1}{2}I_B(\dot{\psi}_0 + \dot{\psi}_s)^2 \\ & + \frac{1}{2}m_1[\dot{y}_s + \ell_0(\dot{\psi}_0 + \dot{\psi}_s) + \dot{y}_1]^2 + \frac{1}{2}I_1[\dot{\psi}_0 + \dot{\psi}_s]^2 \\ & + \frac{1}{2}m_2[\dot{y}_s + \dot{y}_1 + (\ell_0 - \ell_{C2})\dot{\psi}_0 + (\ell_0 - \ell_{C2})\dot{\psi}_s - (\ell_{C2} - \ell_2)\dot{\psi}_2]^2 \\ & + \frac{1}{2}I_2[\dot{\psi}_2 + \dot{\psi}_0 + \dot{\psi}_s]^2 + \frac{1}{2}m_3[\dot{y}_s + \dot{y}_1 + (\ell_0 - \ell_{C3})\dot{\psi}_0 + (\ell_0 - \ell_{C3})\dot{\psi}_s \\ & - (\ell_{C3} - \ell_2)\dot{\psi}_2 - (\ell_{C3} - \ell_3)\dot{\psi}_3]^2 + \frac{1}{2}I_3[\dot{\psi}_3 + \dot{\psi}_2 + \dot{\psi}_0 + \dot{\psi}_s]^2 \end{aligned}$$

Potential Energy:

$$\begin{aligned} V = & \frac{1}{2}k_{z_s}y_s^2 + \frac{1}{2}k_{\psi_s}\psi_s^2 + \frac{1}{2}k_1y_1^2 + \frac{1}{2}k_2\psi_2^2 + \frac{1}{2}k_3\psi_3^2 + \frac{1}{2}k_{y_{aero}} \\ & y_{C3}^2 + \frac{1}{2}k_{\psi_{aero}}(\psi_2 + \psi_1 + \psi_0 + \psi_s)^2 \end{aligned}$$

Dissipation Function:

$$\begin{aligned} D = & \frac{1}{2}c_{y_s}\dot{y}_s^2 + \frac{1}{2}c_{\psi_s}\dot{\psi}_s^2 + \frac{1}{2}c_1\dot{y}_1^2 + \frac{1}{2}c_2\dot{\psi}_2^2 + \frac{1}{2}c_3\dot{\psi}_3^2 + \frac{1}{2}c_{y_{aero}}\dot{y}_{C3}^2 \\ & + \frac{1}{2}c_{\psi_{aero}}(\dot{\psi}_2 + \dot{\psi}_1 + \dot{\psi}_0 + \dot{\psi}_s)^2 \end{aligned}$$

$$\text{Generalized Forces } (Q_i = \mathcal{F}_j \frac{\partial x_j}{\partial q_i}):$$

$$\mathcal{F}_1 = F_y \quad x_1 = y = f(y_1, \psi_2, \psi_3, y_s, \psi_s, \psi_0) = f(q_1, q_2, q_3, \dots)$$

$$y = y_s + (\ell_0 - \ell_2)(\psi_0 + \psi_s) - y_1 - (\ell_3 - \ell_2)$$

$$(\psi_2 + \psi_0 + \psi_s) - (x - \ell_3)(\psi_3 + \psi_2 + \psi_0 + \psi_s)$$

$$F_2 = M_z \quad x_2 = \psi$$

$$\psi = \psi_3 + \psi_2 + \psi_0 + \psi_s$$

$$q_1 = y_1$$

$$Q_1 = F_y \left(\frac{\partial y}{\partial y_1} \right) + M_z \left(\frac{\partial \psi}{\partial y_1} \right) = F_y(1) + M_z(0)$$

$$Q_1 = F_y = \text{the force causing the deflection } y_1$$

$$q_3 = \psi_3$$

$$Q_3 = F_y \left(\frac{\partial y}{\partial \psi_3} \right) + M_z \left(\frac{\partial \psi}{\partial \psi_3} \right) = -F_y(x - \ell_3) + M_z(1) = M_3$$

$$Q_3 = M_3 = \text{the moment causing the deflection } \psi_3$$

Lagrange's Equation for y_1 , the aft moment gage deflection:

$$\frac{d}{dt} \left(\frac{\partial L}{\partial \dot{y}_1} \right) - \frac{\partial L}{\partial y_1} + \frac{\partial D}{\partial \dot{y}_1} = F_y$$

$$\begin{aligned} m_1[\ddot{y}_s + \ell_0(\ddot{\psi}_0 + \ddot{\psi}_s) + \ddot{y}_1] + m_2[\ddot{y}_s + \ddot{y}_1 + (\ell_0 - \ell_{C2})\ddot{\psi}_0 + (\ell_0 - \ell_{C2})\ddot{\psi}_s \\ - (\ell_{C2} - \ell_2)\ddot{\psi}_2] + m_3[\ddot{y}_s + \ddot{y}_1 + (\ell_0 - \ell_{C3})\ddot{\psi}_0 + (\ell_0 - \ell_{C3})\ddot{\psi}_s - (\ell_{C3} - \ell_2)\ddot{\psi}_2 \\ - (\ell_{C3} - \ell_3)\ddot{\psi}_3] + k_1 y_1 + k_{yaero} y_{C3} + c_1 \dot{y}_1 + c_{yaero} \dot{y}_{C3} = F_y \end{aligned}$$

$$\begin{aligned} [m_1 + m_2 + m_3]\ddot{y}_1 + [-m_2(\ell_{C2} - \ell_2) - m_3(\ell_{C3} - \ell_2)]\ddot{\psi}_2 + [(-m_3) \\ (\ell_{C3} - \ell_3)]\ddot{\psi}_3 + [m_1 \ell_0 + m_2(\ell_0 - \ell_{C2}) + m_3(\ell_0 - \ell_{C3})]\ddot{\psi}_s + [m_1 + m_2 + m_3]\ddot{y}_s \\ + [m_1 \ell_0 + m_2(\ell_0 - \ell_{C2}) + m_3(\ell_0 - \ell_{C3})]\ddot{\psi}_0 + k_1 y_1 + c_1 \dot{y}_1 = F_y \end{aligned}$$

Note: k_{yaero} and c_{yaero} have been assumed to be negligible in arriving at the above equation.

Assume that the balance and sting deflections are sinusoidal, e.g.,

$$\psi_j = \bar{\Psi}_j e^{i\omega t} \text{ and } y_j = \bar{Y}_j e^{i\omega t}$$

$$\begin{aligned} A_1(-\omega^2 \bar{Y}_1) + B_1(-\omega^2 \bar{\Psi}_2) + C_1(-\omega^2 \bar{\Psi}_3) + D_1(-\omega^2 \bar{\Psi}_s) + E_1(-\omega^2 \bar{Y}_s) \\ + F_1(-\omega^2 \bar{\Psi}_0) + k_1 \bar{Y}_1 + c_1 i \omega \bar{Y}_1 = \bar{F}_y \end{aligned}$$

The constants A_1 through F_1 are defined in the preceding equation and are tabulated in Table 4.

Lagrange's Equation for ψ_3 , the aft moment gage deflection:

$$\frac{d}{dt} \left(\frac{\partial L}{\partial \dot{\psi}_3} \right) - \frac{\partial L}{\partial \psi_3} + \frac{\partial D}{\partial \dot{\psi}_3} = M_3$$

$$\begin{aligned} m_3[\ddot{y}_s + \ddot{y}_1 + (\ell_0 - \ell_{C3})\ddot{\psi}_0 + (\ell_0 - \ell_{C3})\ddot{\psi}_s - (\ell_{C3} - \ell_2)\ddot{\psi}_2 - (\ell_{C3} - \ell_3)\ddot{\psi}_3] \\ [- (\ell_{C3} - \ell_3)] + I_3[\ddot{\psi}_3 + \ddot{\psi}_2 + \ddot{\psi}_0 + \ddot{\psi}_s] + k_3\psi_3 + k_{\psi_{aero}}(\psi_3 + \psi_2 + \psi_0 + \psi_s) \\ + c_3\dot{\psi}_3 + c_{\psi_{aero}}(\dot{\psi}_3 + \dot{\psi}_2 + \dot{\psi}_0 + \dot{\psi}_s) = M_3 \end{aligned}$$

Note: $k_{\psi_{aero}}$ and $c_{\psi_{aero}}$ have been assumed to be negligible in arriving at the above equation.

$$\begin{aligned} [(-m_3)(\ell_{C3} - \ell_3)]\ddot{y}_1 + [I_3 + (m_3)(\ell_{C3} - \ell_2)(\ell_{C3} - \ell_3)]\ddot{\psi}_2 + [I_3 + (m_3) \\ (\ell_{C3} - \ell_3)^2]\ddot{\psi}_3 + [I_3 - (m_3)(\ell_{C3} - \ell_3)(\ell_0 - \ell_{C3})]\ddot{\psi}_s + [(-m_3)(\ell_{C3} - \ell_3)]\ddot{y}_s \\ + [I_3 - (m_3)(\ell_0 - \ell_{C3})(\ell_{C3} - \ell_3)]\ddot{\psi}_0 + k_3\psi_3 + k_{\psi_{aero}}(\psi_3 + \psi_2 + \psi_0 + \psi_s) + c_3\dot{\psi}_3 \\ + c_{\psi_{aero}}(\dot{\psi}_3 + \dot{\psi}_2 + \dot{\psi}_0 + \dot{\psi}_s) = M_3 \end{aligned}$$

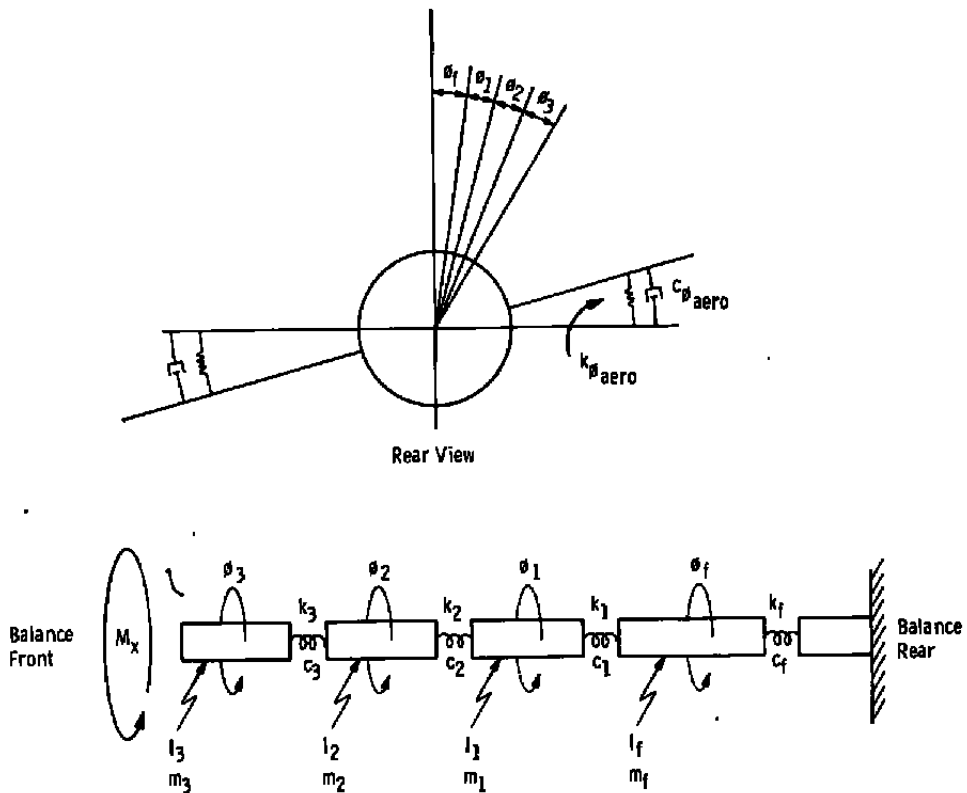
Assume that the balance deflections and sting deflections are sinusoidal, e.g.

$$\psi_j = \bar{\Psi}_j e^{i\omega t} \text{ and } y_j = \bar{Y}_j e^{i\omega t}$$

$$\begin{aligned} A_2(-\omega^2 \bar{Y}_1) + B_2(-\omega^2 \bar{Y}_2) + C_2(-\omega^2 \bar{Y}_3) + D_2(-\omega^2 \bar{Y}_s) - E_2(-\omega^2 \bar{Y}_s) \\ + F_2(-\omega^2 \bar{\Psi}_0) + k_3 \bar{\Psi}_3 + k_{\psi_{aero}}(\bar{\Psi}_3 + \bar{\Psi}_2 + \bar{\Psi}_0 + \bar{\Psi}_s) + c_3 \omega i \bar{\Psi}_3 \\ + c_{\psi_{aero}} \omega i (\bar{\Psi}_3 + \bar{\Psi}_2 + \bar{\Psi}_0 + \bar{\Psi}_s) = \bar{M}_3 \end{aligned}$$

The constants A_2 through F_2 are defined in the preceding equation and are tabulated in Table 4.

Derivation 4. The Roll Derivation



Note: The C.G.'s of the balance sections and the model are assumed to lie on the balance centerline, which is the axis of rotation in roll. Therefore, there are no translations or translational velocities.

Kinetic Energy:

$$T = \frac{1}{2} I_f \dot{\phi}_f^2 + \frac{1}{2} I_1 (\dot{\phi}_f + \dot{\phi}_1)^2 + \frac{1}{2} I_2 (\dot{\phi}_f + \dot{\phi}_1 + \dot{\phi}_2)^2 + \frac{1}{2} I_3 (\dot{\phi}_f + \dot{\phi}_1 + \dot{\phi}_2 + \dot{\phi}_3)^2$$

Potential Energy:

$$V = \frac{1}{2} k_1 \phi_1^2 + \frac{1}{2} k_2 \phi_2^2 + \frac{1}{2} k_3 \phi_3^2 + \frac{1}{2} k_f \phi_f^2 + \frac{1}{2} k_{\phi_{aero}} (\phi_1 + \phi_2 + \phi_3 + \phi_f)^2$$

Dissipation Function:

$$D = \frac{1}{2} c_f \dot{\phi}_f^2 + \frac{1}{2} c_1 \dot{\phi}_1^2 + \frac{1}{2} c_2 \dot{\phi}_2^2 + \frac{1}{2} c_3 \dot{\phi}_3^2 + \frac{1}{2} c_{\phi_{aero}} (\dot{\phi}_f + \dot{\phi}_1 + \dot{\phi}_2 + \dot{\phi}_3)^2$$

Generalized Force $\left(Q_j = \mathcal{F}_i \frac{\partial x_j}{\partial q_i} \right)$:

$$\mathcal{F}_1 = M_x \quad x_1 = \phi = f(\phi_1, \phi_2, \phi_3, \phi_f)$$

$$\phi = \phi_1 + \phi_2 + \phi_3 + \phi_f$$

$$q_1 = \phi_3$$

$$Q_1 = M_x \left(\frac{\partial \phi}{\partial \phi_3} \right) = M_x (1)$$

$Q_1 = M_x \equiv$ the rolling moment which causes the roll deflections

Lagrange's Equation for ϕ_2 , the mid-balance roll deflection:

$$\frac{d}{dt} \left(\frac{\partial L}{\partial \dot{\phi}_2} \right) - \frac{\partial L}{\partial \phi_2} + \frac{\partial D}{\partial \dot{\phi}_2} = M_x$$

$$I_2(\ddot{\phi}_f + \ddot{\phi}_1 + \ddot{\phi}_2) + I_3(\ddot{\phi}_f + \ddot{\phi}_1 + \ddot{\phi}_2 + \ddot{\phi}_3) + k_2\phi_2 + k_{\phi_{aero}}(\phi_1 + \phi_2 + \phi_3 + \phi_f) + c_2\dot{\phi}_2 + c_{\phi_{aero}}(\dot{\phi}_f + \dot{\phi}_1 + \dot{\phi}_2 + \dot{\phi}_3) = M_x$$

Since $I_2 \ll I_3$ and $k_{\phi_{aero}} \ll k_2$, the terms including these parameters are neglected.

Assume that the balance deflections are sinusoidal, i.e., $\phi_j = \bar{\Phi} e^{i\omega t}$.

$$\begin{aligned} & -\omega^2 I_3(\bar{\Phi}_f + \bar{\Phi}_1 + \bar{\Phi}_2 + \bar{\Phi}_3) + k_2 \bar{\Phi}_2 + c_2 \omega i \bar{\Phi}_2 + c_{\phi_{aero}} \omega i (\bar{\Phi}_f + \bar{\Phi}_1 + \bar{\Phi}_2 + \bar{\Phi}_3) \\ & + \bar{\Phi}_3) = \bar{M}_x \\ & \left[1 - \frac{\omega^2 I_3}{k_2 \bar{\Phi}_2} (\bar{\Phi}_f + \bar{\Phi}_1 + \bar{\Phi}_2 + \bar{\Phi}_3) \right] k_2 \bar{\Phi}_2 + c_2 \omega i \bar{\Phi}_2 \\ & + c_{\phi_{aero}} \omega i (\bar{\Phi}_f + \bar{\Phi}_1 + \bar{\Phi}_2 + \bar{\Phi}_3) = \bar{M}_x \end{aligned}$$

$$\text{Substitution: } \bar{\Phi}_f + \bar{\Phi}_1 + \bar{\Phi}_2 + \bar{\Phi}_3 = \bar{\Phi}_{TOTAL} = \frac{k_2 \bar{\Phi}_2}{k_{total}}$$

$$\bar{\Phi}_f + \bar{\Phi}_1 + \bar{\Phi}_2 + \bar{\Phi}_3 = k_2 \bar{\Phi}_2 \left(\frac{1}{k_{total}} \right)$$

$$\left[1 - \omega^2 I_3 \left(\frac{1}{k_{total}} \right) \right] k_2 \bar{\Phi}_2 + c_2 \omega i \bar{\Phi}_2 + c_{\phi_{aero}} \omega i (\bar{\Phi}_f + \bar{\Phi}_1 + \bar{\Phi}_2 + \bar{\Phi}_3) = \bar{M}_x$$

$$\text{Substitution: } \frac{I_3}{k_{\text{total}}} = \frac{1}{\omega_{n\text{total}}^2}$$

$$\left[1 - \left(\frac{\omega}{\omega_{n\text{total}}}\right)^2\right] k_2 \bar{\Phi}_2 + c_2 \omega i \bar{\Phi}_2 + c_{\phi\text{aero}} \omega i (\bar{\Phi}_f + \bar{\Phi}_1 + \bar{\Phi}_2 + \bar{\Phi}_3) = \bar{M}_x$$

$$\text{Substitution: } k_2 \bar{\Phi}_2 = M'_x$$

$M'_x \equiv$ the apparent moment measured by the rolling moment gage element as determined using a static calibration sensitivity.

$$\left[1 - \left(\frac{\omega}{\omega_{n\text{total}}}\right)^2\right] M'_x + \frac{c_2}{k_2} \omega i M'_x + c_{\phi\text{aero}} \omega i \bar{\Phi}_{\text{total}} = \bar{M}_x$$

$$\text{Substitution: } \bar{\Phi}_{\text{total}} = \frac{M'_x}{k_{\text{total}}}$$

$$\left[1 - \left(\frac{\omega}{\omega_{n\text{total}}}\right)^2\right] \bar{M}'_x + \frac{c_2}{k_2} \omega i \bar{M}'_x + \frac{c_{\phi\text{aero}}}{k_{\text{total}}} \omega i \bar{M}'_x = \bar{M}_x$$

$$\left\{ \left[1 - \left(\frac{\omega}{\omega_{n\text{total}}}\right)^2\right] + \omega i \left[\frac{c_2}{k_2} + \frac{c_{\phi\text{aero}}}{k_{\text{total}}} \right] \right\} \bar{M}'_x = \bar{M}_x$$

APPENDIX C

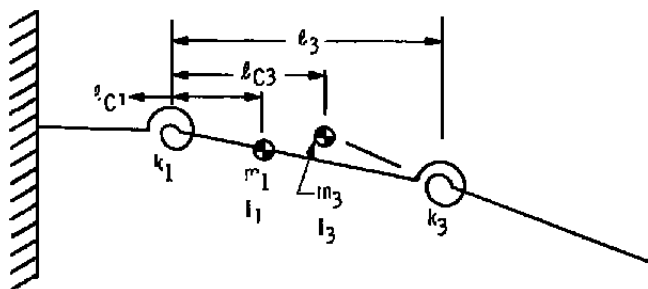
THE DETERMINATION OF CONSTANTS NEEDED FOR DATA REDUCTION

Basically there are three types of constants that must be determined before the complete equations of balance motion can be used: (1) moment of inertia and mass constants along with c.g. locations, (2) spring constants, and (3) damping constants.

The first type of constants can usually be fairly accurately determined from balance and model dimensions and the density of the material from which they are constructed. The moments of inertia of some aerodynamic models are somewhat more difficult to obtain than the balance inertias since the models often have irregularly shaped surfaces for which it is hard to calculate a volume. However, through the use of a torque tube or possibly using a trifler pendulum it is possible to obtain these inertias to within less than one percent uncertainty.

The second type of constant, the spring constant, is somewhat more difficult to obtain. To most accurately model the system, all degrees of freedom permitted by the balance/sting system must be included in the equations of motion, and a spring constant must be determined for each of the flexible elements permitting a degree of freedom. However, each balance is designed and gaged for particular primary degrees of freedom, and other extraneous degrees of freedom than those which are gaged and monitored are considered negligible. The confirmation of these primary degrees of freedom and the determination of these spring constants using holographic interferometry are discussed in detail in Appendix A. Besides this load versus deflection technique, it is also possible to determine the spring constants from knowledge of the masses and moments of inertias, as discussed above, and balance mode frequencies measured with the C.C. balance mounted to a rigid support (inertial reference frame).

As an example, a solution is given below for the spring constants of a 2-DOF moment balance on which a known mass is mounted and for which the masses of the "floating" balance sections are known. This is a model that could be used for the moment balance if the central roll gage element is considered rigid in pitch. A simplified sketch of the system is given below.



The characteristic equation for such a 2-DOF system is

$$\lambda^4(m_{11}m_{22} + m_{12}^2) - \lambda^2(k_3m_{11} + k_1m_{22}) + k_1k_3 = 0$$

or

$$\lambda^4(a) - \lambda^2(b) + c = 0$$

where a, b, and c are equation constants to be determined, and where the mass terms m_{11} , m_{12} , and m_{22} are defined below.

$$m_{11} = I_1 + m_1\ell_{C1}^2 + I_3 + m_3\ell_{C3}^2$$

$$m_{22} = I_3 + m_3(\ell_3 + \ell_{C3})^2$$

$$m_{12} = m_{21} = I_3 + m_3\ell_{C3}(\ell_3 + \ell_{C3})$$

If the balance is mounted to a rigid support, the mode frequencies of such a 2-DOF system are fairly easy to distinguish when a spectral analyzer is used to display the frequency content of the freely oscillating balance. Defining these frequencies as

$$\lambda_1 = \text{frequency of 1st mode}$$

$$\lambda_2 = \text{frequency of 2nd mode}$$

they can be used in the above characteristic equation to yield two equations in two unknowns.

$$a\lambda_1^4 - b\lambda_1^2 + c = 0$$

$$a\lambda_2^4 - b\lambda_2^2 + c = 0$$

These two equations can be solved for b/a and c/a.

From the identities

$$b/a = \frac{k_3m_{11} + k_1m_{22}}{m_{11}m_{22} + m_{12}^2} \text{ and } c/a = \frac{k_1k_3}{m_{11}m_{22} + m_{12}^2}$$

and the known mass constants, m_{11} , m_{12} , and m_{22} , the spring constants k_1 and k_3 can be determined.

Aside from the mechanical spring constants themselves, the free-stream flow over the model surface also provides a restoring moment which can be thought of as a spring constant. This constant, $k_{\theta_{aero}}$ or $k_{\phi_{aero}}$, must be obtained from previous static stability tests or dynamic stability, direct derivative tests. While they are included in the initial steps of the derivations in Appendix B, they have been neglected in the final equations since they are relatively small compared to the balance spring constants. In most cases they would represent much less than one percent of the total spring constant.

The third type of constant, the damping constant, can be divided into two categories: (1) the aerodynamic damping constants such as $c_{\theta_{aero}}$ and $c_{\phi_{aero}}$, and (2) the mechanical damping constants of the balance gage elements. As with the aerodynamic spring constants the aerodynamic damping constants must be known from previous dynamic stability, direct derivative tests. Unlike the aerodynamic spring constants, the aerodynamic damping constants cannot be neglected in the equations of motion. They could be of the same magnitude or larger than the mechanical damping constants. An example showing the effects of neglecting the aerodynamic damping constants on a typical test is given in Appendix D.

The mechanical damping constants can be determined in the laboratory before a test using a similar procedure to that used to obtain C.F. balance mechanical damping constants. When the dual balance system with an attached model or calibration body is oscillated in a vacuum, the aerodynamic force and aerodynamic damping terms drop out. By using a calibration body with known cross products of inertia, a known load can be applied to the balance. This load will have a real component only, i.e., it will have zero phase with respect to the impressed balance motion, since it is strictly an inertial load. Using the equation of motion for the moment balance as an example, the complete equation of motion,

$$- \omega^2(A_1 \bar{\Theta}_1 + B_1 \bar{\Theta}_2 + C_1 \bar{\Theta}_3 + D_1 \bar{\Theta}_s + E_1 \bar{Z}_s + F_1 \bar{\Theta}_0) + k_1 \bar{\Theta}_1 + c_1 \omega i \bar{\Theta}_1 + c_{\theta_{aero}} \omega i (\bar{\Theta}_3 + \bar{\Theta}_2 + \bar{\Theta}_1 + \bar{\Theta}_s + \bar{\Theta}_0) = \bar{M}_1$$

takes the form

$$c_1 \omega i \bar{\Theta}_1 = \omega^2(A_1 \bar{\Theta}_1 + B_1 \bar{\Theta}_2 + C_1 \bar{\Theta}_3 + D_1 \bar{\Theta}_s + E_1 \bar{Z}_s + F_1 \bar{\Theta}_0) - k_1 \bar{\Theta}_1 + \bar{M}_1$$

or

$$c_1 i = \omega A_1 + \left\{ \omega B_1 \frac{\bar{\Theta}_2}{\bar{\Theta}_1} + \omega C_1 \frac{\bar{\Theta}_3}{\bar{\Theta}_1} + \omega D_1 \frac{\bar{\Theta}_s}{\bar{\Theta}_1} + \omega E_1 \frac{\bar{Z}_s}{\bar{\Theta}_1} + \omega F_1 \frac{\bar{\Theta}_0}{\bar{\Theta}_1} - \frac{k_1}{\omega} + \frac{\bar{M}_1}{\omega \bar{\Theta}_1} \right\}$$

Therefore, c_1 is equal to the imaginary part of the bracketed term, and the real part should be equal to zero. In a similar manner any of the balance equations of motion can be solved for the mechanical damping constants if the system is oscillated under vacuum.

The roll equation of motion poses a somewhat different problem. In this particular equation [Eq. (2) of Table 3], the constant c_2/k_2 is required. A simple approach to obtaining this combined constant can be used if the total system damping is known, similar to the case described by Buchanan in Ref. 4.

For a single-degree-of-freedom roll system, the equation of motion takes the form

$$I_2 \ddot{\phi}_2 + c_2 \dot{\phi}_2 + k_2 \phi_2 = M$$

or

$$-\omega^2 I_2 \bar{\Phi}_2 + c_2 \omega i \bar{\Phi}_2 + k_2 \bar{\Phi}_2 = \bar{M}$$

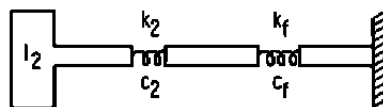
where the displacement ϕ_2 takes the form $\phi_2 = \bar{\Phi}_2 e^{i\omega t}$ and the resulting moment is assumed to take the form $\bar{M} e^{i\omega t}$. For a two-degree-of-freedom roll system, where the two degrees of freedom are considered to be the rolling motion of the roll gage of the C.C. balance and the rolling motion of the C.F. balance, the equation takes the form

$$I_2 (\ddot{\phi}_2 + \ddot{\phi}_f) + c_2 \dot{\phi}_2 + k_2 \phi_2 = M$$

or

$$-\omega^2 I_2 (\bar{\Phi}_2 + \bar{\Phi}_f) + c_2 \omega i \bar{\Phi}_2 + k_2 \bar{\Phi}_2 = \bar{M}$$

In this particular equation I_2 is the total inertia supported by the series of two springs, k_2 and k_f as shown below.



The primary difference between the equations of the two different systems is that the deflection in the inertia term of the 2-DOF system includes the deflection of both springs. For a general static moment M , this total deflection can be rewritten as follows.

$$\phi_{\text{total}} = \frac{M}{k_{\text{total}}} = M \left(\frac{1}{k_2} + \frac{1}{k_f} \right) = \phi_2 \left(1 + \frac{k_2}{k_f} \right)$$

where

$$M = k_2 \phi_2 = k_f \phi_f$$

The 2-DOF equation now takes the form

$$- \omega^2 I_2 \left(1 + \frac{k_2}{k_f} \right) \bar{\Phi}_2 + c_2 \omega i \bar{\Phi}_2 + k_2 \bar{\Phi}_2 = \bar{M}$$

If the term $(1 + k_2/k_f)I_2$ is looked upon as an effective mass, then this equation takes the same form as the 1-DOF equation, which can be written in the form

$$\ddot{\phi}_2 + 2\zeta \omega_n \dot{\phi}_2 + \omega_n^2 \phi_2 = \omega_n^2 \frac{M}{k_2} e^{i\omega t} + \gamma$$

where

$$\omega_n = \sqrt{\frac{k_2}{I_2(1 + k_2/k_f)}}$$

and

$$\zeta = \frac{c_2}{2I_2(1 + k_2/k_f)\omega_n} = \frac{c_2 \omega_n}{2k_2}$$

The solution for this system results in the definition of γ and $k_2 \Phi_2/M$ as follows:

$$\gamma = \tan^{-1} \frac{2\zeta \frac{\omega}{\omega_n}}{1 - (\frac{\omega}{\omega_n})^2}$$

$$\frac{k_2 \Phi_2}{M} = \frac{1}{\sqrt{(1 - \frac{\omega}{\omega_n})^2 + 4\zeta^2 (\frac{\omega}{\omega_n})^2}}$$

By experimentally determining γ and $k_2 \Phi_2/M$, commonly referred to as magnification factor μ , for several values of ω/ω_n , the value of ζ and ω_n can be determined through a curve-fitting process as was done by Buchanan (Ref. 4). Knowing ζ , the value of c_2 can be determined if k_2 and k_f are known, which requires another laboratory procedure. However, this can be avoided because only the ratio c_2/k_2 is required in the roll equation of motion. From the definition of ζ , the term c_2/k_2 can be defined as

$$\frac{c_2}{k_2} = \frac{2\zeta}{\omega_n}$$

where ω_n is the natural frequency of the total system in roll. Although for this 2-DOF system there would be two mode frequencies, the mass between the two springs is relatively small. For practical purposes the system behaves like a 1-DOF system with the primary mode frequency showing up as the above-mentioned single natural frequency. This has been confirmed by experiment.

APPENDIX D

THE EFFECT OF NEGLECTING THE AERODYNAMIC DAMPING CONSTANT FROM THE DATA REDUCTION PROCEDURE

As discussed in Sec. 3.0 and Appendix B, the complete equations of motion require both mechanical damping constants and aerodynamic damping constants. In some cases the aerodynamic damping constants may not be available, and it becomes a question of how accurate the dynamic moment can be if the aerodynamic damping is neglected. There is no general answer to this question because the aerodynamic moment depends on so many other parameters besides aerodynamic damping. To illustrate this point the roll equation of motion will be used with some typical input constants from a previous test run with a dual-balance system. When all of the constants in the roll equation of motion are input it simplifies from

$$\left\{ \left[1 - \left(\frac{\omega}{\omega_{n\text{total}}} \right)^2 \right] + i\omega \left[\frac{c_2}{k_2} + \frac{c_{\phi\text{aero}}}{k_{\text{total}}} \right] \right\} \bar{M}'_x = \bar{M}_x$$

to

$$\left\{ \left(\frac{1}{\mu} \right) e^{i\Delta\gamma} \right\} \bar{M}'_x = \bar{M}_x.$$

The vector constant by which the measured moment is multiplied serves to demagnify and phase shift the measured moment \bar{M}'_x to yield the aerodynamic load \bar{M}_x . The demagnification constant $1/\mu$ would normally not show a significant effect from ignoring $c_{\phi\text{aero}}$ since $c_{\phi\text{aero}}/k_{\text{total}}$ is much less than one in most cases. The effect on phase shift ($\Delta\gamma$) would normally be more significant since $\Delta\gamma$ varies directly with the imaginary part (damping term) for small angles. Therefore, in terms of the final result \bar{M}_x , the primary error resulting from ignoring $c_{\phi\text{aero}}$ would be in the form of a phase error.

Using the mechanical characteristics of the 4,000-lb dual balance roll derivative system used for the roll tests described in Ref. 4, $1/\mu$ and $\Delta\gamma$ are plotted in Fig. D-1 versus aerodynamic damping for several values of balance system natural frequency in roll, which was varied by changing roll moment of inertia I_x . As mentioned above, the phase shift $\Delta\gamma$ is affected significantly while the demagnification constant sees little change. In Fig. D-2 this phase angle shift is shown in terms of percent error in phase angle for several values of neglected aerodynamic damping constants. As would be expected, the errors get very large for small values of phase angle.

Considering that aerodynamic cross or cross-coupling moments will have small phase angles, and considering the errors which could result if all of the damping constants are not well defined, the future of these measurements might be considered bleak at best. However, below a certain threshold level of cross or cross-coupling damping, these derivatives will be of little concern to the aircraft stability anyway, and can be ignored. The high uncertainty in damping measurements is unimportant. In fact, it might be more correct to quote cross and cross-coupling moments in their vector form with an absolute uncertainty in phase angle rather than to divide the moment into its in-phase and out-of-phase (with position) components.

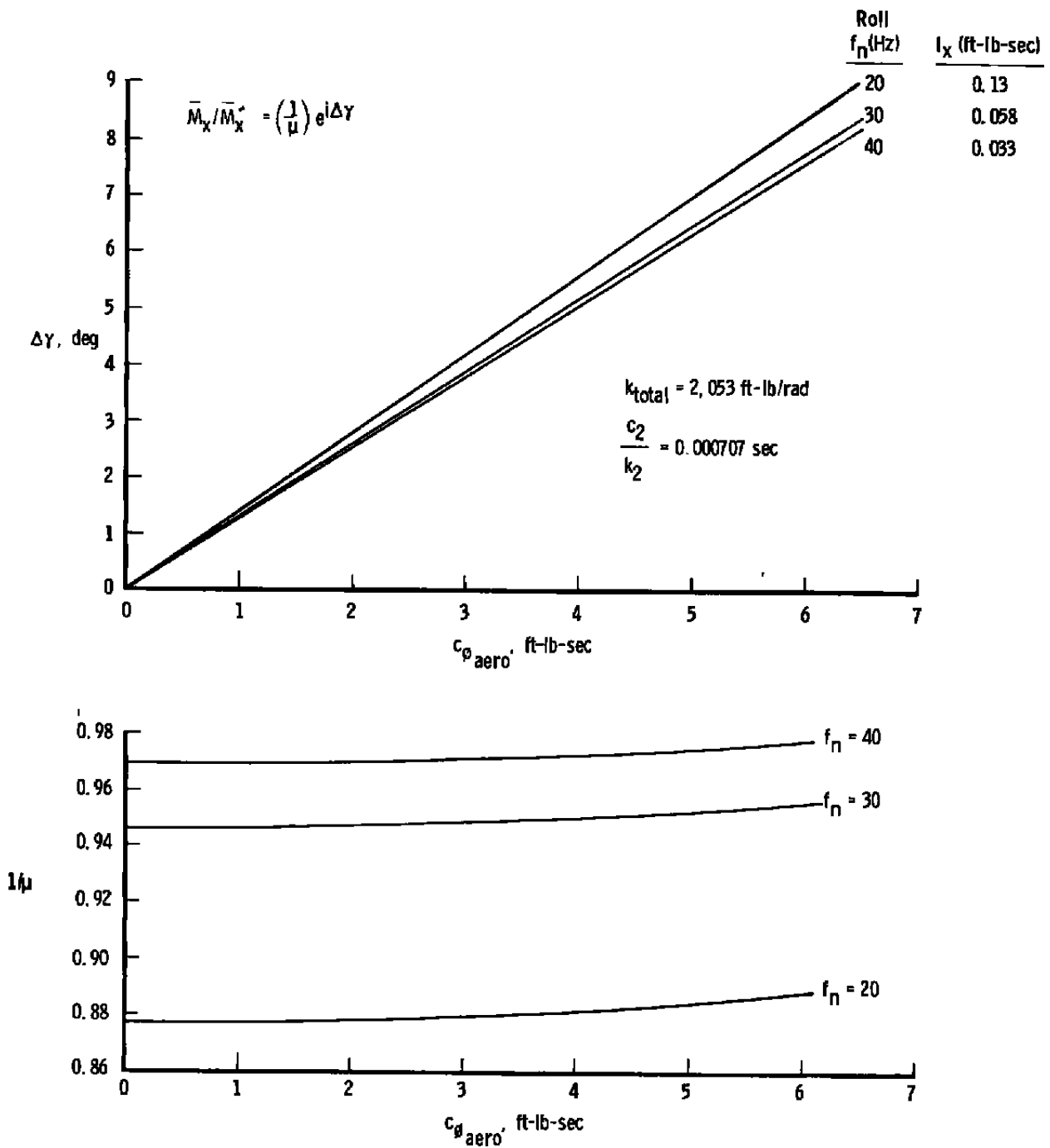
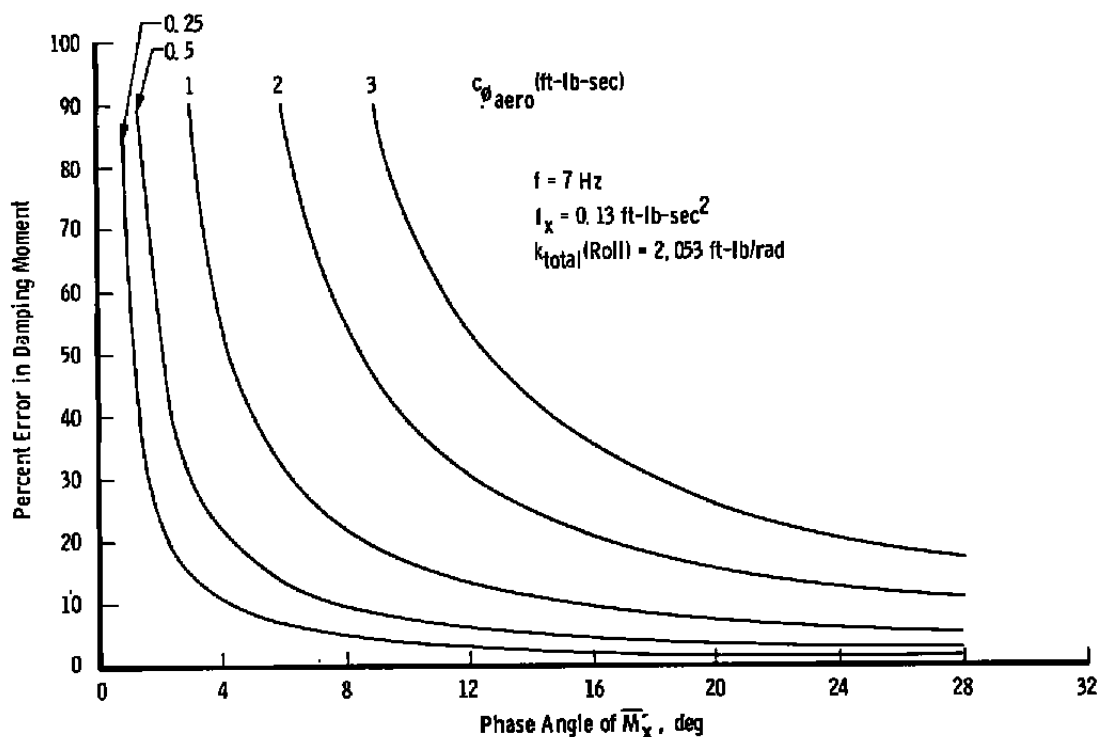
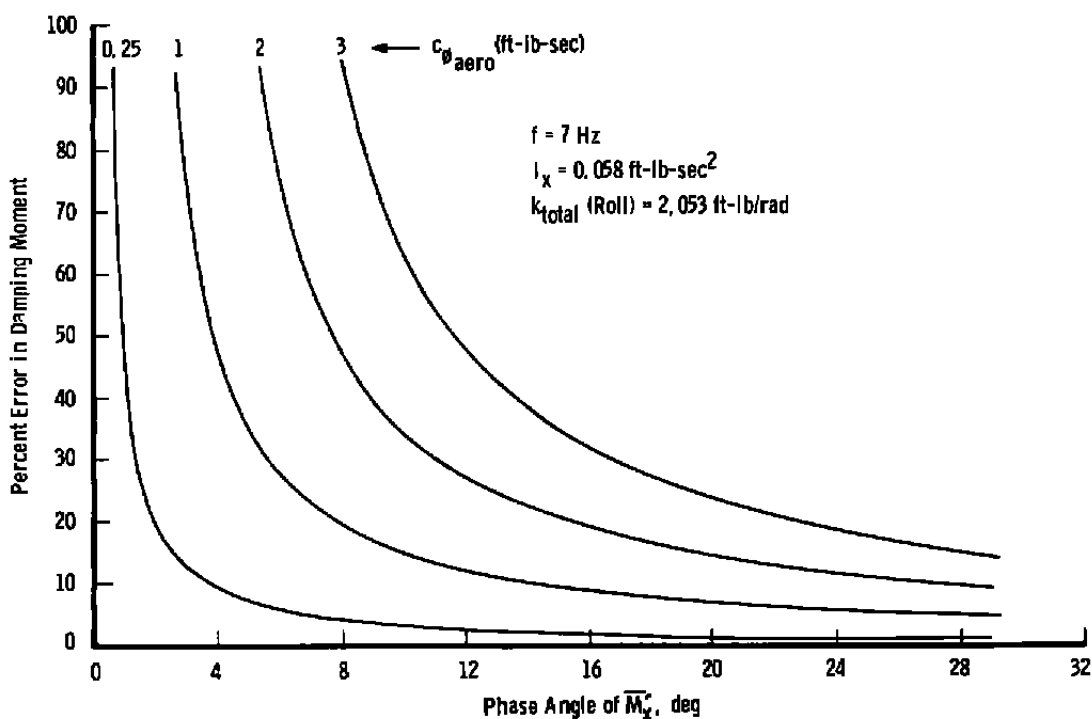


Figure D-1. Magnification and phase shift effects due to $c_{\phi_{aero}}$.

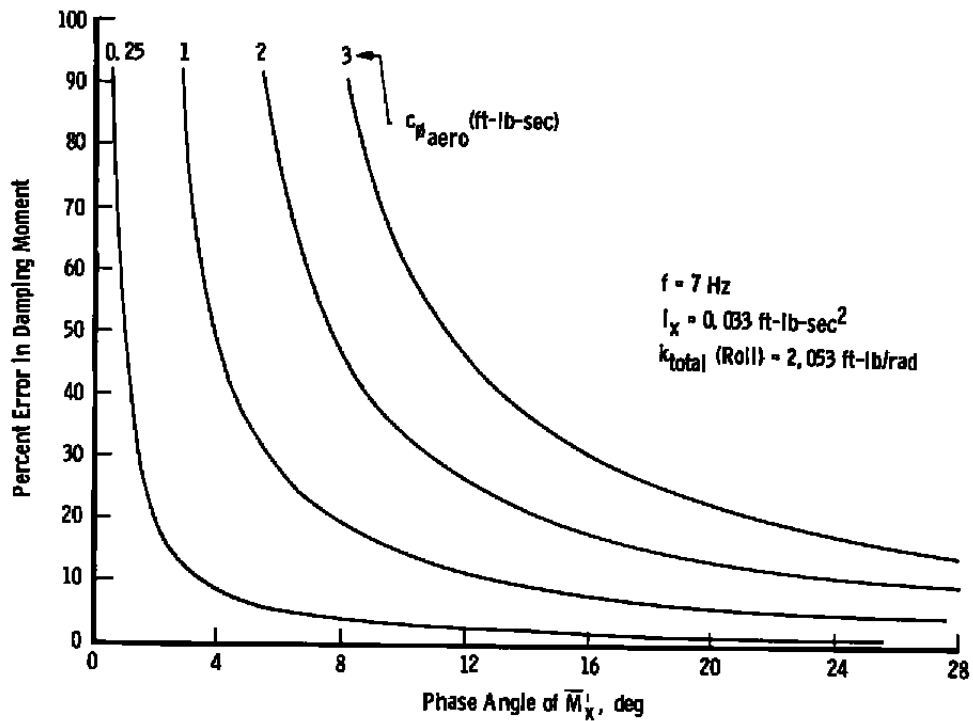


a. $f_n(\text{Roll}) = 20 \text{ Hz}$



b. $f_n(\text{Roll}) = 30 \text{ Hz}$

Figure D-2. The possible error in cross-coupling roll damping moment resulting from neglecting $c_{\phi_{aero}}$.



c. $f_n(\text{Roll}) = 40 \text{ Hz}$
 Figure D-2. Concluded.

NOMENCLATURE

a	Real part of a complex number
b	Imaginary part of a complex number
c	Damping coefficient, ft-lb-sec/rad or lb-sec/ft
\bar{c}	Wing mean aerodynamic chord, ft
c_j	The damping force or moment attributable to the jth component ft-lb-sec/rad or lb-sec/ft
C_l	Rolling moment coefficient
C_{l_q}	$\partial C_l / \partial (q\bar{c}/2V_\infty)$, rad^{-1}
C_{l_α}	Slope of C_l versus α curve, $\partial C_l / \partial \alpha$, rad^{-1}
$C_{l_{\dot{\alpha}}}$	$\partial C_l / \partial (\dot{\alpha}\bar{c}/2V_\infty)$, rad^{-1}
C.R.	Center of rotation
$c_{y_{\text{aero}}}$	Translational aerodynamic damping coefficient in the yaw plane, lb-sec/ft
c_{y_s}	Translational sting damping coefficient in the yaw plane, lb-sec/ft
$c_{z_{\text{aero}}}$	Translational aerodynamic damping coefficient in the pitch plane, lb-sec/ft
c_{z_s}	Translational sting damping coefficient in the pitch plane, lb-sec/ft
$c_{\theta_{\text{aero}}}$	Rotational aerodynamic damping coefficient in pitch, ft-lb-sec
c_{θ_s}	Rotational sting damping coefficient in pitch, ft-lb-sec
$c_{\phi_{\text{aero}}}$	Rotational aerodynamic damping coefficient in roll, ft-lb-sec
$c_{\psi_{\text{aero}}}$	Rotational aerodynamic damping coefficient in yaw, ft-lb-sec
c_{ψ_s}	Rotational sting damping coefficient in yaw, ft-lb-sec
D	Energy dissipation function, ft-lb/sec
E	Voltage
F	Force, lb
f	Oscillation frequency of C.F. balance, Hz

\mathcal{F}_j	Load applied to a balance in one of the six degrees of freedom, i.e., a force in the direction of or a moment about one of the three Cartesian coordinate axes, lb or ft-lb
\bar{F}_j	Force vector measured by the jth component, $\bar{F}_j = F_j e^{i\gamma_j}$
F_j	Magnitude of the force vector of the jth component, lb
f_n	Natural frequency, Hz
F_y	Force parallel to the balance y axis, lb
F_z	Force parallel to the balance z axis, lb
F_θ	Force proportional to angular position i.e., the component of the force vector which is in phase with the oscillatory deflection vector $\bar{\Theta}_T$, lb
$F_\dot{\theta}$	Force proportional to angular velocity, i.e., the component of the force vector which is 90-deg out-of-phase with the oscillatory deflection vector Θ_T , lb
i	$\sqrt{-1}$ (when not used as a dummy subscript)
I_j	Mass moment of inertia supported by the jth component (see Figs. 3 through 6 and Figs. 8 through 10), slug ft ²
I_x	Mass moment of inertia about the x axis, slug ft ²
I_{xy}	Cross product of inertia relative to the xy plane, slug ft ²
k_f	Spring constant of a pitch/yaw cross flexure balance in roll, ft-lb/rad
k_j	Spring constant of the jth component, lb/ft or ft-lb/rad
k_{total}	Resultant spring constant of a system having two or more springs in series, lb/ft or ft-lb/rad
$k_{y_{aero}}$	Translational aerodynamic spring constant in the yaw plane, lb/ft (assumed to be zero)
k_{y_s}	Translational spring constant of the sting in the yaw plane, lb/ft
$k_{z_{aero}}$	Translational aerodynamic spring constant in the pitch plane, lb/ft (assumed to be zero)
k_{z_s}	Translational spring constant of the sting in the pitch plane, lb/ft
$k_{\theta_{aero}}$	Rotational aerodynamic spring in the pitch plane, ft-lb/rad

k_{θ_s}	Rotational spring constant of the sting in the pitch plane, ft-lb/rad
$k_{\phi_{aero}}$	Rotational aerodynamic spring constant in roll, ft-lb/rad
$k_{\psi_{aero}}$	Rotational aerodynamic spring constant in the yaw plane, ft-lb/rad
k_{ψ_s}	Rotational spring constant of the sting in the yaw plane, ft-lb/rad
L	Lagrangian function, T-V, ft-lb
ℓ_j	The distance from the forward C.C. balance gage to the jth component, ft
m	Mass, slug
M	Moment, ft-lb
m_j	Mass supported by the jth component, slug (See Figs. 3 through 6 and Figs. 8 through 10)
M_j	Amplitude of the vector moment about the jth component, ft-lb
\overline{M}_j	Vector moment about the jth component, ft-lb
\overline{M}_{REF}	Moment vector about a designated model reference point, ft-lb
M_x	Moment about the balance x axis, ft-lb
\overline{M}_x	Vector moment about balance x axis, ft-lb
M_y	Moment in the balance pitch plane, ft-lb
M_z	Moment in the balance yaw plane, ft-lb
M_{θ}	Moment proportional to angular position, i.e., the component of the moment vector which is in-phase with the oscillating deflection vector $\overline{\theta}_T$, ft-lb
$M_{\dot{\theta}}$	Moment proportional to angular velocity, i.e. the component of the moment vector which is in-phase with the oscillatory deflection vector $\overline{\Theta}_T$, ft-lb
$m_{11},$ $m_{12},$ m_{21}, m_{22}	Inertia terms appearing in the characteristic equation of a 2-degree-of-freedom spring - mass system, slug ft ²
q	Rotational velocity in pitch, rad/sec

Q_j	Generalized force relative to the j th component, lb or ft-lb
q_j	Generalized coordinate, ft or rad
s	Gage sensitivity, volt/lb or volt/ft-lb
T	Kinetic energy, ft-lb
t	Time, sec
V	Potential energy, ft-lb
V_∞	Free-stream velocity, ft/sec
x	Distance from balance forward gage station measured along balance axis, ft (see sign conventions on Figs. 1 and 2)
y_j	Translational deflection in y -axis direction of the j th component, ft (see sign conventions on Figs. 1 and 2)
Y_j	Magnitude of the translational deflection vector of the j th component in the y direction, ft
\overline{Y}_j	Translational deflection vector of the j th component in the y direction, ft
z_j	Translational deflection in the z -axis direction of the j th component, ft (see sign conventions on Figs. 1 and 2)
Z_j	Magnitude of the translational deflection vector of the j th component in the z direction, ft
\overline{Z}_j	Translational deflection vector of the j th component in the z direction, ft
α	Angle of attack, deg or rad
γ_j	Phase of the load vector or the deflection vector of the j th component, deg or rad
γ_{TF}	Phase of force vector relative to the total deflection vector $\overline{\Theta}_T$, deg or rad
γ_{TM}	Phase of moment vector relative to the total deflection vector $\overline{\Theta}_T$, deg or rad
ζ	Damping factor, $\zeta = c/2m\omega_n$
θ_j	Pitch plane rotational deflection of the j th component, deg or rad
Θ_j	Magnitude of the pitch plane rotational deflection vector of the j th component, deg or rad

$\bar{\Theta}_j$	Pitch plane rotational deflection vector of the jth component, deg or rad
Θ_T	Total pitch plane rotational deflection of a wind tunnel model, deg or rad
$\bar{\Theta}_T$	Total pitch plane rotational deflection vector of a wind tunnel model, deg or rad
μ	Magnification factor
ϕ_j	Roll deflection of the jth component, deg or rad
Φ_j	Magnitude of the roll deflection vector of the jth component, rad
$\bar{\Phi}_j$	Roll deflection vector of the jth component, deg or rad
x_j	Ordinary coordinates used in the Lagrangian formulation. See Appendix B
ψ_j	Yaw plane rotational deflection of the jth component, deg or rad
Ψ_j	Magnitude of the yaw plane rotational deflection vector of the jth component, rad
$\bar{\Psi}_j$	Yaw plane rotational deflection vector of the jth component, rad
ω	Oscillation frequency, rad/sec
ω_n	Natural frequency, rad/sec
$\omega_{n_{total}}$	Predominant (first mode) frequency exhibited by a multispring system, rad/sec
$(\)'$	Quantity as measured by a balance
$(\dot{\ })$	$d(\)/dt$
$(\ddot{\ })$	$d^2(\)/dt^2$

SUBSCRIPTS

0	Motion as input by the C.F. balance
1	Balance gage element located structurally nearest the sting support
2	Balance gage element located at mid-balance position and used to measure roll deflection
3	Balance gage element structurally farthest from the sting support

B	That mass or moment of inertia attributed to the “nonfloating” portion of the C.C. balance
s	Sting
f	Cross flexure
C1	Center of gravity of the balance mass located between the forward C.C. balance gage element and either the roll gage element (for 3-degree-of-freedom balance) or the aft gage element (for 2-degree-of-freedom balance)
C2	Center of gravity of the balance mass located between the roll gage element and the aft gage element
C3	Center of gravity of the balance and model mass supported by the aft balance gage element